S

Scale-Up of the Ionic Liquid-Based Biomass Conversion Processes

Gabriella Papa[1,2], Blake A. Simmons[2,3] and Ning Sun[1,2]
[1]Advanced Biofuels and Bioproducts Process Development Unit (ABPDU), Lawrence Berkeley National Laboratory, Emeryville, CA, USA
[2]Biological Systems and Engineering Division, Lawrence Berkeley National Laboratory, Berkeley, CA, USA
[3]Joint BioEnergy Institute, Lawrence Berkeley National Laboratory, Emeryville, CA, USA

Introduction

The future biobased economy will be realized by industrial biorefineries that produce sustainable biofuels and multiple bioproducts from renewable biomass sources. As energy demand rises and fossil reserves dwindle, societies will need new resources for sustainable energy and green chemistry sectors. Over the last decade, great efforts and remarkable progress have been made, in developing scalable technologies for conversion of nonfood lignocellulosic biomass to biofuels and biobased chemicals that could replace petroleum-based products.

In the biochemical conversion processes of biomass-to-biofuel, renewable chemicals and materials, it is essential to enhance high conversion yield of all biomass components that are source of sugars and aromatics. A critical role in this effort is the conversion of cellulose, hemicellulose, and lignin fractions from lignocellulose biomass to C6/C5 sugars and aromatics for processing these precursors to intermediate products toward a wide variety of biochemicals through fermentation or chemical catalysis. One of the major challenges in this conversion is related to the need of biomass fractionation into its components (i.e., cellulose, hemicelluloses, and lignin), and processing of heterogeneous lignocellulose biomass for sugar production.

In this regard, the pretreatment step, which alters or removes structural and compositional impediments to digestibility of the plant cell wall polysaccharides, is highly essential and represents a central unit operation affecting the overall yields and the economic viability of biorefinery system [1]. Since the digestibility of cellulose in lignocellulosic biomass is impeded by various chemical and physical factors, an efficient pretreatment of lignocellulosic biomass is required in order to deconstruct the complex, highly cross linked and recalcitrant matrix involving carbohydrates and lignin, and to achieve the maximum sugar released [2].

In general, the success of any pretreatment highly depends on physicochemical properties of the pretreated feedstock as well as the employed conditions [3]. Biomass pretreatment conditions are optimized based on the accessibility of the biopolymers, which is generally indicated by

S. Zhang (ed.), *Encyclopedia of Ionic Liquids*,
https://doi.org/10.1007/978-981-33-4221-7

sugar yields. Throughout the years, many different pretreatment processes were developed (e.g., steam explosion, hot water, dilute acid, alkaline, sulfite pulping, mechanical pulping, and organosol processes). Recently, significant progress has been made with ionic liquid (IL) pretreatment [4] due to their unique solvation properties, disrupting the intermolecular forces that hold biomass biopolymers together and superior performance compared to other types of pretreatment processes.

Typically, biomass is mixed with IL and heated to 120–160 °C during pretreatment process, so that IL could penetrate into the lignocellulosic matrix, enable some solubilization of the main components, partially remove lignin and/or carbohydrates, and delocalize their moieties. Several ILs are very effective at breaking biomass tissues, which also facilitates lignocellulosic biomass dissolution. In particular, the solubility of lignocellulose in ILs has been reported in various ILs. In fact, the correlation between the hydrogen bond basicity of the anion and the solvation ability of ILs to swell and/or dissolve biomass has been studied in literature [5]. Thus, the carbohydrates (i.e., cellulose and hemicellulose) are accessible for hydrolysis with high cellulose conversion. There have been thousands of different structures described in the literature. This opened up the possibility of tuning the properties of the ILs to match a specific application. The studies demonstrated the ability of certain ILs to promote the dissolution of cellulose, through interaction with the anion and to dissolve and remove lignin from biomass [6]. It has been shown that IL pretreatment of biomass is very effective in fractionation of carbohydrates from lignin in a wide range of feedstocks such as herbaceous biomass, softwood, hardwood, agricultural residue, and densified pellets of mixed feedstocks as well; thus, it is considered to be a robust feedstock-agnostic pretreatment technology [4].

More information and details about IL-based lignocellulosic biomass pretreatment can be found in an excellent book chapter, which summarizes performance of the most common ILs on various feedstocks, employing different pretreatment conditions [7]. In particular, the authors provide comprehensive data to define the overall efficiency of IL pretreatment as a function of parameters such as biomass tissue type, solid loading, and severity (temperature/time).

Among the ILs that have been utilized on biomass-related research, imidazolium-based ILs, in particular 1-ethyl-3-methylimidazolium acetate ($[C_2C_1Im][OAc]$), are widely used and chosen as the gold standard for biomass processing. This IL has been proven to be superior in terms of biomass solubilization and saccharification yields, with >90% and at both lab and pilot scale tests [8, 9]. However, both cost and recyclability render challenges for its commercial feasibility, resulting in being less competitive compared to other biocompatible and cheaper ILs. For example, cholinium-based ILs such as cholinium lysinate [Ch][Lys] are less expensive and still facilitate efficient biomass fractionation, which is highly desirable for biorefinery [3, 5, 10].

Since the use of ILs is a relatively new approach to pretreat and fractionate lignocellulose materials, ILs conversion technologies are still at early stage with research focusing on developing new ILs, processes, and concepts in order to reduce or eliminate water wash step due to the inhibition effect to downstream biological conversion steps. This entry discusses the experimental outcomes of pilot scale studies related to IL pretreatment, in consideration of various process configurations and different feedstocks. In particular, conventional water-wash route followed by enzymatic or acid hydrolysis is compared to results from the recent developed "one pot"-consolidated approach. Figure 1 shows two common approaches for IL-based biomass conversion pathways. Table 1 summarizes bench to pilot scale studies on sugars production from lignocellulosic raw materials, adopting various process configurations and IL pretreatment at various conditions.

We also provide a brief overview of different ILs used for pretreatment along with their effect on biomass chemical-physical properties, considering the parameters affecting the performance and reported data on process optimization. The information will help to identify the current

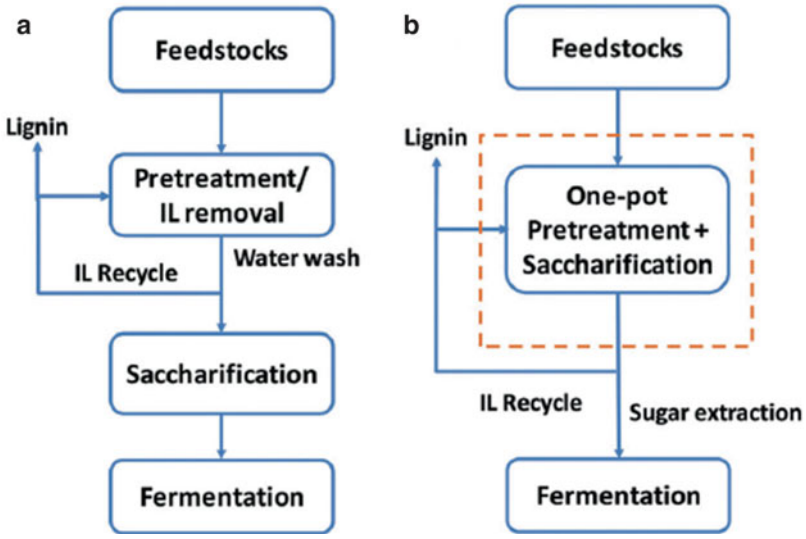

Scale-Up of the Ionic Liquid-Based Biomass Conversion Processes, Fig. 1 Process configurations for conversion of IL-pretreated biomass to advanced biofuels: (**a**) fully separated unit operations; (**b**) one pot deconstruction and saccharification [4] (By kind permission of Royal Society of Chemistry, license no. 4617060721104)

technical challenges and the scenarios of IL pretreatment for future biorefineries.

Process Configurations of IL Pretreatment

Different solid loadings, temperatures, retention times, and various types of ILs were investigated at bench or pilot scale for biomass conversion. As mentioned above, the most common IL tested in pilot scale studies is imidazolium-based IL[C_2C_1Im][OAc] [8]. Few other scale-up studies reported the performances observed by using other ILs such as chloride-based ILs, 1-butyl-3-methylimidazolium chloride ([C_4C_1Im]Cl), and 1-ethyl-3-methylimidazolium chloride ([C_2C_1Im]Cl) that were used followed by acid hydrolysis to produce sugar monomers [11]. While only tested at bench scale, protic ILs are receiving more attention in lignocellulose fractionation studies, where up to 85% of the lignin solubilization and sugars yields >77% were found after pretreating herbaceous feedstocks with triethylammonium hydrogen sulfate [12]. Moreover, the potential of using protic ILs in one-pot configuration without pH adjustment was suggested by Sun et al. [13], who successfully employed the whole slurry derived from pretreated switchgrass with ethanolamine acetate ([EOA][OAc]) for simultaneous saccharification and fermentation (SSF) to produce ethanol at high yields (no water wash, solid-liquid separations, or pH adjustment).

Even though bioderived ILs, "bionic liquid," such as cholinium lysinate [Ch][Lys] show promising results on lab scale level [3, 10], no large-scale demonstration has been reported in literature on the use of this IL in conventional water wash approach. On the other hand, this renewable IL has been successfully employed at pilot scale with the integrated system approach and evaluation of process scale-up-assessed technical feasibility of this process configuration and significant improvements in process economics [14].

Conventional Process with Water Wash

As shown in Fig. 1a., the conventional IL pretreatment process consists of three steps: mixing, washing, and solid/liquid separation. In the first step, the reaction takes place by mixing the IL with biomass. In the second step, an antisolvent, typically water or ethanol, is used to wash off the IL from the regenerated or undissolved biomass. The addition of antisolvent also results in precipitation of dissolved macromolecules; thus, one solid mass (precipitated and undissolved) is recovered. Lignin and xylan that stay soluble

Scale-Up of the Ionic Liquid-Based Biomass Conversion Processes, Table 1 Comparison of scale-up studies on sugars production from lignocellulosic raw materials, adopting various process configurations and ionic liquid pretreatment at various conditions

Lignocellulosic substrate	Ionic liquid	Process configurations Pretreatment conditions (solid loading, temperature, and time)	Reactor volume	Total mass pretreated kg	Yield after saccharification %		Reference
					Glucose	Xylose	
Switchgrass	$[C_2C_1Im][OAc]$	Conventional water wash 15% solid, 160 °C, 3 h	10	0.9	95	77	[20]
Mixed feedstocks (switchgrass and eucalyptus)	$[C_2C_1Im][OAc]$	Conventional water wash 10% solid, 140 °C, 1 h	10	0.6	99.7	62.8	[8]
Switchgrass	$[C_2C_1Im][OAc]$	Conventional water wash 15% solid, 160 °C, 2 h	210	6	83.1	30.7	[15]
Municipal solid waste (MSW)	$[C_2C_1Im]Cl$ $[[C_4C_1Im]Cl$	One pot IL acidolysis 10–15% solid, 120–160 °C, 2 h	10	0.34–0.51	58	35	[17]
MSW/corn stover blends	$[C_2C_1Im]Cl$ $[C_4C_1Im]Cl$, 0.6–1.8% HCl	One pot IL acidolysis 10–15% solid, 120–160 °C, 2 h	10	0.34	44.5–70.9	34.6–55.7	[11]
Sorghum	Water:[Ch][Lys] (9:1, w/w)	One pot consolidated 30 and 20% solid, 140 °C, 1 h	1	0.07	75 ± 1.2	57 ± 3	[14]
Sorghum	Water:[Ch][Lys] (9:1)	One pot consolidated 30 and 20% solid, 140 °C, 1 h	10	2.3	88 ± 1.1	57 ± 0.8	[14]
Sorghum	Water:[Ch][Lys] (9:1)	One pot consolidated 30 and 20% solid, 140 °C, 1 h	210	17.5	68 ± 0.5	63 ± 0.3	[14]

during precipitation and washing steps could be extracted or recovered by water or solvent removal. In the third step, the solid with features which are helpful for efficient enzymatic hydrolysis, such as disrupted matrix structure, altered fibrillar structure, increased surface area, less crystallinity of cellulose, and less lignin content, is recovered. Then this material is subjected to enzymatic hydrolysis, where the long-chain carbohydrates (cellulose and hemicellulose) are

converted to water-soluble monosaccharides. Any remaining solid is collected as lignin-rich residue. Conventional IL process (i.e., water-wash route) requires extensive washing procedure of the pretreated biomass to remove residual ILs to avoid inhibition effect in the downstream saccharification and successive fermentation. This process could result in losses of soluble sugars and generate large volumes of waste water.

Since 2010, biomass pretreatment, using imidazolium-based ILs, has been reported in the literature. However, the majority of the reported pretreatments have been performed using low biomass loadings (3–15 wt.%) and only at lab scale [5, 9].

Investigations on the scale-up effect of water-wash conventional IL pretreatment can be found in studies by Li et al. [8], who evaluated the response of mixed milled feedstock in comparison with two single feedstocks (i.e., switchgrass and eucalyptus), to $[C_2C_1Im][OAc]$ pretreatment performed at solid loading of 10% (w/w) and temperature of 160 °C for 3 h. After pretreatment of 0.6 kg biomass with 5.4 kg IL $[C_2C_1Im][OAc]$ in a 10 L Parr reactor, 6 L hot water was added to the slurry to remove the IL from precipitated biomass. A further homogenization step was conducted by employing additional four water-wash cycles (9 L DI water each time) to mechanically break the gel and facilitate IL removal with water. They found a significant biomass loss into the water washes due to the solubilization of components such as xylan, lignin, and other extractives during pretreatment with IL. They concluded that solid recovery and prevention of gel formation could be improved with scaling to higher solid loadings, larger volumes, and milder severity. The authors also investigated the enzymatic hydrolysis performance and found rapid sugar release with maximum sugar titers of 62.1 g L^{-1} for glucose and 15.0 g $L^{-1}$for xylose (i.e., 95.9 and 98.3% glucose and xylose, based on glucan and xylan in pretreated biomass), after 72 h saccharification.

In a more recent study [15], the authors demonstrated $[C_2C_1Im][OAc]$ pretreatment on switchgrass at 40 kg scale in a 210 L reactor with high sugars yields (i.e., 83.1 wt% of glucan and 30.7 wt% of xylan conversion based on initial carbohydrate content) after 166 h enzymatic hydrolysis. The IL pretreatment was conducted at 160 °C for 2 h with 15 wt% solid loading; a relative high dissolution of biomass (>40 wt%) was observed. In particular, 56.6 wt% of the starting switchgrass (6 kg) was recovered as solids after washing and solid/liquid separation. This pilot scale study provided a full mass flow, with valuable data tracking the solid and liquid streams, and showed that >95 wt% glucan was preserved in the IL-pretreated material with >60 wt% xylan removed in liquid stream. They suggested to recover soluble sugars from aqueous stream; however, this process has only been demonstrated at lab scale studies.

One-Pot Biomass Conversion: Acidolysis Process

Acid catalyst has been used to hydrolyze polysaccharides to monosaccharides following IL pretreatment, which could potentially provide an enzyme-free process with significant reduction of the processing time and material cost [16, 17]. It was reported that over 80% glucose and 90% xylose were released with the integrated IL-acidolysis process at lab (10 g) and bench (6 L) scale. Biomass pretreatment was carried out at either 105 °C/6 h or 160 °C/1.5 h in chloride-based ILs such as $[C_4C_1Im]Cl$ or $[C_2C_1Im]Cl$. At the end of the pretreatment, the temperature was maintained at 105 °C, and acidolysis takes another 1 h. Water was added either at defined time intervals (0 min, 10 min, 20 min, 30 min, and 60 min) or continuously pumped in during acidolysis. It was found that time intervals for water addition played an important role on the sugar yields, which is attributed to the kinetics of the glucose hydrolysis. Maximum glucose yields occur at the expense of reduced xylose yields. At more severe process conditions, more glucan can be hydrolyzed, but this also results in spontaneous xylose degradation. The maximum solid loading was tested at 15% (w/w) with 15 g/L glucose and 7 g/L xylose in the hydrolysate [16].

One-Pot Biomass Conversion: Bionic Liquid Process

The use of bioderived ILs (e.g., cholinium lysinate ([Ch][Lys]) in a one-pot process has been showed as an integrated and efficient biomass conversion process eliminating the water-washing step. The one-pot process was first reported by Shi et al. [4] with pretreatment of switchgrass in $[C_2C_1Im][OAc]$, which was proved to reduce significantly the water usage by 2–15 fold as compared to the conventional approach. Progress in one-pot corn stover processing using cholinium-based ILs was reported by Xu et al. [18]. Over 80 g/L glucose was achieved in the hydrolysate with high-gravity experiments (i.e., fed-batch with solid loading >30%), and 41.1 g/L (74.8% theoretical yield based on glucose) ethanol was obtained with yeast fermentation. Techno-economic analysis (TEA) showed significant economic and environmental benefits for cellulosic biorefineries by reducing the amount of IL required by 90% and wastewater generation by 85%. In turn, these improvements can reduce net electricity use, greenhouse gas-intensive chemical inputs for wastewater treatment, and waste generation. The result showed an overall 40% reduction in the cost of cellulosic ethanol produced and a reduction in local burdens on waste management infrastructure. Additional encouraging results were obtained at laboratory scale [13], using the low-cost protic IL (PIL) ethanolamine acetate, which demonstrated improvement of the economic performance and opened avenues for developing efficient IL-based biomass conversion technology.

The [Ch][Lys]-based one-pot process has been scaled up at the Advanced Biofuels and Bioproducts Process Development Unit (ABPDU) in a recent study [14]. The study presented a scalable separation-free process to convert lignocellulosic biomass to an advanced biofuel, revealing the feasibility of integrating most of the biomass conversion unit operations within the biorefinery (Fig. 2). The authors demonstrated bisabolene production, a sesquiterpene

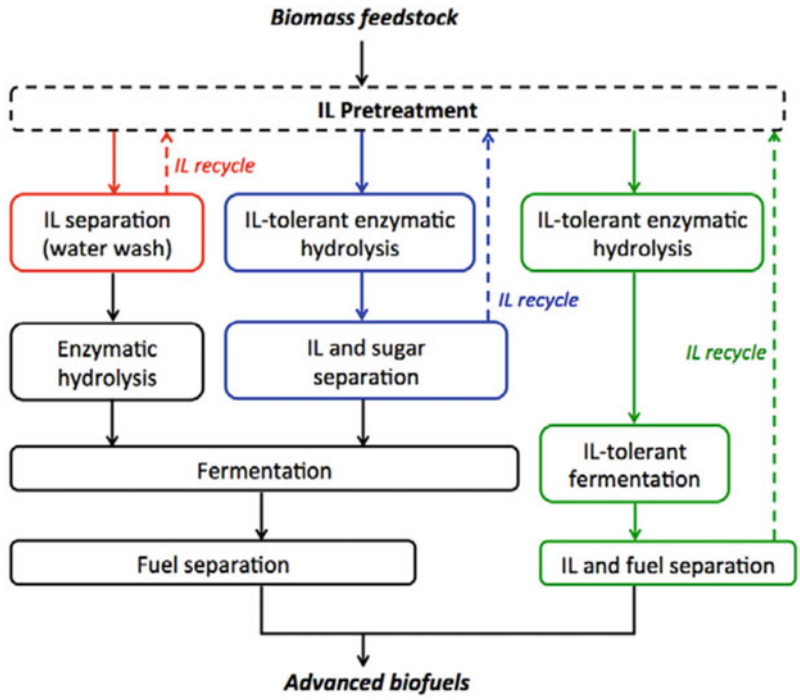

Scale-Up of the Ionic Liquid-Based Biomass Conversion Processes, Fig. 2 The fully consolidated process eliminates the requirement for IL separation prior to saccharification and fermentation but requires IL-tolerant enzyme cocktails and an IL-tolerant host organism. Separation of both fuel molecules and residual ionic liquids can then be consolidated into a single step following fermentation [14]

diesel and jet fuel precursor, from milled sorghum (<2 mm). The pretreatment and hydrolysis steps were conducted in a 210 L vessel, with a total working mass of 17.5 kg. The C5-C6 sugars in the sorghum hydrolysate were further fermented with genetically modified *R. toruloides* in a 50 L bioreactor without solid-liquid separations or water-washing steps.

The process conditions and sugars yields are summarized in Table 1. By conducting [Ch][Lys] pretreatment (140 °C for 1 h) of sorghum at 30% solid loading and diluting to 20% for enzymatic saccharification, the authors compared the sugars yields of three scales (i.e., 1 L, 10 L, and 210 L reaction vessels). The improvement in performance with process scale-up (over 87% glucose and 80% xylose released) was ascribed to the improved dynamics on mass transfer during the mixing in the larger-scale reactor. The fermentation scale-up experiments were also conducted in different scales of fermenters with working volume: 2 and 20 L. Higher bisabolene production was obtained at larger scale with 2.2 g/L bisabolene produced at 20 L fermentation. This was attributed to a combination of improved mixing, media composition, oxygen transfer, DO control, and pH control in the bioreactor. This work was the first scale-up study to demonstrate a separation-free IL-based process for biomass conversion and the first to demonstrate full consumption of sugars and organic acids in the presence of [Ch][Lys]. With further optimization and by routing additional carbon flux to the mevalonate pathway, improved bisabolene titers, rates, and yields could be achieved.

Application of the Residual Lignin Fraction

After pretreatment and hydrolysis steps, the solid stream is rich in lignin (40–80%) and could be further upgraded after further carbohydrates removal. Catalytic hydrogenolysis of the lignin stream after biomass conversion using the [Ch][Lys]-based one-pot process is reported by Carrozza et al. [19]. The lignin-rich fraction was recovered after enzymatic saccharification and converted to low-molecular weight aromatic phenolic compounds through catalytic hydrogenolysis reactions. Maximum 35% (wt% on lignin basis) lignin monomers such as guaiacol, phenol, syringone, acetosyringone, etc. are relseased by reduction over metal catalysts Pd/C and $NiSO_4$. The insights gained from this work contributed to better understanding of the lignin stream generated during [Ch][Lys]-based process.

Outlook and Perspectives

IL is a promising pretreatment technology with advantages including feedstock agnostic, efficient sugar conversion, fast kinetics, and consolidated process configuration. However, there are still challenges to make it an economic viable process.

Increased biomass loading during pretreatment and saccharification is crucial to generate enough sugar concentrations for fermentation. Since most of the lignocellulosic feedstocks contain 30–40% of polysaccharides, high biomass loading (> 30%) is needed so that the fuel product could be recovered [20]. The high solid loading also leads to economic benefit by cutting costs associated with water consumption and IL usage. On the other hand, high solid loadings pose process challenges such as reduced mass and heat transfer and material handling which could affect the sugars yield [21]. With >15% solid loading, there is no free liquid due to the hydroscopic properties of the biomass. Continuous reactors (e.g., extruders) may allow improved solid loading and mass/heat transfer in this regard.

Up to now, the most hitch in the commercialization of biomass conversion employing ILs is the IL recyclability, and the recovery and reuse of ILs has not been proved at large scale, albeit promising techniques, such as membrane-based processes (i.e., nanofiltration, pervaporation, reverse osmosis, and electrodialysis) are currently under development and stimulating scientific community to keep working on this research area.

References

1. Blanch HW, Simmons BA, Klein-Marcushamer D (2011) Biomass deconstruction to sugars. Biotechnol J 6:1086–1102
2. Kumar P, Barrett DM, Delwiche MJ, Stroeve P (2009) Methods for pretreatment of lignocellulosic biomass for efficient hydrolysis and biofuel production. Ind Eng Chem Res 48:3713–3729
3. Papa G, Feldman T, Sale KL, Adani F, Singh S, Simmons BA (2017) Parametric study for the optimization of ionic liquid pretreatment of corn Stover. Bioresour Technol 241:627–637
4. Shi J, Gladden J, Sathitsuksanoh N, Kambam P, Sandoval L, Mitra D, Zhang S, George A, Singer S, Simmons B, Singh S (2013) One-pot ionic liquid pretreatment and saccharification of switchgrass. Green Chem 15:2579–2589
5. Sun N, Parthasarathi R, Socha AM, Shi J, Zhang S, Stavila V, Sale KL, Simmons BA, Singh S (2014) Understanding pretreatment efficacy of four cholinium and imidazolium ionic liquids by chemistry and computation. Green Chem 16:2546–2557
6. Sun N, Rodríguez H, Rahman M, Rogers RD (2011) Where are ionic liquid strategies most suited in the pursuit of chemicals and energy from lignocellulosic biomass? Chem Commun (Camb) 47: 1405–1421
7. Dutta T, Shi J, Sun J, Zhang X, Cheng G, Simmons BA, Singh S (2015) Ionic liquids in the biorefinery concept: challenges and perspectives. In: Bogel-Lukasik R (ed) Ionic liquid pretreatment of lignocellulosic biomass for biofuels and chemicals. RSC Green Chem, pp 65–94
8. Li C, Tanjore D, He W, Wong J, Gardner JL, Thompson VS, Yancey NA, Sale KL, Simmons BA, Singh S (2015) Scale-up of ionic liquid-based fractionation of single and mixed feedstocks. Bioenergy Res 8: 982–991
9. Li C, Knierim B, Manisseri C, Arora R, Scheller HV, Auer M, Vogel KP, Simmons BA, Singh S (2010) Comparison of dilute acid and ionic liquid pretreatment of switchgrass: biomass recalcitrance, delignification and enzymatic saccharification. Bioresour Technol 101:4900–4906
10. Dutta T, Papa G, Wang E, Sun J, Isern NG, Cort JR, Simmons BA, Singh S (2018) Characterization of lignin streams during bionic liquid-based pretreatment from grass, hardwood, and softwood. ACS Sustain Chem Eng 6(3):3079–3090
11. Li C, Liang L, Sun N, Thompson VS, Xu F, Narani A, He Q, Tanjore D, Pray TR, Simmons BA, Singh S (2017) Scale-up and process integration of sugar production by acidolysis of municipal solid waste/ corn Stover blends in ionic liquids. Biotechnol Biofuels 10:13
12. Brandt-Talbot A, FJV G, Fennell PS, Lammens TM, Tan B, Weale J, Hallett JP (2017) An economically viable ionic liquid for the fractionation of lignocellulosic biomass. Green Chem 19:3078–3102
13. Sun J, Konda NVSNM, Parthasarathi R, Dutta T, Valiev M, Xu F, Simmons BA, Singh S (2017) One-pot integrated biofuel production using low-cost biocompatible protic ionic liquids. Green Chem 19: 3152–3163
14. Sundstrom E, Yaegashi J, Yan J, Masson F, Papa G, Rodriguez A, Mirsiaghi M, Liang L, He Q, Tanjore D, Pray TR, Singh S, Simmons B, Sun N, Gladden J (2018) Demonstrating a separation-free process coupling ionic liquid pretreatment, saccharification, and fermentation with Rhodosporidium toruloides to produce advanced biofuels. Green Chem 20:2870–2879
15. Liang L, Yan J, He Q, Luong T, Pray TR, Simmons BA, Sun N (2018) Scale-up of biomass conversion using 1-ethyl-3-methylimidazolium acetate as the solvent. GEE. https://doi.org/10.1016/j.gee.2018.07.002
16. Sun N, Liu H, Sathitsuksanoh N, Stavila V, Sawant M, Bonito A, Tran K, George A, Sale KL, Seema S, Simmons BA, Holmes BM (2013) Production and extraction of sugars from switchgrass hydrolyzed in ionic liquids. Biotechnol Biofuels 6:39
17. Liang L, Li C, Xu F, He Q, Yan J, Luong T, Simmons BA, Pray TR, Singh S, Thompson VS, Sun N (2017) Conversion of cellulose rich municipal solid waste blends using ionic liquids: feedstock convertibility and process scale-up. RSC Adv 7: 36585–36593
18. Xu F, Sun J, Konda NVSNM, Shi J, Dutta T, Scown CD, Simmons BA, Singh S (2016) Transforming biomass conversion with ionic liquids: process intensification and the development of a high-gravity, one-pot process for the production of cellulosic ethanol. Energy Environ Sci 9:1042
19. Carrozza CF, Papa G, Citterio A, Sebastiano RS, Simmons BA, Singh S (2019) One-pot bio-derived ionic liquid conversion followed by hydrogenolysis reaction for biomass valorization: a promising approach affecting the morphology and quality of lignin of switchgrass and poplar. Bioresour Technol 294:122214–122223
20. McIntosh S, Palmer J, Zhang Z, Doherty WOS, Yazdani SS, Sukumaran RK, Vancov T (2017) Simultaneous saccharification and fermentation of pretreated *Eucalyptus grandis* under high solids loading. Ind Biotechnol 13:131–140
21. Li C, Tanjore D, He W, Wong J, Gardner JL, Sale KL, Simmons BA, Singh S (2013) Scale-up and evaluation of high solid ionic liquid pretreatment and enzymatic hydrolysis of switchgrass. Biotechnol Biofuels 6:154
22. Sun J, Shi J, Murthy KNVSN, Campos D, Liu D, Nemser S, Shamshina J, Dutta T, Berton P, Gurau G, Rogers RD, Simmons BA, Singh S (2017) Efficient Dehydration and Recovery of Ionic Liquid After Lignocellulosic Processing Using Pervaporation. Biotechnol Biofuels, 10, 154:1–14

Selective Dissolution of Biomass with Ionic Liquids

Hiroyuki Ohno, Mizuki Shimo, Takashi Akiba and Mao Nagatani
Department of Biotechnology, Tokyo University of Agriculture and Technology, Tokyo, Japan

Introduction

Effective utilization of biomass is one of the methods expected to solve future energy problems. Besides using as a material, biomass has been used as a fuel. Although it is convenient and therefore dried biomass has widely been used as a fuel, energy conversion efficiency by direct combustion is not so high. Since burning them generates carbon dioxide, it is not a desirable energy conversion method. Therefore, effective utilization of biomass has widely been studied, but the chemical stability of biomass is the big issue to transform them into usable materials. That is, there was no solvent capable of efficiently dissolving the biomass under mild condition. Of course, it can be dissolved in some kind of solvents under heating, but it is not desirable from the viewpoint of energy balance to input a large amount of energy to extract energy.

On the other hand, studies on ionic liquids, which are salts having extremely low melting point, are active. Since it is a salt, it is studied as various reaction solvents as a safe substitute for flammable organic solvents, taking advantage of the feature of liquids with extremely low vapor pressure. However, since the performance is not much different from that of conventional organic solvents, development as a solvent for chemical reaction has been rapidly downgraded. On the other hand, some ionic liquids, having high polarity and the feature of dissolving sparingly soluble substances, have come to attract keen attention. Rogers and his co-workers succeeded in dissolving cellulose by heating pyridinium chloride and/or imidazolium chloride based ionic liquids. Since this research, it has been reported that various highly polar ionic liquids dissolve cellulose, partial lysis of lignin under relatively mild conditions, and dissolution (swelling) of biomass itself. Under such a background, ionic liquids with various functions are designed, and a new flow for biomass treatment is about to be created.

This entry mentions the introduction of ionic liquids that can dissolve cellulose and lignin, which are the main components of biomass, and discusses a possible method to selectively dissolve them or isolate them from biomass.

Dissolution of Cellulose in Ionic Liquids

Early Study with Chloride Salts

It was already found in the 1930s that a solution of an amine with ethyl pyridinium chloride salt dissolved cellulose [1]. The chloride salt of ethyl pyridinium was not recognized as an ionic liquid at that time, and it was handled as mere addition salt. After a while, Rogers and his colleagues in the United States reported dissolution of cellulose using ionic liquids [2]. Rogers et al. found that pulp cellulose melts when 1-butyl-3-methylimidazolium chloride ($[C_4mim]$ Cl) (Fig. 1, left) was heated above 100 °C. When combined with microwave and ultrasonic treatment, it is said that 25 wt% cellulose solution can be made, but the disadvantage is that the melting point of the chloride salt is high. We have reported that introducing an allyl group into the imidazolium cation greatly reduces the melting point of the chloride salt [3]. This is a rare chloride salt that can be treated as a liquid at room temperature. In response to this report, Zhang and colleagues dissolved cellulose using 1-allyl-3-methylimidazolium chloride salt ([Amim] Cl) (Fig. 1, right) [4]. On the other hand, Heinze et al. compared chloride salts with alkyl pyridinium cation and quaternary ammonium cation and reported that the difference in cation structure affects the solubility of cellulose [5].

Strategy to Design Ionic Liquids to Dissolve Cellulose Under Ambient Condition

Based on the basic idea that the chloride salt is not the only solvent of cellulose, there were attempts to make new ionic liquids from a physicochemical approach. First, ionic liquids with various anions were prepared, and correlation with solubility of cellulose was sorted out through polarity evaluation. Kamlet-Taft parameters [6, 7], calculated empirically from the solvatochromism of dye molecules, were chosen as polarity parameters. Three parameters of hydrogen bond donation (α value), hydrogen bond acceptability (β value), and bipolarity ($\pi*$ value) are individually calculated. We have searched ionic liquids having hydrogen bonding ability equal to or higher than that of the chloride salt. As a result of examining a series of ionic liquids, we have found some ionic liquids containing carboxylic acid anions such as acetic acid have equivalent or higher hydrogen bond ability than chloride salts. It was expected that an acetic acid-based ionic liquid was effective for dissolving cellulose, and actually 10 wt% of cellulose can be dissolved in it at 55 °C. Therefore, since a series of organic carboxylic acids can be obtained relatively easily, various carboxylates have been synthesized and looked for more powerful structure. As a result, as the alkyl chain length of the carboxylic acid however became longer, the physical properties of the salt tended to gradually deteriorate. Therefore, the formate salt was expected to have good properties, and the formate salt has certainly high hydrogen bonding ability and has cellulose-dissolving ability comparable to that of acetic acid [8]. It was also found that the formate salt is an ionic liquid with a lower viscosity than the acetate salt. However, a series of carboxylate salts are not excellent in long-term stability and thermal stability. Then these carboxylates were evaluated not to be excellent solvent for cellulose.

The anion species were investigated further expanded, and a few new polar ionic liquids were found instead of chloride salt and carboxylate. It was found that even a sulfonic acid or phosphoric acid derivatives were good cellulose solvents. Synthesis of these salts is not so complicated. For example, they can be obtained by reacting acid ester with tertiary amine [9]. It was also found to be an excellent point that high-purity ionic liquids can easily be synthesized due to no bi-product. To check the cellulose solubilizing ability of the obtained ionic liquids, cellulose powder was added and mixed so as to be 2.0 wt%. As a result, only 1-ethyl-3-methylimidazolium dimethylphosphate ($[C_2mim](MeO)_2PO_2$) completely dissolved cellulose under mild stirring at 45 °C for 30 min [10]. This $[C_2mim](MeO)_2PO_2$ is an ionic liquid that can dissolve cellulose without causing decomposition like chloride salts. Through this examination, a few ionic liquids having various phosphate derivative anions were newly found to be solvents for cellulose (Fig. 2). All of these phosphate-based salts were liquid at room temperature. As a result of differential scanning calorimetry study, $[C_2mim](MeO)_2PO_2$ showed a melting point at around 20 °C, but the other two ionic liquids showed no melting point, but only the glass transition temperature. Even when these ionic liquids were cooled at −20 °C for more than 1 month, no crystallization occurred. These results show that

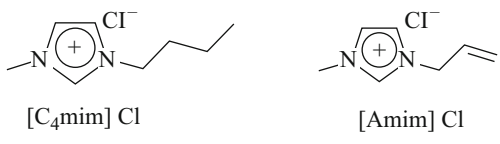

Selective Dissolution of Biomass with Ionic Liquids, Fig. 1 Typical ionic liquids containing chloride anion

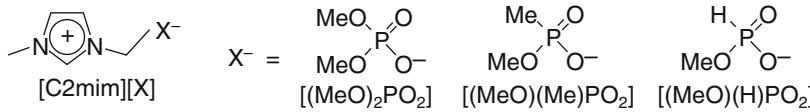

Selective Dissolution of Biomass with Ionic Liquids, Fig. 2 Examples of ionic liquids containing phosphate and phosphonate anion analogs

the newly prepared 1-ethyl-3-methylimidazolium methylphosphate ($[C_2mim](MeO)(H)PO_2$) and $[C_2mim]$ $(MeO)(Me)PO_2$ maintain a stable super-cooled state even at room temperature. It was revealed that ionic liquids with phosphate derivative newly prepared have high hydrogen bond acceptability (β value of 1.0 or more). The polarity values of ionic liquids capable of dissolving cellulose are summarized in Table 1. As obvious from these, the necessary condition of the hydrogen bond-donating property (α value) is 0.47 or more, and the hydrogen bond acceptability (β value) is 0.62 or more. These values are good reference to design new ionic liquids as cellulose solvents.

On the other hand, the viscosity of these ionic liquids greatly varies from 100 to 500 cP at 25 °C depending on the anion structure. For the cellulose solvent, it is desirable that the viscosity be as low as possible. Among the ionic liquids in Table 1, $[C_2mim](MeO)(H)PO_2$ showed the lowest viscosity. Regarding these viscosity values, there is room for improvement as compared with general-purpose organic solvents. However, some of these are highly polar ionic liquids with relatively low viscosity. Furthermore, it was confirmed that any newly prepared ionic liquid did not volatilize and thermally decompose to about 250 °C. There was no weight loss and chemical structure change even when they were heated for a long time at 100 °C. However, gradual decomposition was observed when it was kept at high temperature for a long period of time, so that further improvement in stability is strongly desired.

Selective Dissolution of Biomass with Ionic Liquids, Table 1 Polarity parameters of typical ionic liquids used as solvents for cellulose

Ionic liquid	α	β
$[C_4mim]Cl$	0.47[a]	0.87[a]
$[C_4mim](MeO)(H)PO_2$	0.52	1.02
$[Amim](MeO)(H)PO_2$	0.51	0.99
$[C_3mim](MeO)(H)PO_2$	0.54	1.00
$[C_2mim](MeO)(H)PO_2$	0.52	1.00
$[C_2mim](EtO)(H)PO_2$	0.55	1.02
$[C_2mim](i\text{-}PrO)(H)PO_2$	0.55	1.03
$[C_2mim](n\text{-}BuO)(H)PO_2$	0.56	1.06
$[C_2mim]H_2PO_2$	0.52	0.97
$[C_4mim]MeOSO_3$	0.59	0.62
$[C_4mim]CF_3CO_2$	0.62	0.81
$[C_4mim](MeO)_2PO_2$	0.52	1.00
$[C_4mim]HCO_2$	0.56	1.01

[a]At 90 °C, because this is solid at 25 °C

Solubility of cellulose was evaluated in the prepared ionic liquid, and we found that about 10% of finely powdered cellulose was dissolved under mild condition within a short stirring time. The temperature required for dissolving cellulose varied depending on the ion species used and final concentration. For example, a 10% cellulose solution can be prepared by stirring at 45 °C for 30 min when $[C_2mim](MeO)(H)PO_2$ was used as solvent, but $[C_2mim](MeO)_2PO_2$ required heating at 65 °C in order to obtain the same concentration of cellulose solution by stirring within 30 min. These differences may be due to the difference in the polarity as well as that in the viscosity of the system that affects the dispersibility of the cellulose. Naturally, the temperature required for dissolution of cellulose can be reduced by prolonging the stirring time. In other words, cellulose can be dissolved even without heating when sufficiently long stirring time was allowed. With these newly prepared ionic liquids, up to about 8% of cellulose solution can be obtained by stirring for several hours at room temperature.

Dissolution and Extraction of Cellulose from Plant Biomass

Some biomass samples such as cotton, rice hulls, coconuts shell, and even disposable chopsticks were added into polar ionic liquids, and their dissolution capacity was examined at room temperature or under mild heating. Although the cotton completely dissolved, all the other samples were swollen, but most parts were remained insoluble. From this experiment, cellulose was confirmed to easily be dissolved in polar ionic liquids, but lignin network and other biomass staffs are hardly soluble under mild condition. This result also suggested that cellulose could be extracted from biomass under mild condition. Figure 3 shows the result of extracting cellulose from wheat hull (bran) using polar ionic liquids such as $[C_2mim](MeO)(H)PO_2$ [11]. Bran was

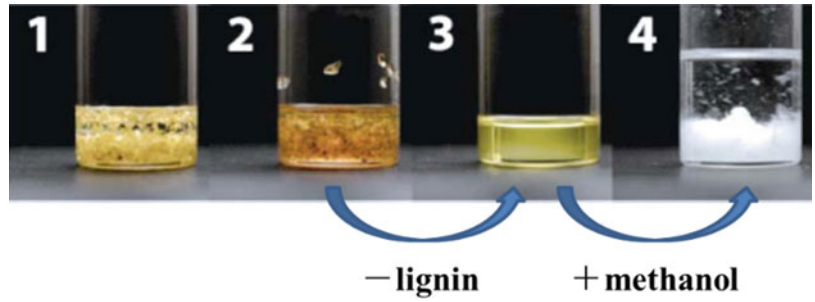

Selective Dissolution of Biomass with Ionic Liquids, Fig. 3 Extraction and separation of cellulose from bran [11]. (With permission of Royal Society of Chemistry)

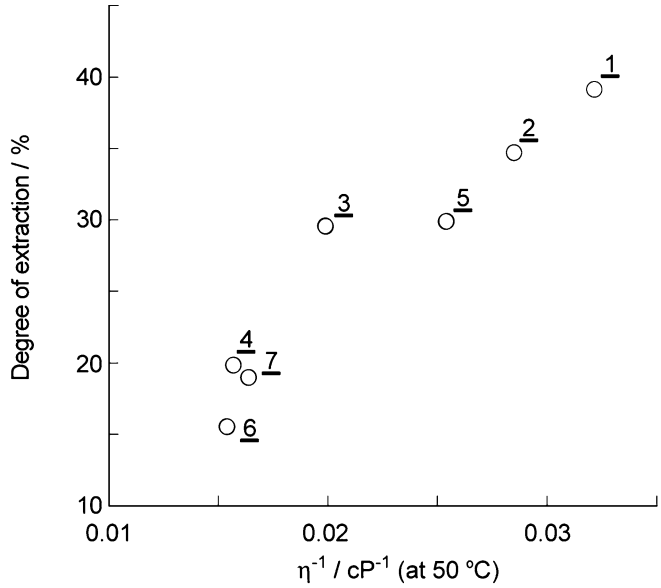

Selective Dissolution of Biomass with Ionic Liquids, Fig. 4 Relationship between degree of extraction of polysaccharides and inverse viscosity. (50 °C) of a series of ILs used [11]. (With permission of Royal Society of Chemistry). (1) $[C_2mim](MeO)(H)PO_2$, (2) [Amim] $(MeO)(H)PO_2$, (3) $[C_3mim](MeO)(H)PO_2$, (4) $[C_4mim]$ $(MeO)(H)PO_2$, (5) $[C_2mim](EtO)(H)PO_2$, (6) $[C_2mim]$ $(i\text{-}PrO)(H)PO_2$, (7) $[C_2mim](BuO)(H)PO_2$

added to this ionic liquid to form 5.0 wt% suspension (step 1) and then stirred for 10 min at 50 °C (step 2). Some insoluble components such as lignin have been removed by filtration (step 3), and then methanol was added to the filtered solution to precipitate cellulose (step 4). The dried cellulose obtained was confirmed to have low crystallinity by X-ray diffraction analysis. All these steps (especially step 2) can be done to extract cellulose at room temperature, but it took longer time. After separation of cellulose and heating, separation of ionic liquid and methanol can be repeatedly used as an extraction solvent and a poor solvent to precipitate cellulose, respectively. Therefore, since biomass was added and after gentle mixing, insoluble components such as lignin were separated by filtration, this system can be considered as a closed system. In spite that precipitates are composed of cellulose, 100% of cellulose cannot be extracted from bran, and some were still contaminated in the insoluble part. Further trial is needed to improve the separation efficiency.

There is an interesting relation between extraction degree of cellulose (after stirring for 2 h) from bran and reciprocal viscosity of ionic liquids used as shown in Fig. 4 [11]. This relation shows that less viscous ionic liquids are better to extract more amount of cellulose from bran under the limited

stirring time. Since the ionic liquids used here have almost similar polarity, the difference in the extraction degree of cellulose (within the limited time) can be considered to be due to the solution viscosity.

Dissolution of Lignin in Ionic Liquids

Lignin is the second most abundant plant biomass. Lignin is the cross-linked aromatic polymers which impart physical strength to maintain the shape of plants. Since lignin is the component for structure preservation of plants, they are quite stable. In other words, it is quite difficult to dissolve lignin. Generally, wood chips were treated with strong acid or alkali at high temperature such as 150 °C or more to partly decompose the cross-linked structure and solubilize lignin. However, such harsh condition is corrosive and needs large amounts of energy. For the effective use of lignin, we should think about a new method to extract lignin (fragments) without consuming huge energy. One possible way is the use of wood-rotting fungus. A lignin-degrading enzyme from the wood-rotting fungus is known to fragmentize the lignin. With the use of such enzyme, it is possible to decompose lignin (or wood chip) under mild condition, but it takes a long time. To develop innovative method that can decompose and dissolve lignin under mild condition, many ionic liquids have been tested. There should be a different strategy to design ionic liquids as solvents for lignin from that for cellulose.

Strategy to Design Ionic Liquids to Dissolve Lignin

First, the effect of polarity of the ILs on the dissolution of lignin has been analyzed. For this experiment alkali lignin was mainly used. Alkali lignin is relatively easy to dissolve and should be a good reference to analyze the physicochemical properties of ionic liquids required for lignin dissolution. Figure 5 shows the effect of polarity on the dissolution ability of lignin. Soda lignin was added to a series of ionic liquid (numbered from 1 to 18) to reach the final concentration of 10 wt%, and the mixtures were gently stirred at 60 °C for 30 min. The ionic liquids that could dissolve soda lignin were

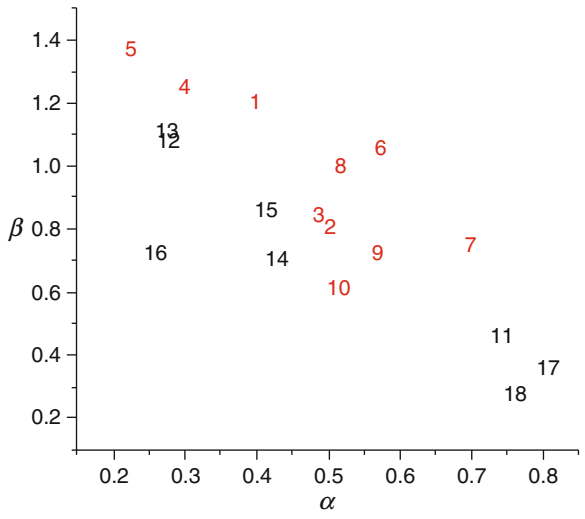

1: $[Pyr_{12O1}]CH_3CO_2$
2: $[Pyr_{12O1}]CF_3CO_2$
3: $[Pyr_{14}]CF_3CO_2$
4: $[P_{4444}]CH_3O(H)PO_2$
5: $[P_{4448}]\ CH_3CO_2$
6: $[C_2mim]CH_3CO_2$
7: $[C_2mim]CF_3CO_2$
8: $[C_2mim]CH_3O(H)PO_2$
9: $[C_2mim]CH_3SO_3$
10: $[C_2mim]N(CN)_2$
11: $[C_2mim]CF_3SO_3$
12: $[P_{4444}]\ CH_3CO_2$
13: $[P_{4448}]\ CF_3CO_2$
14: $[Mor_{14}]\ CF_3CO_2$
15: $[Pip_{14}]\ CF_3CO_2$
16: $[P_{4444}]\ N(CN)_2$
17: $[C_2mim]BF_4$
18: $[C_2mim]\ [Tf_2N]$

Selective Dissolution of Biomass with Ionic Liquids, Fig. 5 Effect of polarity of ionic liquids on the solubilization of soda lignin. The number related to the ionic liquids which can dissolve soda lignin is marked in red. Those cannot were plotted in black

S

depicted as numbers in red in Fig. 5. Namely, those with numbers 1–10 were confirmed to dissolve soda lignin under this condition. Other eight ionic liquid species could not dissolve soda lignin. It is obvious that there is a borderline between these two groups. In other words, different from the case of cellulose dissolution, soda lignin was soluble in some ionic liquids having two related parameters. When ionic liquids with very large β value were prepared, they could dissolve soda lignin even small α value such as entry 5 in Fig. 5. On the other hand, those with relatively small β value could dissolve soda lignin only when α value should be large like entries 7, 9, and 10 in the same figure. Figure 5 is quite helpful to preliminarily evaluate the ability of ionic liquids to dissolve soda lignin. In other words, solubility of soda lignin can be controlled by selecting proper counter ion even when cation or anion was fixed as components of ionic liquids used.

Effect of Water

There is an interesting effect of water addition on the dissolution of soda lignin. A series of ionic liquids containing $CH_3O(H)PO_2$ anion could dissolve certain amount of soda lignin. Some of them showed not so excellent solubility, but the solubility increased by the addition of water as seen in Fig. 6. As in the case of $[P_{4444}]$ $CH_3O(H)PO_2$, the soda lignin solubility was less than 3 wt %, but it reached more than 7 wt% after adding 20 wt% water (see Fig. 6, closed black square). Since pure water is a poor solvent for lignin, the solubility decreased by the addition of more amount of water. In some cases, the soda lignin dissolution ability was found only after adding water to moderately polar ionic liquids such as 1-ethyl-3-methylimidazolium trifluoromethanesulfonate ($[C_2mim]CF_3SO_3$). Pure $[C_2mim]CF_3SO_3$ can dissolve no soda lignin, but it becomes possible after adding 10 wt% water. The β value of $[C_2mim]CF_3SO_3$ was 0.47. When both $[C_2mim]BF_4$ and $[C_2mim][Tf_2N]$ were used (their β value was 0.37 and 0.23, respectively), no improvement on the soda lignin dissolution was found after addition of any amount of water. It is clear that the positive effect of water addition to improve soda lignin dissolution ability can be seen only when these ionic liquids have certain polarity.

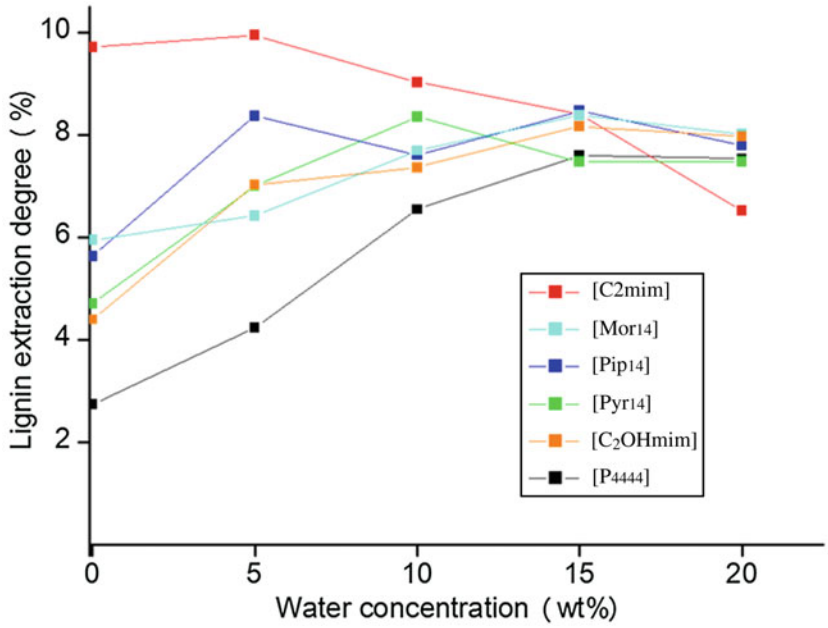

Selective Dissolution of Biomass with Ionic Liquids, Fig. 6 Effect of water content of a series of ionic liquids on the dissolution degree of soda lignin in them. In this study, anion species was fixed to $CH_3O(H)PO_2$

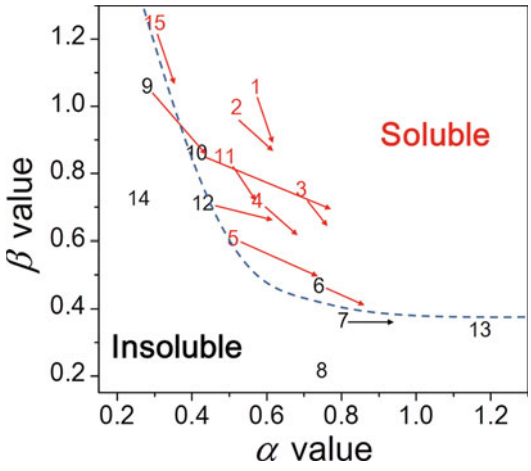

1: $[C_2mim]CH_3CO_2$
2: $[C_2mim]CH_3O(H)PO_2$
3: $[C_2mim]CF_3CO_2$
4: $[C_2mim]CH_3SO_3$
5: $[C_2mim]N(CN)_2$
6: $[C_2mim]CF_3SO_3$
7: $[C_2mim]BF_4$
8: $[C_2mim][Tf_2N]$
9: $[P_{4444}]CF_3CO_2$
10: $[Pip_{14}]CF_3CO_2$
11: $[Pyr_{14}]CF_3CO_2$
12: $[Mor_{14}]CF_3CO_2$
13: $[C_2OHmim][Tf_2N]$
14: $[P_{4444}]N(CN)_2$
15: $[P_{4444}]$ $CH_3O(H)PO_2$

Selective Dissolution of Biomass with Ionic Liquids, Fig. 7 Effect of water addition (10 wt%) on the solubilization of soda lignin in a series of ionic liquids [12] (with permission of Royal Society of Chemistry). Red and black numbers mean that these ionic liquids can and cannot dissolve lignin, respectively. Red arrows mean the changes of polarity parameters after adding water

Figure 7 summarizes the effect of water addition on the solubilization of soda lignin in a series of ionic liquids [12]. As shown in Fig. 7, it is clear that the addition of water changed the polarity parameters of the ionic liquids. Generally α value increased and β value decreased by the addition of water. The point is that some ionic liquids gain the solubilization ability of lignin in spite of decreasing in β value; α value increased to cross the border (see dashed blue line in Fig. 7) from insoluble region to soluble region by water addition. For example, in case of $[P_{4444}]CF_3CO_2$, this ionic liquid has no power to dissolve soda lignin, but the lignin turned soluble after adding water to this ionic liquid (see Fig. 7, #9). We firstly found such experimental results of enhanced solubility, but we could not explain the reason why lignin turned soluble after adding water. Water is a poor solvent for lignin. Results shown in Fig. 7 considerably helped us to understand the effect of polarity change on the solubility change of ionic liquids after water addition. In small conclusion, water addition is quite effective to add a power to dissolve lignin to some ionic liquids only when the polarity changed to cross the border shown in Fig. 7.

Effect of Hydrogen Peroxide

It is known that the addition of hydrogen peroxide (H_2O_2) aqueous solution is a typical oxidation agent and has bleaching power. So it is easy to think that the addition of H_2O_2 to polar ionic liquids accelerates the dissolution of lignin. Addition of H_2O_2 aqueous solution to a series of carboxylate-type ionic liquids certainly improved the solubility of lignin. So we challenged to dissolve Klason lignin with polar ionic liquids. Klason lignin powder was preliminarily treated in an aqueous solution containing 20 wt% H_2O_2. After 2 h treatment with H_2O_2, solubility of Klason lignin in $[C_2mim]CH_3CO_2$ at 80 °C was improved. As seen in Fig. 8, solubility was improved in some polar ionic liquids. Here in Fig. 8, numbers and closed circles printed in red mean Klason lignin was partly soluble in pure ionic liquids at 80 °C. Font size means solubility of Klason lignin, for example, the solubility in $[N_{2222}]CH_3CO_2$ (#4 in Fig. 8) was considerably improved by the pretreatment with H_2O_2. Dissolution ability of these ionic liquids was not only the function of polarity such as α and β values but also the cation species. This can be comprehended to be due to the steric effect of cations to affect the interaction between anions and (may be hydroxyl groups of) lignin.

It is noteworthy that the most hardly soluble Klason lignin was solubilized in ionic liquid below 100 °C. The improved solubility of Klason lignin was also found when mixtures of polar acetate-type ionic liquids and H_2O_2 aqueous solution were used. However, it is known that the addition of H_2O_2 aqueous solution to carboxylic acids such as acetic acid generates peracetic acid. This peracetic acid has bleaching power but is explosive. So the mixture of carboxylate-type

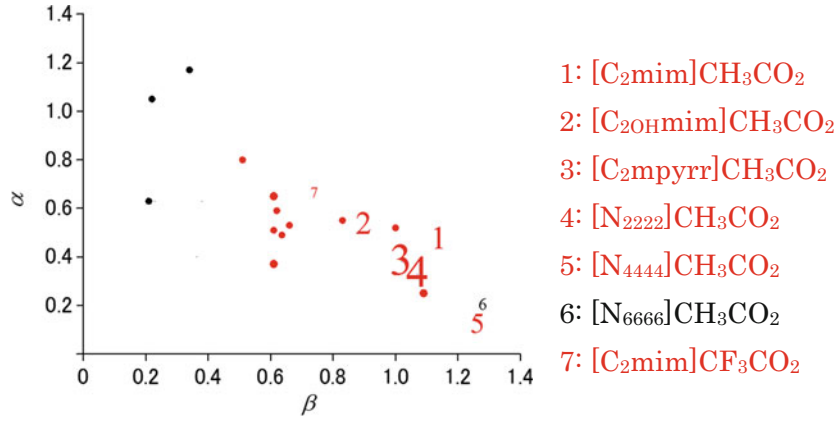

Selective Dissolution of Biomass with Ionic Liquids, Fig. 8 Effect of cation species on the solubility of Klason lignin (pretreated in 20 wt% H_2O_2 aqueous solution for 2 h) in a series of ionic liquids at 80 °C. Larger font size means better solubility of Klason lignin

ionic liquids with H_2O_2 is not suitable for ordinary use as a solvent. Instead of acetates, some other anions were studied not to form explosive mixtures. Some of phosphonate type ionic liquids such as $[C_2mim](MeO)(H)PO_2$ form stable mixture with H_2O_2, because phosphates are known as one of stabilizers of H_2O_2. We have examined solubilization of Klason lignin with the mixtures of phosphate-type ionic liquids and H_2O_2. Their Klason lignin dissolution ability was not better than acetates, but they were found to be stable solvents for Klason lignin. Further design of cations of phosphate-type ionic liquids should be needed to improve the dissolution ability of lignin.

Dissolution and Extraction of Lignin from Plant Biomass

Based on the results obtained above, we tried to extract lignin directly from biomass. Cedar wood powder was used as typical biomass, and the powder was added to $[C_2mim]CH_3CO_2$ to reach the final concentration of 5.0 wt%. About 4% of lignin was extracted from cedar powder in $[C_2mim]CH_3CO_2$ at 80 °C. On the other hand, 25% of lignin was extracted under the same condition from cedar powder pretreated with 20 wt% H_2O_2 aqueous solution for 2 h. It was obvious that the pretreatment with H_2O_2 aqueous solution was effective to enhance the extraction degree of lignin from biomass. However, there remains fear of explosion depending on the ionic liquid species. Furthermore, dissolution of cellulose was also found by this treatment, so that other candidate should be searched to enhance the solubility of lignin.

Dissolution of Plant Biomass in Ionic Liquids Derivatives

Dissolution of Lignin in Organic Onium Hydroxide Aqueous Solution

There are some discussions on the effect of anions on the dissolution of major components of biomass. Chloride anion has already been recognized to be potential component ions for ionic liquids to dissolve cellulose and lignin. For further search on effective anions to design ionic liquids as potential solvents for biomass, we have discussed on the anion size. Small anions are empirically recognized to be effective for biomass dissolution. Bromide anion was found to be effective but less powerful than chloride anion. Then hydroxide anion was newly proposed. Of course organic onium hydroxides are not ionic liquids but strong base. However, we have examined the dissolution of cellulose in organic onium hydroxide such as tetrabutylphosphonium hydroxide (($[P_{4444}]OH$): TBPH) aqueous solution to find the excellent solubility of cellulose in this alkaline solution [5]. Solubility of cellulose in this organic onium hydroxide solution was found to be much more than that in NaOH aqueous solution [13].

The NaOH aqueous solution needed to cool it down to around 0 °C to dissolve cellulose, but maximum concentration to be dissolved was less than 10 wt%. Against this, TBPH aqueous solution containing 40 wt% water could dissolve 20 wt% cellulose under stirring at room temperature for only 5 min [14]. Through a series of experiments, dissolution and/or swelling of wood chips was found by simply soaking them into TBPH aqueous solution [13–16].

Dissolution of Biomass in Organic Onium Hydroxide Aqueous Solution

Dissolution (or at least swelling) of whole wood chips meant (partial) solubilization of lignin by the TBPH aqueous solution. Since it is not easy to break the cross-links of lignin under mild condition, there seems to be a small amount of uncross-linked lignin which can be solubilized by this solution. Some of cross-links can be broken by soaking them in this solution for relatively longer time. Effectiveness of hydroxide anions on the dissolution of lignin was confirmed by comparing a series of onium hydroxide aqueous solutions. As mentioned above, alkali lignin and Klason lignin are used as typical extremes of lignin, i.e., former is relatively easy to dissolve and latter is not. Table 2 shows the maximum solubility of both lignin samples in a series of onium hydroxide aqueous solutions. It is obvious that alkali lignin was easily dissolved in all onium hydroxide aqueous solutions applied here just by simple stirring for 30 min without heating. This means that the OH^- has power to dissolve lignin. On the other hand, little solubility was found when Klason lignin was examined. This big difference is attributed to both different molecular weight and degree of cross-linking of the lignin. In spite of small number in Table 2, left column, it was surprising to find that Klason lignin was partly solubilized in these aqueous solution at 60 °C. In case of 60 wt% TBPH aqueous solutions (Nw = 10, in Table 2), 3 wt% Klason lignin was found to be dissolved. Increase in the water content decreased the solubilization power, for example, 36 wt% TBPH aqueous solution (Nw = 25, in Table 2) has no power to dissolve Klason lignin. The solubility was further improved by the addition of H_2O_2 aqueous solution. The positive effect of H_2O_2 aqueous solution on the dissolution of Klason lignin was also found here.

Selective Dissolution of Biomass with Ionic Liquids, Table 2 Maximum amount of Klason lignin and alkali lignin solubilized in a series of onium hydroxide aqueous solutions

Cation	Nw[a]	Maximum solubility (wt%)	
		Klason lignin (60 °C, 24 h)	Alkali lignin (r.t., 30 min)
$[P_{4444}]$	10	3	40
	25	0	40
	40	–[b]	30
$[Pyr_{14}]$	10	1	40
	25	0	30
	40	–[b]	20
$[Mor_{14}]$	10	0	40
	25	0	20
	40	–[b]	20

[a]Nw: water/hydroxide anion ratio (mol/mol)
[b]Not evaluated

Is Water Addition Effective to Separate Cellulose and Lignin After Dissolution of Woody Biomass?

As has been previously reported, TBPH aqueous solution can effectively solubilize (or swell) woody biomass under mild condition [13]. Experimental steps are schematically shown in Fig. 9. As mentioned above, hydrogen peroxide aqueous solution was also added to promote the dissolution of wood powder [17, 18]. Point of this section is the change of solution property of TBPH aqueous solution for selective dissolution of the biomass components.

Dissolution of woody biomass has been carried out according to our previous report [17]. Hydrogen peroxide aqueous solution was mixed with TBPH aqueous solution. Then cedar powder, used as a model of woody biomass, was added to this aqueous solution (5.0 wt%), and the mixture was stirred gently at 60 °C. After removal of residue by centrifugation (10,000 G, 10 min), more than 80% of the powder was confirmed to be solubilized in this solution. Some higher molecular weight and cross-linked lignin fraction were remained insolubilized. Then this mixture was filtered and removed the remained solid

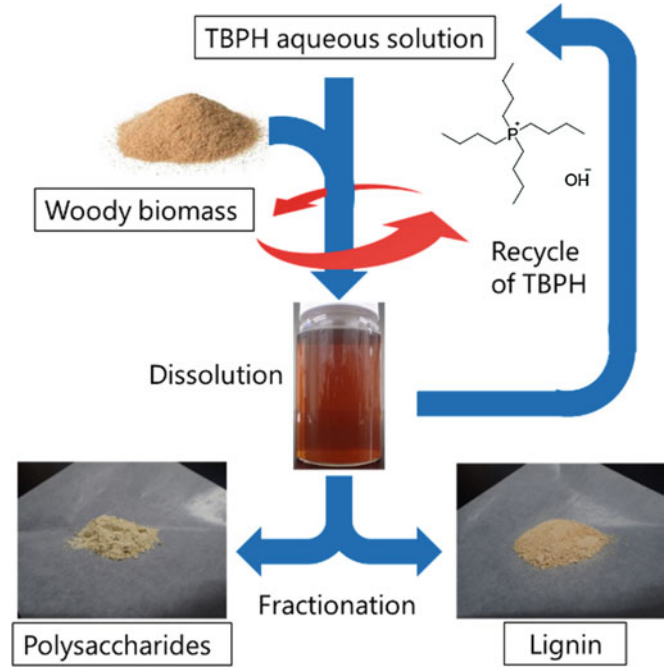

Selective Dissolution of Biomass with Ionic Liquids, Fig. 9 Schematic diagram of dissolution of biomass with TBPH aqueous solution. After suitable treatments, polysaccharides and lignin fraction are easily separated

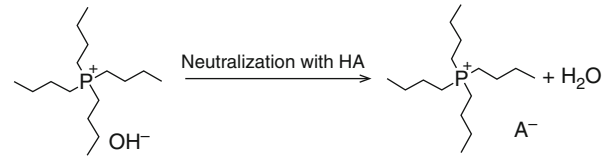

Selective Dissolution of Biomass with Ionic Liquids, Fig. 10 Switching solubility power by the counter anion exchange of TBPH

Solubility of cellulose: ☺ ☹
Solubility of lignin: ☺ ☺

fraction. Then, the supernatant was neutralized with hydrochloric acid. This step is quite important to change the solvent properties from organic onium hydroxide aqueous solution to ionic liquid/water mixture. As seen in Fig. 10, it is easy to convert the properties of these mixed solutions; just add acids to neutralize the TBPH aqueous solution. TBPH aqueous solution (left) has power to dissolve both polysaccharide and lignin, but only lignin can be soluble in the neutralized aqueous salt solution such as $[P_{4444}]Cl$ containing certain amount of water (right). As previously shown in Fig. 7, suitable amount of water is essential to solubilize lignin. More or less amount of water do not work to dissolve lignin, and the suitable amount of water deeply depended on the ionic liquid species used.

As expected, polysaccharides dissolved in TBPH aqueous solution were selectively precipitated after the neutralization. This is well comprehended to be the change of solvent properties, because ionic liquid/water mixture is a poor solvent for polysaccharides but is still a good solvent for lignin. As shown in Fig. 10, it is easy to switch the solubility power of THPB aqueous solution by switching counter anions. The precipitated polysaccharides were collected using centrifugation and washed with water. Lignin was dissolved in the ionic liquid ($[P_{4444}]Cl$) aqueous solution, and the dissolved lignin can be

precipitated further by the addition of poor solvent such as ethanol or water. The precipitated lignin was collected using centrifugation and washed with water. Obtained polysaccharides and lignin were dried in vacuo. Yield of polysaccharides and lignin was calculated according to their mass balance.

As a result, both polysaccharides and lignin were selectively obtained with high yield. After collecting dissolved compounds in $[P_{4444}]Cl$ aqueous solution, the aqueous solution was converted into TBPH aqueous solution again by passing through column filled with anion exchange resin. Structural characterization of TBPH was carried out with ^1H NMR, and no significant degradation was confirmed to occur during the treatment. Since TBPH aqueous solution was recyclable after anion exchange from X^- to OH^-, this procedure is quite useful to extract both lignin and polysaccharides from woody biomass and then separate dissolved lignin from precipitated polysaccharides.

Conversion of Lignin to Valuable Compounds

Since lignin is known to be highly cross-linked aromatic polymers, their fragments should be potential candidates for aromatic compounds. A few aromatic compounds such as vanillin, vanillic acid, and p-hydroxybenzaldehyde were found in the heat treated TBPH aqueous solution after dissolution of lignin. This strongly suggests that the TBPH aqueous solution is also a potential solvent to convert lignin into aromatic molecules [18, 19]. Yield of vanillin and vanillic acid from lignin was 21% and 1.7% (lignin-based value) when Japanese cedar powder was dissolved in TBPH aqueous solution and heated 120 °C for 72 h [20]. Many other aromatic compounds can be prepared from lignin or even biomass with the aid of TBPH aqueous solution. Effect of cation structure on the conversion performance is under progress.

Conclusion

Design of component ions of ionic liquids enables enhancement of dissolution power of biomass. In this entry, we report possible way to selectively dissolve biomass components with the aid of ionic liquids under mild condition. Performance of the selective dissolution and/or separation of components of biomass is possible but still not 100%, so that there are strong demands to accelerate structural design of the ionic liquids suitable for selective dissolution of biomass.

Cross-References

- ▶ Depolymerization of Lignin by Catalytic Oxidation in Ionic Liquids
- ▶ Design of Amino Acid ILs for Dissolution of Lignocellulosic Biomass
- ▶ Design of Functional Imidazolium-Based Ionic Liquids for Biomass Processing

References

1. Graenacher C (1934) Cellulose solution. US Patent No. 1,943,176
2. Swatloski RP, Spear SK, Holbrey JD, Rogers RD (2002) Dissolution of Cellose with Ionic Liquids. J Am Chem Soc 124:4974
3. Mizumo T, Marwanta E, Matsumi N, Ohno H (2004) Allylimidazolium Halides as Novel Room Temperature Ionic Liquids. Chem Lett 33:1360
4. Zhang H, Zhang WJ, He J (2005) 1-Allyl-3-methylimidazolium Chloride Room Temperature Ionic Liquid: A New and Powerful Nonderivatizing Solvent for Cellulose. Macromolecules 38:8272
5. Heinze T, Schwikal K, Barthel S (2005) Ionic Liquids as Reaction Medium in Cellulose Functionalization. Macromol Biosci 5:520
6. Crowhurst L, Mawdsley PR, Perez-Arlandis JM, Salter PA, Welton T (2003) Solvent–solute interactions in ionic liquids. Phys Chem Chem Phys 5:2790
7. Baker SN, Baker GA, Bright FV (2002) Temperature-dependent microscopic solvent properties of 'dry' and 'wet' 1-butyl-3-methylimidazolium hexafluorophosphate: correlation with ET(30) and Kamlet–Taft polarity scales. Green Chem 4:165
8. Fukaya Y, Sugimoto A, Ohno H (2006) Superior Solubility of Polysaccharides in Low Viscosity, Polar, and Halogen-Free 1,3-Dialkylimidazolium Formates. Biomacromolecules 7:3295
9. Himmler S, Hörmann S, Hal RV, Schulz PS, Wasserscheid P (2006) Transesterification of methylsulfate and ethylsulfate ionic liquids—an environmentally benign way to synthesize long-chain and functionalized alkylsulfate ionic liquids. Green Chem 8:887

10. Fukaya Y, Hayashi K, Wada M, Ohno H (2008) Cellulose dissolution with polar ionic liquids under mild conditions: Required factors for anions. Green Chem 10:44
11. Abe M, Fukaya Y, Ohno H (2010) Extraction of polysaccharides from bran with phosphonate or phosphinate-derived ionic liquids under short mixing time and low temperature. Green Chem 12:1274
12. Akiba T, Tsurumaki A, Ohno H (2017) Induction of lignin solubility for a series of polar ionic liquids by the addition of a small amount of water. Green Chem 19:2260
13. Abe M, Yamada T, Ohno H (2014) Dissolution of wet wood biomass without heating. RSC Adv 4:17136
14. Abe M, Fukaya Y, Ohno H (2012) Fast and facile dissolution of cellulose with tetrabutylphosphonium hydroxide containing 40 wt% water. Chem Commun 48:1808
15. Abe M, Yamanaka S, Yamada H, Yamada T, Ohno H (2015) Almost complete dissolution of woody biomass with tetra-n-butylphosphonium hydroxide aqueous solution at 60 °C. Green Chem 17:432
16. Abe M, Kuroda K, Ohno H (2015) Maintenance-free cellulose solvents based on onium hydroxides. ACS Sus Chem Eng 3:1771
17. Yamanaka S, Yoshioka K, Miyafuji H, Ohno H (2017) Effect of hydrogen peroxide on the extraction of components of cedar powder with tetrabutylphosphonium hydroxide aqueous solution at 60 °C. Aust J Chem 70:322
18. Yamada H, Miyafuji H, Ohno H, Yamada T (2017) Rapid and complete dissolution of softwood biomass in tetra-n-butylphosphonium hydroxide with hydrogen peroxide. Bioresources 12:4515
19. Yamamoto K, Hosoya T, Yoshioka K, Miyafuji H, Ohno H, Yamada T (2017) Tetrabutylammonium hydroxide 30-hydrate as novel reaction medium for lignin conversion. ACS Sus Chem Eng 5:10111
20. Maeda M, Hosoya T, Yoshioka K, Miyafuji H, Ohno H, Yamada T (2018) Vanillin production from native soft wood lignin in the presence of tetrabutylammonium ion. J Wood Sci 64:810

SIL, Supported Ionic Liquid

▶ Immobilization of Ionic Liquids, Types of Materials, and Applications

SILLP, Supported Ionic Liquid-Like Phase

▶ Immobilization of Ionic Liquids, Types of Materials, and Applications

SILP, Supported Ionic Liquid Phase

▶ Immobilization of Ionic Liquids, Types of Materials, and Applications

Solubility of Polymers in Ionic Liquids

Jinming Zhang, Chenyang Liu and Jun Zhang
CAS Key Laboratory of Engineering Plastics, Institute of Chemistry, Chinese Academy of Sciences, Beijing, China

Introduction

As ambient temperature molten salts, ionic liquids (ILs) have attracted considerable attention, due to their unique properties such as nonvolatility, nonflammability, excellent stability, high ion conductivity, and strong solvating power. In particular, ILs exhibit high flexibility in designing cationic and anionic structures and their combinations, thus their properties can be manipulated in principle as required. ILs have been generally regarded as the "designer solvents" or "the third liquid," following conventional water and organic solvents. ILs are useful in many chemical applications. For example, ILs are capable of dissolving complex macromolecules and polymeric materials with high efficiency, and then a further chemical transformation or materials processing step can be carried out [1–5]. ILs offer new progress, challenges, and opportunities in polymer materials science.

The dissolution of polymers in ILs is complex and not readily predicted due to multiple solute-solvent interactions. The solubility parameter (SP, or Hildebrand parameter) δ, based on the paradigm of "like dissolves like," which has frequently been applied to account for the solubility of polymers in organic solvents, cannot serve as a qualitative guide for predicting polymer solubility in ILs [4, 5]. Because there are multiple interactions

between polymers and ILs, including coulombic interactions, hydrogen-bonding interactions, van der Waals interactions, and cation-π interactions, which play an important role in controlling the solubility of polymer solutes in ILs. For example, the solubilities of poly(methyl methacrylate) (PMMA, SP = 18.3 $Mpa^{1/2}$) are quite different in three ILs ($[C_4mim][NTf_2]$, $[C_6mim]PF_6$, and $[C_8mim]BF_4$) that have essentially identical solubility parameters (21.5–22.0 $MPa^{1/2}$) [6]. On the other hand, PMMA has good solubilities in $[C_4mim][NTf_2]$, while polystyrene (PS), which has a similar SP value (18.6 $MPa^{1/2}$) with PMMA, is incompatible with $[C_4mim][NTf_2]$ [4].

Dissolution of Biopolymers in Ionic Liquids

It is interesting to discover that some ILs can effectively dissolve hard-to-dissolve biopolymers, including polysaccharides, lignin,

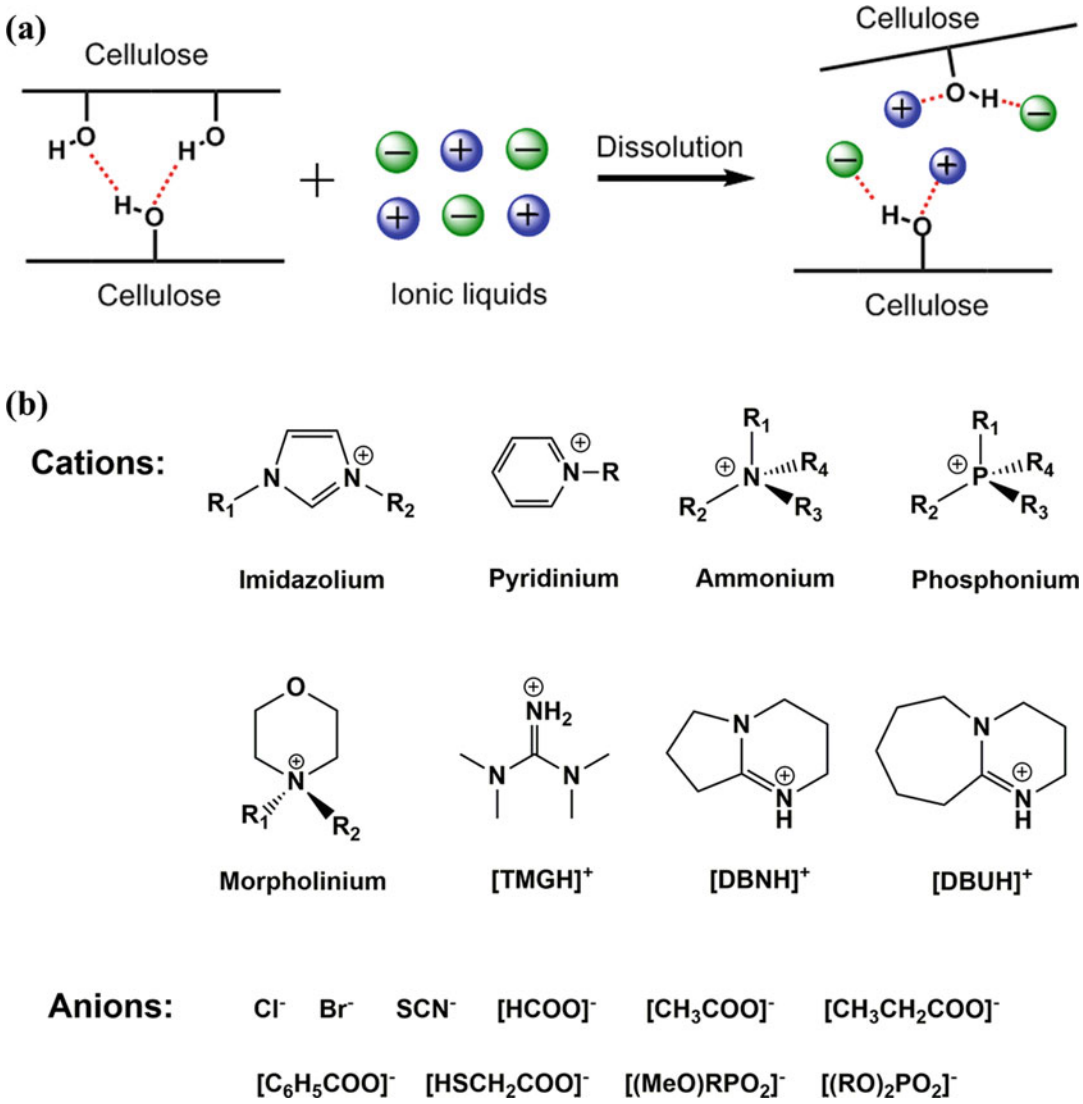

Solubility of Polymers in Ionic Liquids, Fig. 1 (**a**) Dissolution mechanism of cellulose in ILs [25]; (**b**) Cation and anion structures of typical ionic liquids for dissolving cellulose [7]

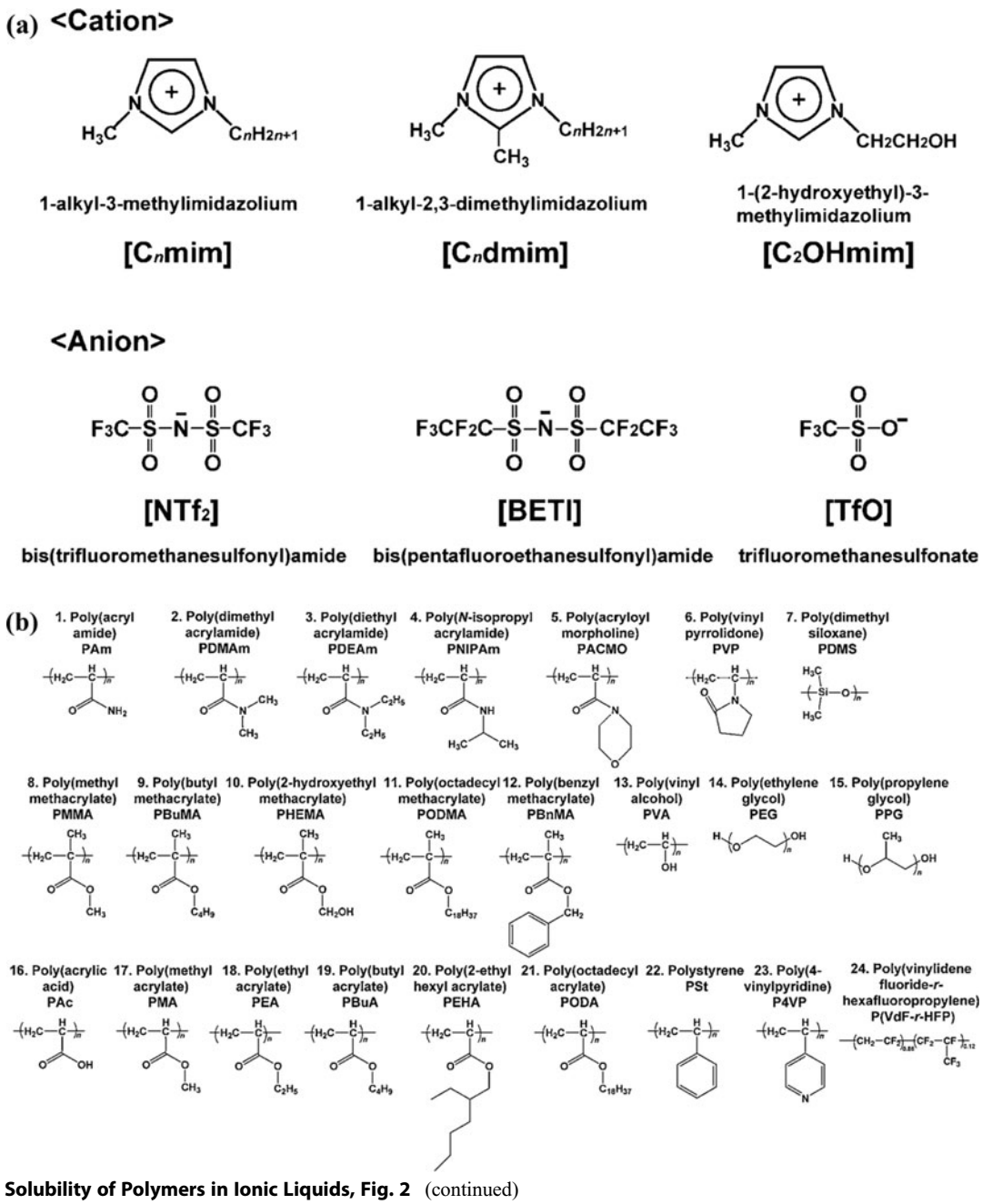

Solubility of Polymers in Ionic Liquids, Fig. 2 (continued)

(c)

Entry No.	1	2	3	4	5	6	7	8
Polymer	PAm	PDMAm	PDEAm	PNIPAm	PACMO	PVP	PDMS	PMMA
SP/(cal cm^{-3})$^{1/2}$	27.1[37]	18.1[37]	10.5[38]	19.8[37]	n.d.	14.7[39]	7.4[40]	8.9[30]
[C_2mim][NTf_2]	UCST	Yes	Yes	UCST	Yes	Yes	Yes	Yes
[C_4mim][NTf_2]	UCST	Yes	Yes	UCST	Yes	Yes	Yes	Yes
[C_4mim]PF_6	No	Yes	Yes	UCST	Yes	Yes	Yes	Yes
[C_2mim]BF_4	No	Yes	No	UCST	No	Yes	No	No
Entry No.	9	10	11	12	13	14	15	16
Polymer	PBuMA	PHEMA	PODMA	PBnMA	PVA	PEG	PPG	PAc
SP/(cal cm^{-3})$^{1/2}$	9.0[30]	16.8[41]	7.8[30]	n.d.	10.6[42]	9.8[43]	8.0[44]	n.d.
[C_2mim][NTf_2]	Yes	No	UCST	LCST	No	Yes	No	No
[C_4mim][NTf_2]	Yes	No	UCST	LCST	No	Yes	No	No
[C_4mim]PF_6	Yes	No	UCST	LCST	No	Yes	No	No
[C_2mim]BF_4	No	Yes	UCST	No	No	UCST	LCST	No
Entry No.	17	18	19	20	21	22	23	24
Polymer	PMA	PEA	PBuA	PEHA	PODA	PSt	P4VP	P(VdF-*r*-HFP)
SP/(cal cm^{-3})$^{1/2}$	8.9[30]	8.9[30]	10.0[30]	9.0[30]	n.d.	9.1[30]	5.9[45]	n.d.
[C_2mim][NTf_2]	Yes	Yes	Yes	Yes	UCST	No	No	UCST (sol–gel)
[C_4mim][NTf_2]	Yes	Yes	Yes	Yes	UCST	No	No	UCST (sol–gel)
[C_4mim]PF_6	Yes	Yes	Yes	Yes	UCST	No	No	UCST (sol–gel)
[C_2mim]BF_4	Yes	Yes	Yes	No	UCST	No	No	UCST (sol–gel)

a) Yes and No indicate compatible and incompatible, respectively. Numbers indicated by superscripts express

Solubility of Polymers in Ionic Liquids, Fig. 2 (**a**) Chemical structure of ILs with different cations and anions [4]; (**b**) Chemical structure of synthetic polymers [4]; (**c**) Solubility of conventional polymers in four ILs [4]

lignocellulose, and proteins, thereby providing an available, versatile, and fascinating platform for processing these natural resources [7–12]. The disruption of the hydrogen bonding network in biopolymers is crucial for their dissolution (Fig. 1a). Thus, the hydrogen bonding capabilities of the anions and cations in ILs play a predominant role in the solubility of biopolymers.

Take cellulose, for example, Swatloski et al. discovered that 1-butyl-3-methylimidazolium chloride (BmimCl) had a high dissolving capability of up to 10 wt% concentration of cellulose by heating, and to 25 wt% by microwave-assisted heating [13]. The ILs with higher hydrogen-bonding capability, such as 1-ethyl-3-methylimidazolium acetate (EmimAc) and 1,3-dialkylimidazolium formate, are more powerful solvents for cellulose [14, 15]. In addition, the low viscosity is beneficial to the cellulose dissolution. Compared with BmimCl, 1-allyl-3-methylimidazolium chloride (AmimCl), and EmimAc have lower melting points and viscosities, and higher dissolving capability. By using AmimCl or EmimAc as the solvent, a solution containing up to 30 wt% cellulose with a degree of polymerization (DP) as high as 650 was readily prepared in only 30 min [7]. Moreover, the addition of polar and aprotic co-solvents (DMAc, DMSO, DMF, etc.) to ILs can enhance their solvating power, because these co-solvents decrease the solvent viscosity without significant influence on the specific interactions between ILs and cellulose [16–19]. In contrast, the addition of protic co-solvents, such as water and ethanol, dramatically worsens the dissolving capability. So far, many ILs have been found to dissolve cellulose (Fig. 1b). The dissolving capability of ILs follows

the order of imidazolium-based ILs > pyridinium-based ILs > ammonium-based ILs, and carboxylate-based ILs > alkylphosphate-based ILs > halide-based ILs. The most favorite and typical ILs are AmimCl, BmimCl, and EmimAc. Via two high-throughput screening tests, Zavrel et al. indicated that EmimAc was the most efficient one for dissolving cellulose, and AmimCl for dissolving wood chips [20]. Based on a similar mechanism, many studies have been conducted on the solubilization of other hard-to-dissolve biopolymers such as silk, wool, keratin, chitosan, and chitin in ILs [8–12, 21–24].

Dissolution of Synthetic Polymers in Ionic Liquids

Winterton et al. screened the solubilities of 17 different polymers in three different ILs, 1-ethyl-3-methylimidazolium tetrafluoroborate ($[C_2mim]BF_4$), 1-butyl-3-methylimidazolium hexafluorophosphate, ($[C_4mim]PF_6$), and 1-octyl-3-methylimidazolium bis(trifluoromethanesulfonyl) amide ($[C_8mim][NTf_2]$) (Fig. 2a), and concluded that $[C_8mim][NTf_2]$ was the most effective solvent for a series of polymers [26]. Ueki et al. summarized the solubility of 24 synthetic polymers in four

(a)

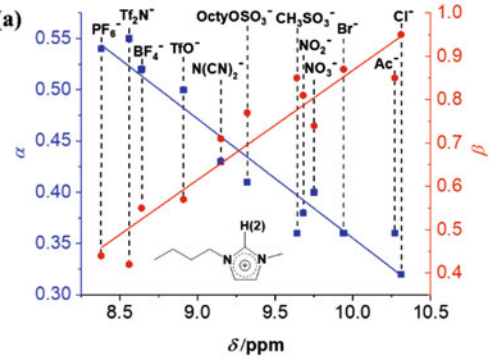

(b)

Ionic Liquids	α		β	
$[C_4mim]PF_6$	0.67	0.63	0.19	0.19
$[C_4mim][Tf_2N]$	0.69	0.64	0.25	0.25
$[C_8mim][Tf_2N]$	-	0.60	-	0.29
$[C_8mim]BF_4$	-	0.62	-	0.41
$[C_4mim]BF_4$	0.64	0.63	0.41	0.37
$[C_8mim]PF_6$	0.58	-	0.46	-
$[C_4mim][TfO]$	0.62	0.62	0.46	0.49
[Amim]Br	0.50	-	0.66	-
$[C_4mim]Cl$	0.45	-	0.83	-
[Amim]Cl	0.47	-	0.84	-
$[C_2mim]Ac$	0.51	-	0.99	-

(c)

Structure of Polymer	Name of Polymer	Abbreviation	α_p	β_p	π^*
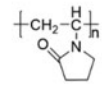	Poly(vinyl pyrrolidone)	PVP	0.01	0.93	0.93
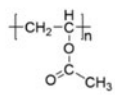	Poly(vinyl acetate)	PVAc	0.00	0.40	0.77
	Polystyrene	PS	0.08	0.06	0.65
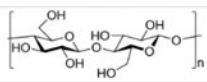	Microcrystalline cellulose	MCC	1.31	0.62	0.34
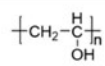	Poly(vinyl alcohol)	PVA	0.66	0.52	1.11
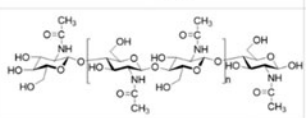	Chitin	-	0.67	0.86	0.91

Solubility of Polymers in Ionic Liquids, Fig. 3 (continued)

(d)

No.	ILs	[C_2mim][Ac]	[Amim][Cl]	[C_4mim][Cl]	[Amim][Br]	[C_4mim][TfO]	[C_8mim][PF_6]	[C_4mim][BF_4]	[C_8mim][BF_4]	[C_8mim][Tf_2N]	[C_4mim][Tf_2N]	[C_4mim][PF_6]
	α_+	0.51	0.47	0.45	0.50	0.62	0.58	0.64	0.62	0.60	0.69	0.67
1	PS (β_P= 0.06)	○, 400	○, 304	○, 285	○, 252	○, 216	○, 200	○, 196	○, 189	○, 120	○, 116	○, 77
2	PDMS	○	○	○	○	○	○	○	○	●	○	○
3	BAPC (β_P= 0.21)	●, 421	○, 315	○, 298	○, 239	○, 163	○, 153	○, 134	○, 130	○, 50	○, 29	○, -14
4	PTT	○	○	○	○	○	○	○	○	○	○	○
5	PET	○	○	○	○	○	○	○	○	○	○	○
6	PBS	○	○	○	○	◓	◓	○	◓	○	◓	◓
7	PMMA (β_P= 0.38)	○, 311	○, 216	○, 203	○, 140	●, 50	●, 46	○, 19	○, 19	●, -54	●, -90	●, -127
8	PVAc (β_P= 0.40)	○, 301	○, 207	○, 194	○, 130	●, 37	●, 35	○, 6	◓, 6	●, -66	●, -104	●, -141
9	PCL (β_P= 0.41)	○, 296	○, 202	○, 189	○, 125	○, 31	◓, 29	○, 0	○, 0	●, -72	◓, -110	○, -147
10	PBC	○	○	○	○	●	●	○	●	●	●	●
11	CTA (β_P= 0.45)	-[b]	○, 183	○, 171	○, 105	●, 6	●, 6	●, -26	●, -25	○, -96	●, -138	●, -174
12	PEO (β_P= 0.65)	○, 173	○, 89	○, 81	○, 5	●, -118	●, -110	●, -154	●, -149	●, -216	●, -276	●, -308
13	PVP (β_P= 0.93)	○, 30	○, -41	○, -44	●, -132	●, -287	●, -268	●, -328	●, -317	●, -378	●, -462	●, -488

No.	ILs	[C_2mim][Ac]	[Amim][Cl]	[C_4mim][Cl]	[Amim][Br]	[C_4mim][TfO]	[C_8mim][PF_6]	[C_4mim][BF_4]	[C_8mim][BF_4]	[C_8mim][Tf_2N]	[C_4mim][Tf_2N]	[C_4mim][PF_6]
	β_-	0.99	0.84	0.83	0.66	0.46	0.46	0.41	0.41	0.29	0.25	0.19
1	Cellobiose (α_P= 1.44)	●, -307	●, -175	●, -168	●, 0	○, 164	○, 172	○, 200	○, 205	○, 311	○, 308	○, 362
2	Amylopectin (α_P= 1.37)	●, -292	●, -171	●, -166	●, -9	○, 143	○, 150	○, 175	○, 180	○, 277	○, 272	○, 322
3	MCC (α_P= 1.31)	●, -296	●, -185	●, -181	○, -32	○, 110	○, 117	○, 141	○, 145	○, 234	○, 229	○, 275
4	CMC0.7 (α_P= 0.94)	●, -34	○, 33	○, 39	○, 110	○, 144	○, 162	○, 150	○, 160	○, 211	○, 165	○, 194
5	Amylose (α_P= 0.83)	●, -102	●, -61	●, -61	●, 3	○, 44	○, 53	○, 49	○, 55	○, 87	○, 59	○, 77
6	BC (α_P= 0.79)	●, -34	●, 10	●, 14	○, 61	○, 70	○, 86	○, 69	○, 78	○, 110	○, 62	○, 82
7	PAA	●	●	●	●	◓	○	○	○	○	○	○
8	PVA (α_P= 0.66)	●, -71	●, -61	●, -65	●, -22	○, 2	○, 5	○, 2	○, 4	○, 14	○, -8	○, -3
9	PAN	-[b]	●	●	●	○	○	○	○	○	○	○
10	PHEMA (α_P= 0.67)	●, -90	●, -82	●, -88	●, -39	●, -2	○, -3	◓, 1	◓, 1	○, 10	○, -4	○, 0
11	CA2.36 (α_P= 0.63)	●, -55	●, -50	●, -54	●, -17	●, 1	◓, 4	●, -1	●, 1	○, 7	◓, -17	◓, -14
12	Chitosan	●	○	○	○	○	○	○	○	○	○	○
13	Chitin (α_P= 0.67)	●, -21	○, 4	○, 7	○, 34	○, 20	○, 36	○, 14	○, 23	○, 40	○, -12	○, 0
14	CMC1.2 (α_P= 0.63)	●, -14	○, 5	○, 7	○, 27	○, 4	○, 21	○, -5	○, 5	○, 17	○, -37	○, -27

Solubility of Polymers in Ionic Liquids, Fig. 3 (**a**) Correlation of α (squares) and β (circles) with the ^{1}H-NMR chemical shift of H2 of [C_4mim]-type ILs [27]. (**b**) KAT parameters α and β for different ILs [27]. (**c**) KAT parameters α, β and π^* of typical polymers [27]. (**d**) Results of solubility tests and values[a] of QHB analysis for H-bond basicity polymers in different ILs [27]. (●: solubilization; ◓: solubilization at high temperatures only; ○: insolubilization. [a]QHB factor as $\Delta\alpha\Delta\beta \times 10^3$. [b]Decomposition in the IL at 120–150 °C)

ILs (Fig. 2b, c) [4]. The results indicate that the solubility of polymers in ILs is predominantly governed by the structure of the anion rather than that of the cation. The SP values do not prove useful in predicting the solubility of a polymer in an IL. In most cases, the paradigm of "like dissolves like" cannot serve as a qualitative guide for predicting polymer solubility in ILs, because of the multiple interactions between polymers and ILs.

Recently, Liu et al. demonstrated that the solubility of polymers in ILs was dominated by hydrogen-bonding complementary principle rather than "like dissolves like" principle [27]. According to Kamlet-Abraham-Taft (KAT) multiple polarity scale, ILs can be categorized as hydrogen bonding acidity or basicity ones. The dissolution experiment confirms that the acidity ILs easily dissolve the basicity polymers and basicity ILs dissolve acidity polymers, indicating the complementary nature of hydrogen bonding interactions (Fig. 3). The solubility of polymers in ILs can be predicted by a quantitative hydrogen-bonding (QHB) analysis, based on the KAT hydrogen-bonding donating or acidity parameter α, and hydrogen-bonding accepting or basicity parameter β. For instance, representative hydrogen-bonding basicity polymers, poly(vinyl pyrrolidone) (PVP: $\alpha_P = 0.01$, $\beta_P = 0.93$), and poly(vinyl acetate) (PVAc: $\alpha_P = 0.0$, $\beta_P = 0.40$) can be dissolved in hydrogen-bonding acidity ILs, e.g., [C_4mim][Tf_2N] ($\alpha_+ = 0.69$, $\beta_- = 0.25$), while is insoluble in hydrogen-bonding basicity ILs, e.g., [C_4mim]Cl ($\alpha_+ = 0.45$, $\beta_- = 0.83$). Representative hydrogen-bonding acidity polymers, microcrystalline cellulose (MCC: $\alpha_P = 1.31$, $\beta_P = 0.62$), poly(vinyl alcohol) (PVA, $\alpha_P =$

S

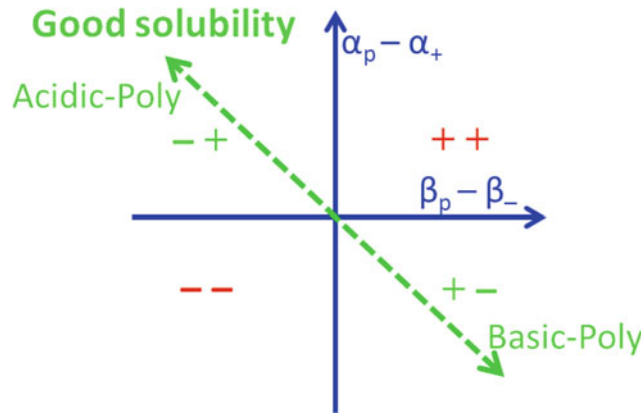

Solubility of Polymers in Ionic Liquids, Fig. 4 QHB analysis by a plot of $(\alpha_p - \alpha_+)$ vs $(\beta_P - \beta_-)$ [27]. Good solubility predicted in the second and fourth quadrants reflects the complementary nature of hydrogen-bonding acidity and basicity scales

0.66, $\beta_P = 0.52$), and chitin ($\alpha_P = 0.67$, $\beta_P = 0.86$) can be dissolved in strong hydrogen bonding basicity ILs, e.g., [C_2mim]Ac ($\alpha_+ = 0.51$, $\beta_- = 0.99$) or [C_4mim]Cl, while are insoluble in hydrogen-bonding acidity ILs, such as [C_4mim][Tf_2N]. Moreover, chitin has a higher β_P value than the β_- values of most ILs listed in Fig. 3, so only [C_2mim]Ac ($\beta_- = 0.99$) can dissolve it. In addition, the reference polymer, PS ($\alpha_P = 0.08$, $\beta_P = 0.06$) has neither hydrogen-bonding accepting capacity nor hydrogen-bonding donating capacity, so no IL solvents can be found for PS.

According to the new hydrogen-bonding complementary principle, a quantitative hydrogen bonding (QHB) analysis is further proposed (Fig. 4) [27]. Hydrogen-bonding acidity polymers, with $(\alpha_p - \alpha_+) > 0$ and $(\beta_P - \beta_-) < 0$, favor the formation of the cross-association hydrogen-bonding with basic ILs, hence their solubility region should appear in the upper-left (second) quadrant of plane coordinates. Similarly, the solubility region of hydrogen-bonding basicity polymers in acidic ILs should appear in the lower-right (fourth) quadrant, where $(\alpha_p - \alpha_+) < 0$ and $(\beta_P - \beta_-) > 0$. Moreover, the greater the acidity and basicity of the intermolecular hydrogen-bonding atoms, the stronger the hydrogen-bonding interactions would be, as indicated by the internal bisector crossing the second and fourth quadrants. So it is expected that the absolute value of the product of $(\alpha_p - \alpha_+)(\beta_P - \beta_-)$ is proportional to the solubility of polymers in ILs.

References

1. Winterton N (2006) Solubilization of polymers by ionic liquids. J Mater Chem 16:4281–4293
2. Ueki T, Watanabe M (2008) Macromolecules in ionic liquids: Progress, challenges, and opportunities. Macromolecules 41:3739–3749
3. Ueki T (2014) Stimuli-responsive polymers in ionic liquids. Polym J 46:646–655
4. Ueki T, Watanabe M (2012) Polymers in ionic liquids: dawn of neoteric solvents and innovative materials. Bull Chem Soc Jpn 85:33–50
5. Liu FY, Zhang JM, Zhang J, Zhang BQ, Liu CY (2012) Solubility of polymers in imidazolium ionic liquids. Polym Bull 10:99–110
6. Ueno K, Fukai T, Nagatsuka T, Yasuda T, Watanabe M (2014) Solubility of poly(methyl methacrylate) in ionic liquids in relation to solvent parameters. Langmuir 30:3228–3235
7. Zhang JM, Wu J, Yu J, Zhang XY, He JS, Zhang J (2017) Application of ionic liquids for dissolving cellulose and fabricating cellulose-based materials: state of the art and future trends. Mater Chem Front 1:1273–1290
8. Zhang T, Chen F, Gai QQ, Qu F, Zhang YK (2011) Ionic liquids and protein/nucleic acid interaction. Prog Chem 23:2132–2139
9. Schindl A, Hagen ML, Muzammal S, Gunasekera HAD, Croft AK (2019) Proteins in ionic liquids: reactions, applications, and futures. Front Chem 7:347
10. Schröder C (2017) Proteins in ionic liquids: current status of experiments and simulations. Top Curr Chem 375:25
11. Li LF, Hu YC (2015) Application of ionic liquids in lignin processing. Chem Ind For Prod 35:163–170
12. Zhu XY, Peng C, Chen HX, Chen Q, Zhao ZB, Zheng Q, Xie HB (2018) Opportunities of ionic liquids for lignin utilization from biorefinery. ChemistrySelect 3:7945–7962
13. Swatloski RP, Spear SK, Holbrey JD, Rogers RD (2002) Dissolution of cellose with ionic liquids. J Am Chem Soc 124:4974–4975

14. Zhang J, Ren Q, He JS (2002) CN Pat., ZL02155945
15. Fukaya Y, Sugimoto A, Ohno H (2006) Superior solubility of polysaccharides in low viscosity, polar, and halogen-free 1,3-dialkylimidazolium formates. Biomacromolecules 7:3295–3297
16. Rinaldi R (2011) Instantaneous dissolution of cellulose in organic electrolyte solutions. Chem Commun 47:511–513
17. Clough MT (2017) Organic electrolyte solutions as versatile media for the dissolution and regeneration of cellulose. Green Chem 19:4754–4768
18. Gale E, Wirawan RH, Silveira RL, Pereira CS, Johns MA, Skaf MS, Scott JL (2016) Directed discovery of greener cosolvents: new cosolvents for use in ionic liquid based organic electrolyte solutions for cellulose dissolution. ACS Sustain Chem Eng 4: 6200–6207
19. Xu AL, Cao LL, Wang BJ (2015) Facile cellulose dissolution without heating in [C4mim][CH3COO]/DMF solvent. Carbohydr Polym 125:249–254
20. Zavrel M, Bross D, Funke M, Buchs J, Spiess AC (2009) High-throughput screening for ionic liquids dissolving (ligno-)cellulose. Bioresour Technol 100: 2580–2587
21. Zhang LH, Wang JQ, Yang M, Ke N, Zhang B, Wang HO, Zheng Q, Xie HB (2019) Dissolution, materialization and derivatization of chitin and chitosan in ionic liquids. Sci Sin Chim 49:1059–1072
22. Shamshina JL, Berton P, Rogers RD (2019) Advances in functional chitin materials: a review. ACS Sustain Chem Eng 7:6444–6457
23. Zhong Y, Cai J, Zhang LN (2020) A review of chitin solvents and their dissolution mechanisms. Chin J Polym Sci 38:1047–1060
24. Kostag M, Jedvert K, El Seoud OA (2021) Engineering of sustainable biomaterial composites from cellulose and silk fibroin: fundamentals and applications. Int J Biol Macromol 167:687–718
25. Zhang JM, Zhang H, Wu J, Zhang J, He JS, Xiang JF (2010) NMR spectroscopic studies of cellobiose solvation in EmimAc aimed to understand the dissolution mechanism of cellulose in ionic liquids. Phys Chem Chem Phys 12:1941–1947
26. Snedden P, Cooper AI, Scott K, Winterton N (2003) Cross-linked polymer-ionic liquid composite materials. Macromolecules 36:4549–4556
27. Yuan YF, Zhang JM, Zhang BQ, Liu JJ, Zhou Y, Du MX, Han LX, Xu KJ, Qiao X, Liu CY (2021) Polymer solubility in ionic liquids: dominated by hydrogen bonding. Phys Chem Chem Phys 23: 21893–21900

Spatial Heterogeneity

► Structure Heterogeneity in Ionic Liquids

Structure Aggregation

► Structure Heterogeneity in Ionic Liquids

Structure Heterogeneity in Ionic Liquids

Song Li and Xiaoxiao Xia
School of Energy and Power Engineering, Huazhong University of Science and Technology, Wuhan, P.R. China

Synonyms

Spatial heterogeneity; Structure aggregation; Structure segregation

Definition

The structure heterogeneity in ionic liquids is the nanoscale spatial segregation of polar and nonpolar domains resulting from the assembly of alkyl chains of cations or anions due to the interplay between van der Waals of nonpolar chains and electrostatic interactions of polar heads.

Introduction

The nanoscale spatial aggregation is commonly observed in ionic liquids (ILs) with long alkyl chains, which can further affect the chemical, thermophysical, and physiochemical properties of ILs. Therefore, exploring the structure heterogeneity in ILs is critical for understanding phenomena resulting from the nanoscale aggregation of ILs. Experimental measurement techniques including small/wide-angle X-ray scattering (S/WAXS), small-angle neutron scattering (SANS), and X-ray diffraction (XRD) as well as molecular dynamics (MD) simulation have been implemented to investigate the impacts of alkyl chain length on structure heterogeneity of

various types of ILs. Both experiment measurement and simulation revealed that more and more evident prepeaks at ~0.3 $Å^{-1}$ in the structure function with the chain length can be observed, which can be ascribed to the long-range anion-anion correlations according to MD simulations. Moreover, the size of heterogeneity is also dependent on the chain length, consistent the heterogeneity order parameter that describes the degree of heterogeneity in the system.

Scientific Fundamentals

The structure heterogeneity in ionic liquids (ILs) resulting from the nanoscale organization of polar heads and nonpolar alkyl chains is crucial for their applications in green solvents, catalysts, and electrolytes. Such heterogeneities in IL solvents may potentially alter the reaction pathways and yields, similar to the effect of micelles or other molecular cages. The structure heterogeneity in ILs may also affect the thermodynamical, physiochemical, and dynamic properties of ILs including the phase transition temperature. So far, experimental measurement integrated with computer simulations has established that ILs can be characterized by three structure regimes depending on the length of alkyl chain (number of $–CH_2$ in alkyl chain = n): (1) short-chain ILs display homogeneous distributions of polar and nonpolar regions; (2) intermediate-chain ILs exhibit structural segregation of polar and nonpolar domains with high heterogeneity; (3) long-chain ILs ($n > 14$ for $[C_nmim][NO_3]$ [1]) present liquid crystal-like behavior with decreased heterogeneity. Herein, the structure heterogeneity in ILs specifically refers to the ILs with intermediate-chain length.

Experimental Measurement

The existence of structural heterogeneity in ionic liquids with long alkyl chains has been evidenced by varying experimental techniques including small/wide-angle X-ray scattering (S/WAXS) [2, 3], small-angle neutron scattering (SANS) [4, 5], and X-ray diffraction (XRD) [6]. The effects of alkyl chains of cations on structure heterogeneity of ILs have been firstly investigated by scattering techniques. The fingerprints of structural heterogeneity in ILs are the presence of the sharp peak at low-Q region of the measured static structure function $S(Q)$ from S/WAXS, SANS, and XRD. The occurrence of nanoscale segregation is characterized by the increased peak intensity with the length of alkyl chain, and the size of aggregates formed by alkyl tails depends on the chain length as well. The diffraction and scattering patterns of $[C_nmim][Cl]$ (n = 3, 4, 6, 8, 10), $[C_nmim][PF_6]$ (n = 4, 6, 8), and $[C_nmim][Tf_2N]$ (n = 2–10) shown in Fig. 1 demonstrate the more and more

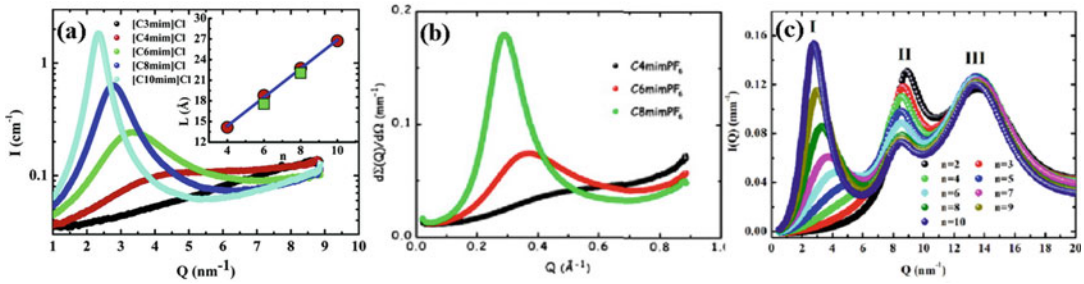

Structure Heterogeneity in Ionic Liquids, Fig. 1 X-ray diffraction (XRD) and small/wide-angle X-ray scattering (S/WAXS) patterns for (**a**) $[C_nmim][Cl]$ (n = 3, 4, 6, 8, 10) [2]. (Reproduced with permission from Ref. [2]. Copyright (2007) of the American Chemical Society); (**b**) $[C_nmim][PF_6]$ (n = 4, 6, 8) [3]. (Reproduced with permission from Ref. [3]. Copyright (2008) of the Elsevier); (**c**) $[C_nmim][Tf_2N]$ (n = 2–10) [8]. In the inset of (**a**), the spatial correlation $L = 2\pi/Q_{MAX}$, Q_{MAX} being the interference peak position, is plotted (circles) as a function of n, the alkyl chain length. (Reproduced with permission from Ref. [8]. Copyright (2009) of IOP Publishing)

significant prepeaks at ~0.3 $Å^{-1}$ in the structure function with increased chain length, which corresponds to the increased aggregation of cationic alkyl chains. The size of the structural heterogeneities (L) that is linearly proportional to the alkyl chain length ($L \sim 2\pi/Q_{MAX}$, Q_{MAX} is the peak position) with a slope of $\partial L_{ILs}/\partial n = 2.1$ Å/CH_2 unit can be estimated in the range of nanometers. Besides, the increased prepeak intensity with chain length of anions is also inspected for $[C_2mim][C_nOSO_3]$ ($n = 2, 4, 6, 8$) [6]. A similar phenomenon has been reported on dicationic ionic liquids(DILs) consisting of cations carrying two positive unit charges linked by one alkyl chain [7], in which $([C_n(mim)_2](Tf_2N)_2$ ($n = 3, 6, 12$)) a low-Q peak located at approximately 0.35–0.4 $Å^{-1}$ was observed with increased intensity as the chain length increases.

The influence of temperature on the structural heterogeneity of ILs has also been investigated experimentally. It has been observed that the shift of the prepeak located at approximately 0.3 $Å^{-1}$ shifts towards the high-Q region with increased temperature for $[C_nMPy][Tf_2N]$ ($n = 2, 3, 6, 8$, and 10), whereas the peaks at 0.9 and 1.4 $Å^{-1}$ shift towards low Q [9]. One the contrary, all the three peaks shift towards low Q with an increase in temperature for the IL tetradecyltrihexylphosphonium bis(trifluoromethylsulfonyl)amide ($[P_{14,666}][Tf_2N]$), indicating that the temperature-dependent peak shift is probably dependent on the type of ionic liquids [10]. In dicationic $[C_n(mim)_2](Tf_2N)_2$ ($n = 3, 6, 12$), the shift of prepeak at 0.3 $Å^{-1}$ towards high Q is trivial, suggesting the temperature insensitivity of heterogeneity in DILs. The slight shift of peaks at 0.9 and 1.4 $Å^{-1}$ towards low Q for DILs is probably due to the decreased density at high temperature and increased distance between ions [7].

Computational Simulation

Experimentally measured structure function is not sufficient to explain the experimentally observed phenomena. Molecular dynamics (MD) simulation is a complementary tool of S/WAXS and SANS by providing direct evidence for the correlation between peaks of S(Q) and the structural heterogeneity of ILs. Direct observation of aggregation of nonpolar chains by MD simulations has been reported for numerous ionic liquids with varying chain lengths [11] including $[C_nmim][C_8SO_4]$ ($n = 2,4,6,8,10,12$) [12] and $[C_nmim][NO_3]$ ($n = 6$–22) [1]. Figure 2a shows the segregation of polar and nonpolar regions of $[C_nmim][PF_6]$ ($n = 2, 4, 6, 8, 12$) highlighted by different colors, and the heterogeneity is more significant in ILs with long alkyl chains, providing a direct evidence of the structure heterogeneity in ILs. In contrast to common monocationic ionic liquids (MILs) consisting of cations carrying a single unit charge, the structure heterogeneity in DILs $[C_n(mim)_2][BF_4]_2$ is less significant than their counterpart MILs, and the aggregate size is smaller due to the dissimilar nano-organization of alkyl tails in DILs and MILs [13].

Structure Function

Instead of direct observation, the total structure function $S(Q)$ can be computed to compare with the experimental measured results from S/WAXS or SANS based on the trajectories of MD simulation by the following equation:

$$S(Q) = 1 + \frac{\sum_{\alpha\beta} \chi_\alpha \chi_\beta f_\alpha(Q) f_\beta(Q) 4\pi \int_0^{r_c} \left[g_{\alpha\beta}(r) - 1 \right] r^2 \frac{\sin(Qr)}{Qr} dr}{\left[\sum_{\alpha\beta} \chi_\alpha f_\alpha(Q) \right]^2}$$

χ_α and χ_β are the fraction of atom species α and β, Q is the wave vector, $f(Q)$ is the form factor of atom species, $g_{\alpha\beta}(r)$ is the correlation function of atom species α and β, and r_c is the integration cutoff which equals one half of the simulation box. It is noted that the intensity of the peaks of $S(Q)$ mostly depends on the types of anions whose constituents usually have large X-ray form factors in comparison to the cation alkyl chains. The consistency in $S(Q)$ between MD simulation and SAXS has been reported on many ILs. Figure 2b shows a good agreement in $S(Q)$ of $[Pyrr_{1,n}][Tf_2N]$ ($n = 4, 6, 8, 10$) from MD simulation and SAXS measurements, in which the intensity of

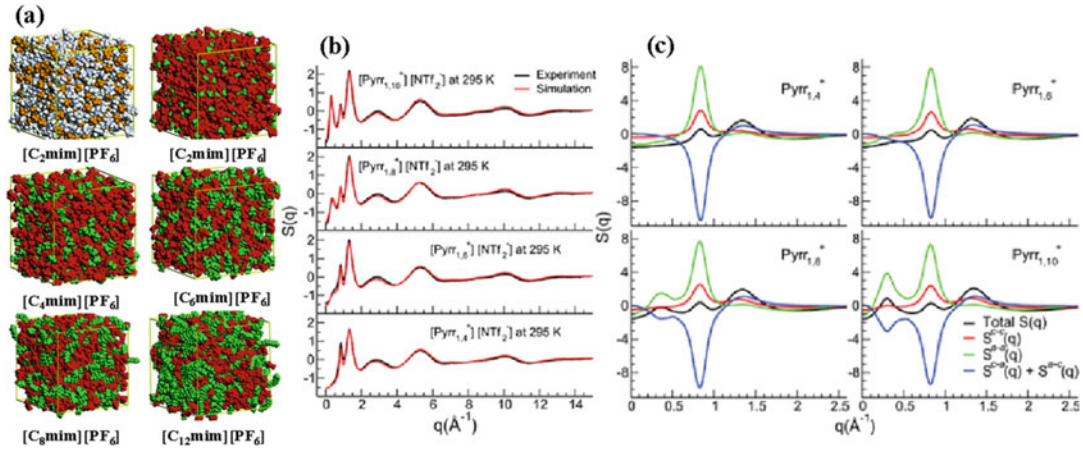

Structure Heterogeneity in Ionic Liquids, Fig. 2 (**a**) Snapshots of $[C_nmim][PF_6]$ ($n = 2, 4, 6, 8, 12$) from MD simulations [14]. (Reproduced with permission from Ref. 14. Copyright (2006) of the American Chemical Society); (**b**) Structure functions for $[Pyrr_{1,n}][Tf_2N]$ ($n = 4, 6, 8, 10$) measured at 295 K from SAXS and experiments; (**c**) Partial structure functions contributed by cation-cation (c-c), anion-anion (a-a), and cation-anion (c-a and a-c) of $[Pyrr_{1,n}][Tf_2N]$ ($n = 4, 6, 8, 10$) [15]. (Reproduced with permission from Ref. 15. Copyright (2012) of the Royal Society of Chemistry)

prepeak located at approximately 0.3 $Å^{-1}$ gradually increases with chain length.

The partial structure function derived from total *S(Q)* can be calculated as follows:

$$S_{\alpha\beta}(Q) = 1 + 4\pi\rho\int_0^{r_c}\left[g_{\alpha\beta}(r) - 1\right]r^2\frac{\sin(Qr)}{Qr}dr$$

Partial structure function $S_{\alpha\beta}(Q)$ is able to quantify the contribution from the interaction of specific groups (i.e., polar/nonpolar) of ILs, which will benefit the identification of the origin of featured peaks in structure function. According to the partial structure functions of $[Pyrr_{1,n}][Tf_2N]$ ($n = 4, 6, 8, 10$) in Fig. 2c, it is found that the prepeak in the structure function is mostly contributed by the long-range anion-anion correlations, due to the large molecular form factor of anionic elements [15]. Therefore, the structure functions of ILs are dominated by anions instead of cations. Besides, the spatial distribution of charge and polarity alternation has been identified to depend on the cation head-anion interaction under the help of partial structure function analysis [16].

Regarding the influences of the temperature variation on the prepeak of *S(Q)*, MD simulation provides similar trends to experimental observations, in which the prepeak shifts towards high Q value at high temperatures. The study on $[C_nMPy][Tf_2N]$ ($n = 2, 3, 6, 8,$ and 10) reveals that the prepeak located at 0.3 $Å^{-1}$ shifts towards the high-Q region with an increased temperature, indicating the reduced polarity alternation distance [9]. On the contrary, the peaks at 0.9 and 1.4 $Å^{-1}$, corresponding to cation-cation/anion-anion and cation-anion correlations, respectively, shift towards low-Q regions with the increase of temperature, which is correlated with the increased distance between ions at high temperature [17]. However, all the three peaks shift towards low Q with an increase in temperature for the tetradecyltrihexylphosphonium bis (trifluoromethyl-sulfonyl)amide ($[P_{14,666}][Tf_2N]$), implicating that the temperature-dependent peak shift may rely on the type of ionic liquids [10].

Heterogeneity Oder Parameter

Another parameter to evaluate the structure heterogeneity in ionic liquids is heterogeneity order parameter (HOP), which quantitatively assesses the degree of structure heterogeneity in MD simulations [18]. In general, HOP is obtained by

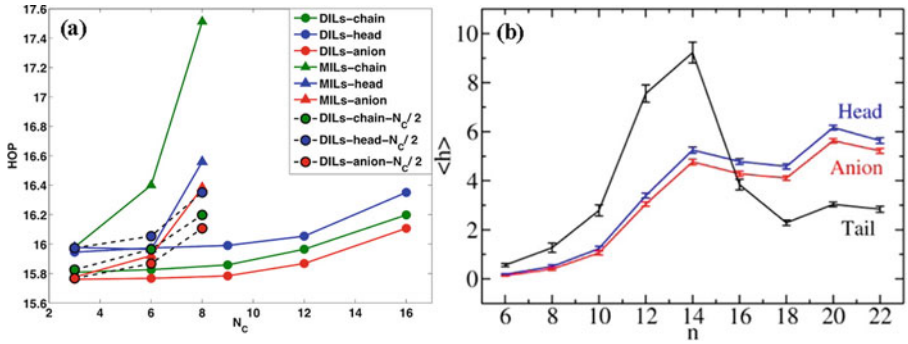

Structure Heterogeneity in Ionic Liquids, Fig. 3. (**a**) Heterogeneity order parameter (HOP) for alkyl chains (green), head groups (blue), and anions (red) of DILs $[C_n(mim)_2](BF_4)_2$ (solid circles) and MILs $[C_nmim][BF_4]$ (solid triangles) as a function of chain length (N_C, the number of -CH_2 in alkyl chain). The solid circles with black dash lines are HOP values of DILs with N_C =N/2 ($N = 6, 12, 16$; N is the number of –CH_2 in the alkyl chain of DILs). The carbon atom in the end of the alkyl tail chain of MILs and the carbon atoms in the middle of the linkage chain for DILs represent the alkyl chain site (for the even-numbered DILs, the site is defined as the center of mass of the two central carbon atoms in an alkyl linkage chain); the center of mass of head groups and anions were used to denote the anion sites and head sites, respectively [13]. (Reproduced with permission from Ref. [13]. Copyright (2013) of the American Chemical Society). (**b**) Heterogeneity order parameters for coarse grain sites A (head), D (anion), and E (tail) of $[C_nmim][NO_3]$ (n = 6–22). It should be noted that all the HOPs of $[C_nmim][NO_3]$ were subtracted by 15.75 for clear comparison [1]. (Reproduced with permission from Ref. [1]. Copyright (2013) of the American Chemical Society)

dividing the simulation space into multiple small cells and counting the number of sites in each cell. The heterogeneity is characterized by the uneven distribution of sites of interest, which could be computed as follows considering the periodic boundary conditions.

$$h = \frac{1}{N_s}\sum_{i=1}^{N_s}\sum_{j=1}^{N_s}\exp\left(\frac{-r_{ij}^2}{2\sigma^2}\right)$$

where N_s is the total number of sites in the system, r_{ij} is the modulation of the vector $r_i - r_j$ corrected with the periodic boundary conditions, $\sigma = L/N^{1/3}$, where L is the side length of the cubic simulation box, and N is the total number of sites. It should be noted that a system consisting of ideally homogeneously distributed particles exhibits a HOP approaching 15.75 [18], suggesting that the indicator of structure heterogeneity in ILs is a deviation from HOP = 15.75

To identify the contributions of cation heads, cation chains and anions to the structure heterogeneity in ILs, their HOPs are usually calculated, respectively. The increased HOP with the chain length corresponds to the increased prepeaks in structure function, suggesting the enhanced structure heterogeneities. The HOP of alkyl chains is generally higher than those of cation heads and anions, especially with the prolongation of alkyl chain for $[C_nmim][BF_4]$ (Fig. 3a), indicating the major contribution of alkyl chains to the structure heterogeneity in ILs. However, when $n > 14$ for $[C_nmim][NO_3]$, there is a dramatic decrease in the HOP of alkyl chain (tail), and a steady increase in the HOPs of polar cation heads and anions (Fig. 3b). Such tendency is ascribed to the transition from spatial heterogeneous phase to liquid crystalline-like phase as chain length increases from n = 14 to 16 [1], after which the alkyl chains tend to be parallel with each other. Whereas, cation heads and anions, mostly perpendicular to the side chains, form a continuous polar network. Compared with DILs, the HOP of MILs is high than that of DILs regardless of the chain length, consistent with the visual inspection in snapshots of MD simulation as well as the more significant prepeaks in *S(Q)* of MILs [13].

S

Summary

In order to understand the structure heterogeneity in ILs, structure function that can be obtained by both experimental techniques and MD simulations is used. Different peaks in structure function can be ascribed to various correlations by integrated experiment and MD simulation studies. The increased prepeaks at ~0.3 $Å^{-1}$ in the structure function with the chain length is ascribed to the long-range anion-anion correlations under the help of partial structure function analysis. In addition, the peaks at ~0.9 and ~1.4 $Å^{-1}$ are contributed by cation-cation/anion-anion and cation-anion correlations, respectively. Heterogeneity order parameter (HOP) is another evaluation criterion to assess the degree of heterogeneity in MD simulations, from which HOP increases with the increase of alkyl chain length and HOP of alkyl chains is higher than HOP of polar cation head/anion. However, further increase in alkyl chain length may result in the reduced HOP due to the transition from heterogeneous phase to crystalline-like phase in ILs.

Outlook

According to X-ray/neutron scattering, X-ray diffraction measurement, and MD simulations, although the correlation between each peak of the structure function and polar/nonpolar interaction in ILs has been revealed, the reported studies only focus on several types of commonly investigated ILs. There may be slight difference for different ILs. Therefore, further investigations can be extended to new types of ILs in future. In addition, the prepeaks in measured structure function is an indirect evidence of the structure heterogeneity in ILs. Direct observation of the structure segregation in ILs with long alkyl chains requires the future development of the advanced imaging techniques. Besides qualitative research, quantitative estimation of the size and distribution of structure heterogeneities in ILs will be the ultimate target for the future experimental measurement techniques.

References

1. Ji YM, Shi R, Wang YT, Saielli G (2013) Effect of the chain length on the structure of ionic liquids: from spatial heterogeneity to ionic liquid crystals. J Phys Chem B 117(4):1104–1109
2. Triolo A, Russina O, Bleif HJ, Di Cola E (2007) Nanoscale segregation in room temperature ionic liquids. J Phys Chem B 111(18):4641–4644
3. Triolo A, Russina O, Fazio B, Triolo R, Di Cola E (2008) Morphology of 1-Alkyl-3-methylimidazolium hexafluorophosphate room temperature ionic liquids. Chem Phys Lett 457(4–6):362–365
4. Fujii K, Kanzaki R, Takamuku T, Kameda Y, Kohara S, Kanakubo M, Shibayama M, Ishiguro S, Umebayashi Y (2011) Experimental evidences for molecular origin of low-Q peak in neutron/X-ray scattering of 1-Alkyl-3-methylimidazolium bis(trifluoromethanesulfonyl) amide ionic liquids. J Chem Phys 135(24):244502
5. Hardacre C, Holbrey JD, Mullan CL, Youngs TGA, Bowron DT (2010) Small angle neutron scattering from 1-Alkyl-3-methylimidazolium hexafluorophosphate ionic liquids ($[C_n mim][PF_6]$, n=4, 6, and 8). J Chem Phys 133(7):074510
6. Macchiagodena M, Ramondo F, Triolo A, Gontrani L, Caminiti R (2012) Liquid structure of 1-ethyl-3-methylimidazolium Alkyl sulfates by X-ray scattering and molecular dynamics. J Phys Chem B 116(45):13448–13458
7. Li S, Banuelos JL, Zhang PF, Feng G, Dai S, Rother G, Cummings PT (2014) Toward understanding the structural heterogeneity and ion pair stability in dicationic ionic liquids. Soft Matter 10(45):9193–9200
8. Russina O, Triolo A, Gontrani L, Caminiti R, Xiao D, Hines LG, Bartsch RA, Quitevis EL, Plechkova N, Seddon KR (2009) Morphology and intermolecular dynamics of 1-Alkyl-3-methylimidazolium bis{(trifluoromethane)sulfonyl}amide ionic liquids: structural and dynamic evidence of nanoscale segregation. J Phys Condens Matter 21(42):424121
9. Li S, Banuelos JL, Guo J, Anovitz L, Rother G, Shaw RW, Hillesheim PC, Dai S, Baker GA, Cummings PT (2012) Alkyl chain length and temperature effects on structural properties of pyrrolidinium-based ionic liquids: a combined atomistic simulation and small-angle X-ray scattering study. J Phys Chem Lett 3(1):125–130
10. Kashyap HK, Santos CS, Annapureddy HVR, Murthy NS, Margulis CJ, Castner EW (2012) Temperature--dependent structure of ionic liquids: X-ray scattering and simulations. Faraday Discuss 154:133–143
11. Hayes R, Warr GG, Atkin R (2015) Structure and nanostructure in ionic liquids. Chem Rev 115(13):6357–6426
12. Kapoor U, Shah JK (2018) Globular, Sponge-like to layer-like morphological transition in 1-&ITn&IT-Alkyl-3-methylimidazolium octylsulfate ionic liquid homologous series. J Phys Chem B 122(1):213–228

13. Li S, Feng G, Banuelos JL, Rother G, Fulvio PF, Dai S, Cummings PT (2013) Distinctive nanoscale organization of dicationic versus monocationic ionic liquids. J Phys Chem C 117(35):18251–18257
14. Lopes JNAC, Padua AAH (2006) Nanostructural organization in ionic liquids. J Phys Chem B 110(7):3330–3335
15. Kashyap HK, Hettige JJ, Annapureddy HVR, Margulis CJ (2012) SAXS anti-peaks reveal the length-scales of dual positive-negative and polar-apolar ordering in room-temperature ionic liquids. Chem Commun 48(42):5103–5105
16. Hettige JJ, Kashyap HK, Annapureddy HVR, Margulis CJ (2013) Anions, the reporters of structure in ionic liquids. J Phys Chem Lett 4(1):105–110
17. Santos CS, Murthy NS, Baker GA, Castner EW (2011) Communication: X-ray scattering from ionic liquids with pyrrolidinium cations. J Chem Phys 134(12):121101
18. Wang YT, Voth GA (2006) Tail aggregation and domain diffusion in ionic liquids. J Phys Chem B 110(37):18601–18608

Structure Segregation

► Structure Heterogeneity in Ionic Liquids

Sulfonium Ionic Liquids

Cheng-tao Yue[1,2], Peng Sun[1] and Fu-wei Li[1]
[1]State Key Laboratory for Oxo Synthesis and Selective Oxidation, Suzhou Research Institute of LICP, Lanzhou Institute of Chemical Physics (LICP), Chinese Academy of Sciences, Lanzhou, China
[2]University of Chinese Academy of Sciences, Beijing, China

Introduction

Over the past decades, ionic liquids have received considerable interest as potential electrolytes for lithium rechargeable batteries due to their excellent stability, non-flammability, and nonvolatility [1–4]. However, while hundreds of ILs have been developed, most of them suffer from low conductivity caused by their intrinsic high viscosity [5–7]. Whereas, in 2005, Wasserscheid and coworkers reported for the first time a series of sulfonium dicyanamides with very low viscosities and high conductivities [8]. Based on this, a variety of functionalized sulfonium ILs were developed as novel low viscous electrolytes [9–13]. On the other hand, apart from their electrochemical applications, sulfonium salts are also being widely used as important synthetic intermediates for the synthesis of massive organic compounds due to the high reactivity of the C-S bond [14]. These sulfonium salts have been designed purposely with specific functional groups for transformation into the targeted compounds. Moreover, the functionalized sulfonium salts also displayed an enhanced biocidal efficacy than the quaternary ammonium counterpart due to their good solubility and antibacterial activity, promising their potential applications as antibacterial agents [15–17]. All these aspects lead to the rapid development of synthetic methods for numerous functionalized sulfonium ILs.

This entry provides a guide to the synthesis and characterization of a variety of sulfonium ILs using different synthetic routes and methods. While traditional sulfonium salts can be synthesized using common routes such as alkylation and metathesis, this entry also describes innovative approaches to produce the functionalized sulfonium ILs, supported sulfonium ILs, and polymeric sulfonium ILs.

Synthesis of Sulfonium ILs

Formation of the Sulfonium Salts

The sulfonium ILs are synthesized similarly to that for the ammonium- and phosphonium-based ILs [18–20], in which the alkylation of thioether with an alkyl halide or alkyl ester produces the corresponding tertiary sulfonium salts. In a typical procedure (Scheme 1), a mixture of dialkylsulphide and equimolar amounts of alkyl halide (ester) in a solvent was stirred and heated for a certain time under the protection of nitrogen. After the completion of the reaction, the solvent was removed under vacuum and the

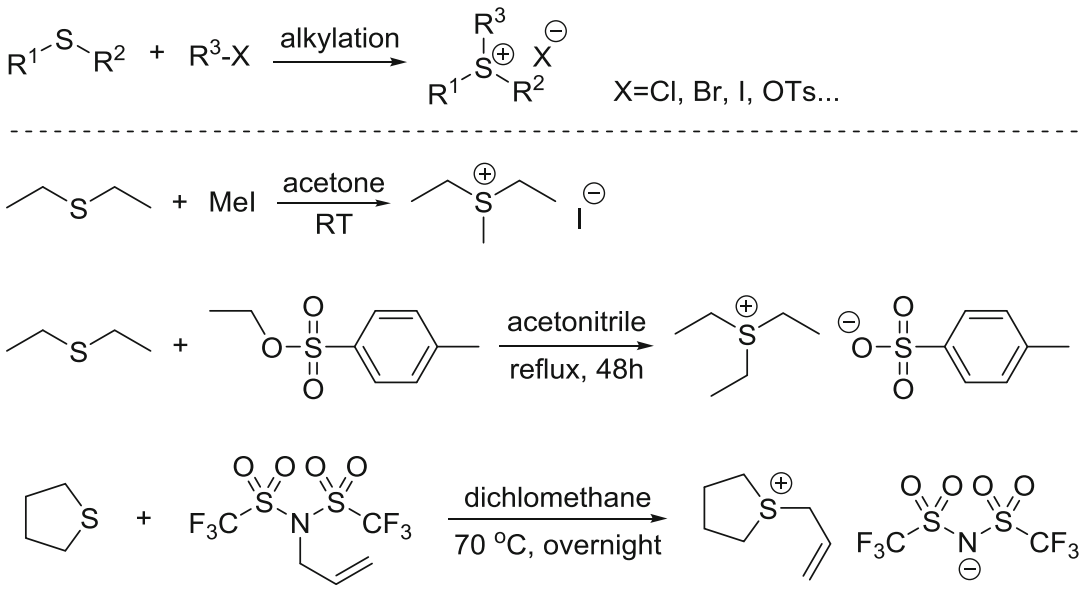

Sulfonium Ionic Liquids, Scheme 1 Formation of sulfonium cations through alkylation of dialkylsulphide with alkyl halide (ester)

resultant crude product was further purified by biphasic extraction or recrystallization. The obtained sulfonium ILs were either a viscous liquid or a white powder. Notably, besides the alkyl halide or alkyl ester, *N*-alkyl trifluoromethanesulfonimide have also been reported as effective alkylation agents for the formation of the sulfonium salts.

Anion Exchange

The anion exchange is the most common way to produce various sulfonium ILs which have different counter-anions, including tetrafluoroborate, hexafluorophosphate, carboxylate, dicycnamide, bis(trifluoromethanesulfonyl)amide, alkylsulfate, trifluoromethanesulfonate, tosylate, etc. [21–23]. This kind of ion-exchange reaction between the halide of sulfonium salts and a different anion is an example of a metathesis reaction (Scheme 2). Depending on the solubility of ILs, the metathesis reaction can be conducted either in water or in an organic solvent. If the sulfonium ILs are water-soluble, the reaction can be conducted in water upon using water-soluble silver salts as the anion source. Whereas, if the sulfonium ILs are water-insoluble, the reaction can be performed in an organic solvent with alkali salts as the anion source. Note that a slight excess of metal salts is used here to ensure the complete conversion of the sulfonium halides. Nonetheless, these excess metal salts as well as the formed metal halides can either be washed off by water or filtered out, facilitating the purification of the resultant products.

Synthesis of Functionalized Sulfonium ILs

Functionalized sulfonium ILs are those sulfonium ILs that consist of tethered functional groups on the sulfonium cation or anion which endow them with unique physicochemical properties for specific tasks. The synthesis of such ILs is accomplished by grafting of functional groups into either the sulfonium cation or anion. In contrast to phosphines which are usually hard to obtain functionalized phosphine precursors, the easy preparation of thioether benefits the construction of functionalized thioether precursors for the subsequent synthesis of functionalized sulfonium cations. Besides, the anion exchange between the halide in phosphonium salts and a functionalized anion can further produce the anion-

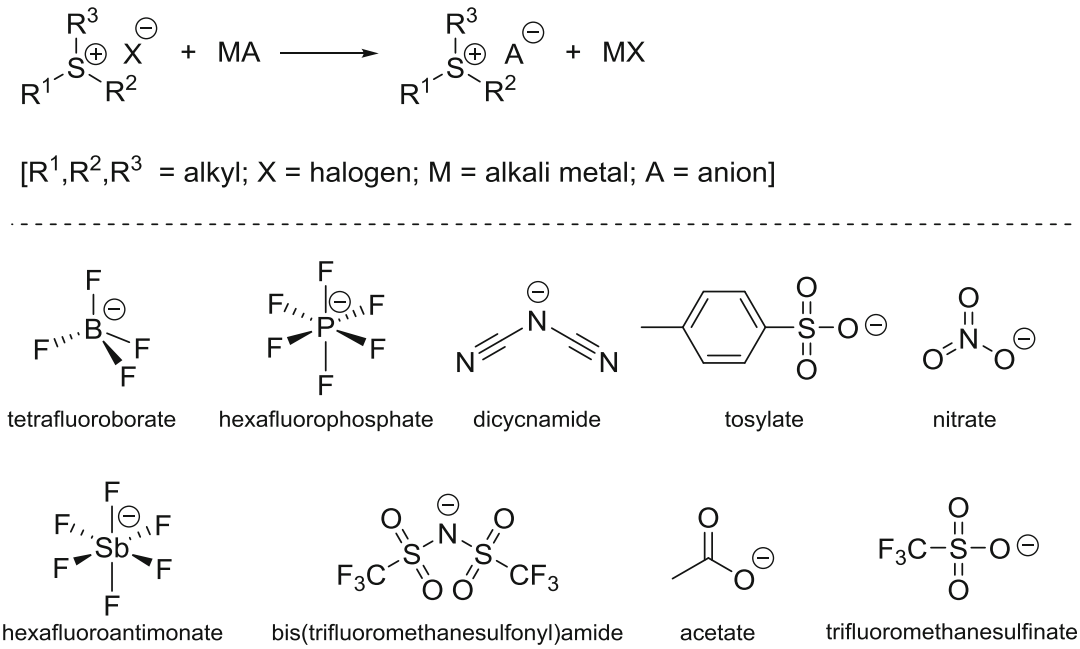

Sulfonium Ionic Liquids, Scheme 2 Mechanism of anion exchange and examples of anions that can be exchanged with halides in ILs

functionalized sulfonium ILs. The following section covers some of the recent advantages made in the synthesis of functionalized sulfonium ILs.

Synthesis of Sulfonium ILs with Specific Groups

Synthesis of Functionalized Sulfonium Cations

The alkylation reaction between dialkylsulphides and functionalized alkyl halides (esters) is the most facile way to fabricate functionalized sulfonium cations [24–27]. For example, Dyson's group used allyl iodide (bromide) as alkylation agents to react with dialkylsulphide which effectively delivered the corresponding allyl-functionalized sulfonium salts ([C_2Allylsul]X) (Scheme 3) [27]. The detailed synthetic procedure is as follows: A mixture of diethyl sulfide and equimolar allyl bromide (or iodide) in acetone was stirred at room temperature (RT) for 24–48 h during which time a white precipitate (or a pale yellow liquid phase) was formed. After removing the acetone, the crude products were washed thoroughly with diethyl ether and dried under vacuum for 24 h to give [C_2Allylsul]Br and [C_2Allylsul]I.

Similarly, Mandal's group reported the use of a pre-synthesized fluorine-containing tosylate (TFEEOTs) as an alkylation agent to prepare fluorine-containing sulfonium ILs ([DESEtTFE]OTs) (Scheme 4) [28]. Here, TFPEOTs was reacted with a large excess of diethyl sulfide (>2 eq) at 70 °C for 3 days to give the desired sulfonium salt with a relatively low yield (32.6%).

Notably, the alkylation reaction between thioether and alkyl halide is highly dependent on the reaction activity of alkyl halide. For instance, Coadou and coworkers reported the synthesis of ether-functionalized sulfonium salts through alkylation of dialkylsulphide by bromoethers. This approach to access ether-functionalized sulfonium salts proved problematic due to the lower alkylation yield (Scheme 5). Alternatively, the employment of pre-synthesized ether-functionalized thioethers to react with more reactive iodomethane can readily generate the sulfonium salt in good yield [29].

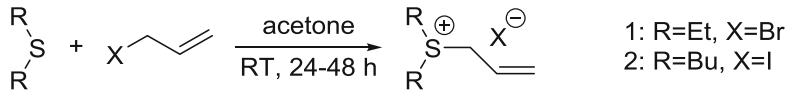

Sulfonium Ionic Liquids, Scheme 3 Typical examples for synthesis of allyl-functionalized sulfonium ILs ([C_2Allylsul]X)

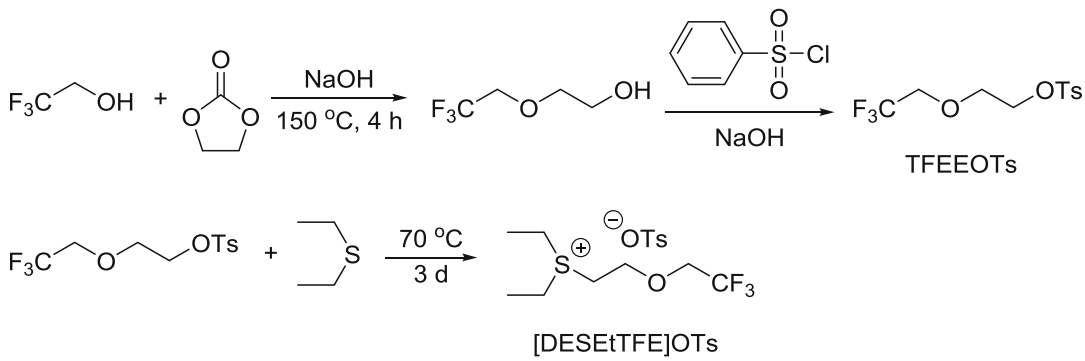

Sulfonium Ionic Liquids, Scheme 4 Synthesis of fluorine-containing sulfonium ILs ([DESEtTFE]OTs) via alkylation of diethyl sulfide with pre-synthesized fluorine-containing tosylate (TFEEOTs)

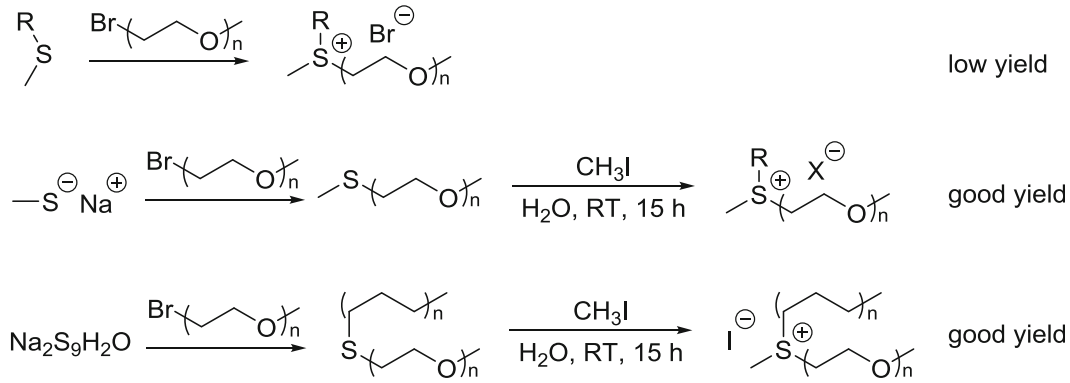

Sulfonium Ionic Liquids, Scheme 5 Strategic routes for the synthesis of ether-functionalized sulfonium ILs

Kim and coworkers described the synthesis of siloxane-functionalized sulfonium ILs via the alkylation reaction between tetrahydrothiophene and 1,3-bis(iodomethyl)tetramethyldisiloxane (Scheme 6) [30]. The high reactive iodosiloxane could readily react with tetrahydrothiophene to furnish the desired ILs in high yield (up to 90%).

The alkylation reaction between functionalized thioethers and alkyl halides provides an alternative way to fabricate functionalized sulfonium cations. For instance, Sundermeyer's group reported the synthesis of ferrocenyl-functionalized sulfonium ILs via the alkylation of alkyl ferrocenyl sulfides by alkylbis(trifluoromethanesulfonyl)imide (TFSI) (Scheme 7) [31]. Here, alkyl ferrocenyl sulfides were pre-synthesized via the functionalization of ferrocene with dimethyl disulfides in the presence of tertbutyllithium and potassium tertbutanolate at −78 °C in THF.

By adopting a multistep reaction, a variety of more complicated thioether can be obtained for the

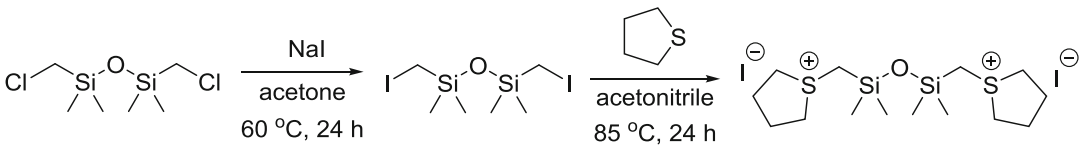

Sulfonium Ionic Liquids, Scheme 6 Strategic routes for the synthesis of siloxane-functionalized sulfonium ILs

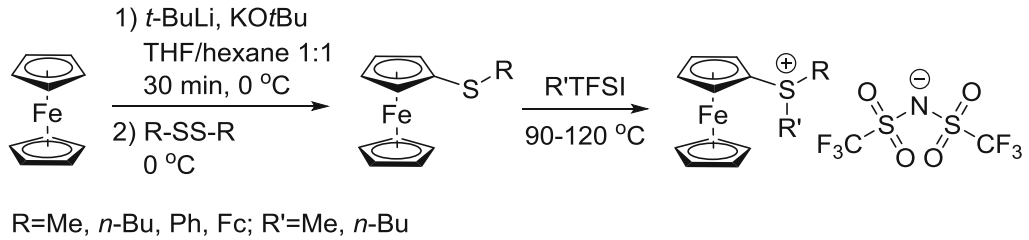

Sulfonium Ionic Liquids, Scheme 7 Synthesis of ferrocenyl-functionalized sulfonium ILs via alkylation of pre-synthesized ferrocenyl thioethers with alkylbis(trifluoromethanesulfonyl)imide

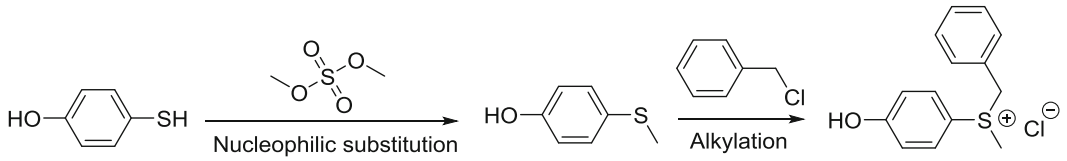

Sulfonium Ionic Liquids, Scheme 8 Synthesis of hydroxyl-functionalized sulfonium ILs from hydroxyl-functionalized thioether

synthesis of functionalized sulfonium ILs containing specific functional groups. For instance, Okai and coworkers prepared a hydroxyl-functionalized sulfonium cation via a two-step nucleophilic substitution alkylation reaction (Scheme 8) [32]. The initial nucleophilic substitution of dimethyl sulfate by 4-mercaptophenol lead to the formation of a hydroxyl-functionalized thioether, after which the alkylation of the obtained thioether with benzyl chloride generated the hydroxyl-functionalized sulfonium chloride.

Jin and coworkers described the synthesis of a conjugated sulfonium salt from 4-aldehyde-triphenylamine through four steps [33]. The detailed synthetic procedure is shown in Scheme 9. First, the Witting-Horner reaction between 4-aldehyde-triphenylamine and diethyl (4-bromobenzyl) phosphonate generated the 4-bromostyryl-triphenylamine (I). Next, the Suzuki reaction was performed with meta-(methylthio)-phenylboronic acid to give triphenylamine-functionalized thioether precursor (II). Then, the alkylation of (II) with methyl trifluoromethanesulfonate produced the triphenylamine-functionalized sulfonium trifluoromethanesulfonate (III). Finally, the anion exchange between (III) and sodium hexafluoroantimonate furnished the desired conjugated sulfonium IL (PI-PAG).

Similarly, Li and coworkers prepared a series of chloramine-functionalized sulfonium salts vi a a four-step synthetic procedure (Scheme 10) [34]. Using 5,5-dimethylhydantoin as the initial synthetic material, this compound underwent a stepwise substitution-alkylation-ion exchange--chlorination to achieve the desired sulfonium salts.

The above synthetic strategies for sulfonium cation have generated a diversity of functionalized sulfonium ILs which have potential applications in synthesis, electrochemistry, and biochemistry. In particular, the use of alkyl- or aryl-sulfonium salts as alkylation (arylation) reagents to forge

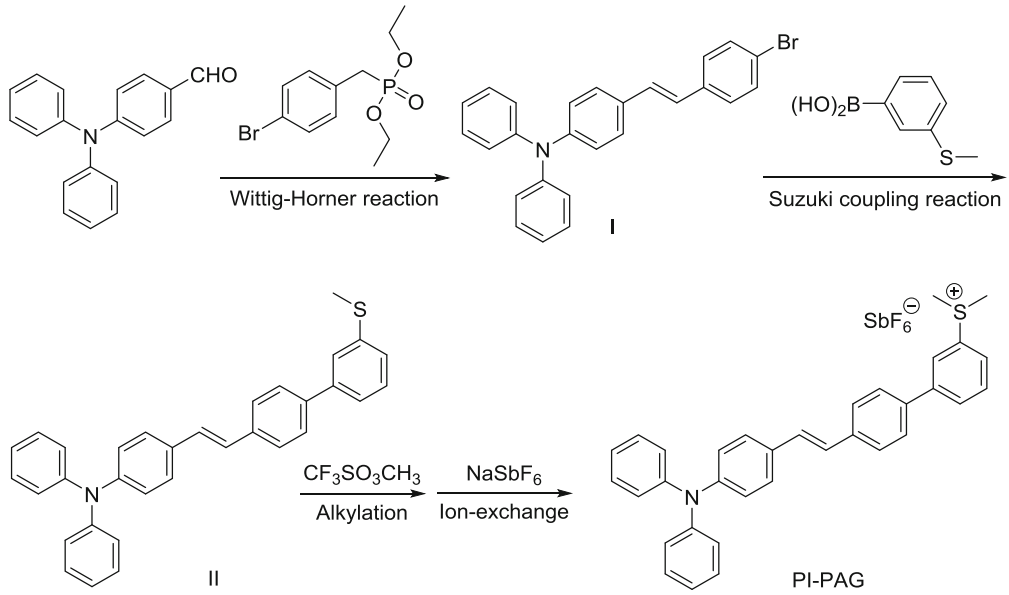

Sulfonium Ionic Liquids, Scheme 9 Synthesis of conjugated sulfonium salt from 4-aldehyde-triphenylamine through four steps

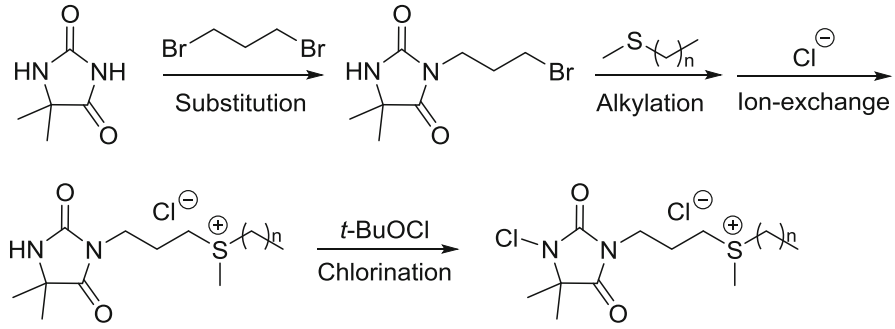

Sulfonium Ionic Liquids, Scheme 10 Synthesis of conjugated sulfonium salt from 4-aldehyde-triphenylamine through four steps

new C-X bonds (X = C, O, S, F,. . .) has recently attracted a great deal of interest in the synthetic organic chemistry due to the high reactivity of the C-S bond in sulfonium cation [35–39]. As shown in Scheme 11, this kind of functionalized sulfonium salts was usually prepared by alkylation of a relatively stable thioether with a reactive alkylation reagent, for the purpose of selective bond breaking.

Synthesis of Anion-Functionalized Sulfonium ILs

Apart from the functionalization of phosphonium cations, the use of functional anions can also generate the corresponding functionalized sulfonium ILs. Typically, this series of anion-functionalized sulfonium ILs are prepared by the anion-exchange of sulfonium halides with those metal salts which have a functional anion. For example, Deng's group reported the synthesis of sulfonium saccharin via the anion-exchange between sulfonium iodide and saccharin silver (Scheme 12) [10]. Stirring the above mixture in the water at 40 °C for 4 h, the desired sulfonium saccharins were readily obtained in high yield (89–92%).

Pradeep's group reported a new series of aromatic sulfonium octamolybdate hybrids via

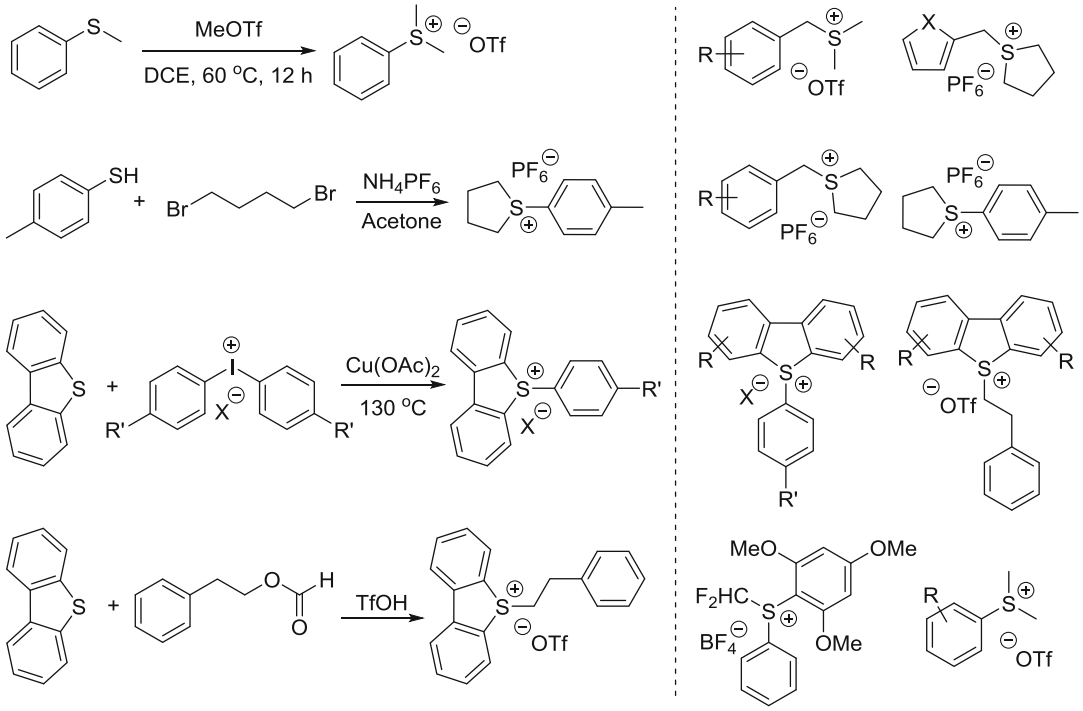

Sulfonium Ionic Liquids, Scheme 11 Synthesis of alkyl- or aryl-sulfonium salts which can be used as alkylation (arylation) reagents to forge new C-X bonds

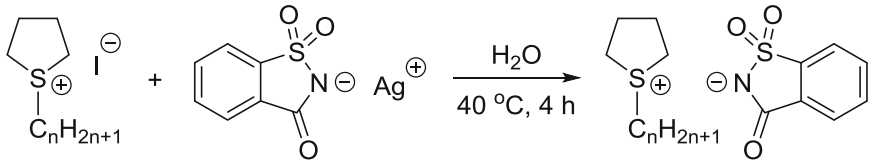

Sulfonium Ionic Liquids, Scheme 12 Synthesis of saccharin-functionalized sulfonium IL via anion-exchange reaction

ion-exchange of sodium molybdate with different aromatic sulfonium ILs (Scheme 13) [40]. The treatment of sodium molybdate (1 equiv.) with sulfonium ILs (1.5 equiv.) in deionized water at pH 4.0 led to the formation of the corresponding sulfonium octamolybdates as white precipitates.

Notably, Matsumoto and coworkers prepared a series of sulfonium fluorohydrogenate ILs via the anion-exchange between sulfonium halides and HF (Scheme 14) [41]. This ion-exchange reaction was conducted in a large excess of anhydrous HF at 0–25 °C without the use of metal salts and bases. After the reaction was complete, the resultant mixture was concentrated by successive pumping with a rotary pump to give the desired sulfonium fluorohydrogenate.

Synthesis of Chiral Sulfonium Salts

Zwitterionic sulfonium ILs represent a kind of sulfonium ILs with the capability of tethering the anion and cation together. This kind of ILs can be directly prepared by alkylation of thioethers with sultones. For instance, Mandal's group reported the synthesis of zwitterionic sulfonium alkylsulfonate via the alkylation reaction between Boc-L-methionine-(2-methacryloylethyl) ester (METMA) and 1,3-propane sultone (Scheme 15) [42]. This reaction was conducted

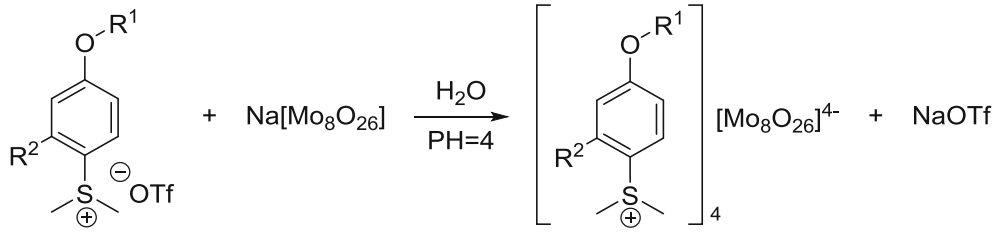

Sulfonium Ionic Liquids, Scheme 13 Synthesis of aromatic sulfonium octamolybdate hybrids via anion-exchange reaction

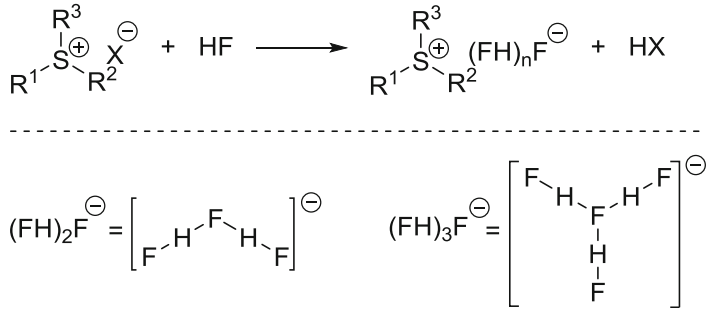

Sulfonium Ionic Liquids, Scheme 14 Synthesis of sulfonium fluorohydrogenate ILs via anion-exchange reaction

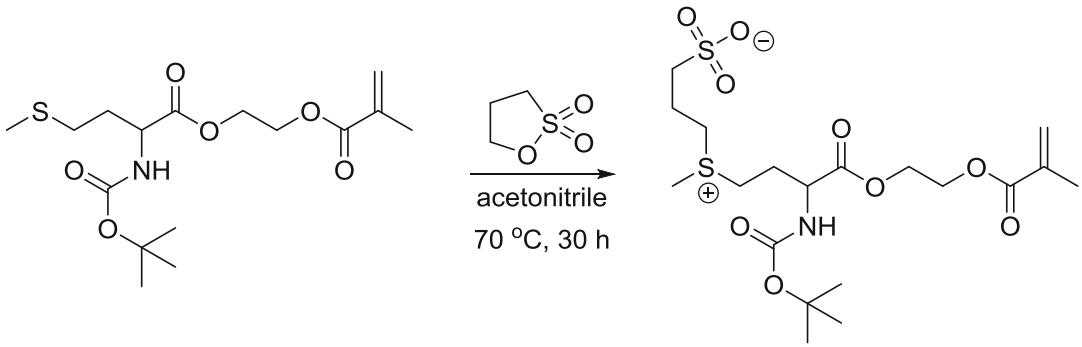

Sulfonium Ionic Liquids, Scheme 15 Synthesis of zwitterionic sulfonium alkylsulfonate via alkylation of thioether with sultone

in acetonitrile at 70 °C for 30 h under a nitrogen atmosphere and the targeted sulfonium alkylsulfonate was obtained as a white precipitate after adding diethyl ether into the resultant mixture.

An alternative synthetic strategy is based on the neutralization of the acid groups in acid-functionalized sulfonium ILs. This synthetic route has been successfully applied to access zwitterionic sulfonium alkylcarboxylate [43, 44]. For example, Forbes and coworkers used silver oxide as the base to deprotonate carboxyl of carboxyl-functionalized sulfonium IL, which quantitatively delivered the corresponding sulfonium betaine after reaction for 20 h in methanol under a stream of nitrogen (Scheme 16) [44].

Synthesis of Chiral Sulfonium Salts

Chiral sulfonium salts are widely presented in various natural products such as salaprinol, ponkoranol, kotalanol, and neosalaprinol. Based on this, great efforts have been paid to develop

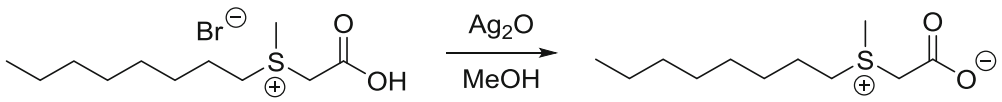

Sulfonium Ionic Liquids, Scheme 16 Synthesis of zwitterionic sulfonium alkylcarboxylate via neutralization of the acid groups

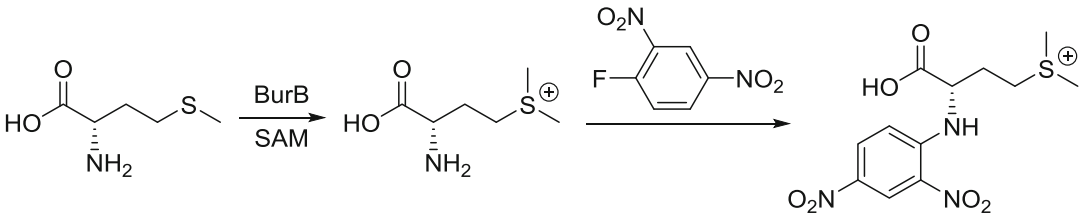

Sulfonium Ionic Liquids, Scheme 17 Synthesis of s chiral sulfonium salts via alkylation of a pre-synthesized chiral thioether

new practical synthetic approaches to access chiral sulfonium salts [45]. One of the most promising approaches to the above sulfonium salts is through the alkylation of a pre-synthesized chiral thioether. For instance, Hertweck and coworkers reported the use of L-methionine to produce chiral sulfonium salts via a two-step procedure (Scheme 17) [46]. The alkylation of L-methionine by S-adenosylmethionine (SAM) under the catalysis of methyltransferase (BurB) led to the formation of L-methionine with built-in sulfonium cation, after which dinitrobenzene-functionalized L-methionine were further obtained by nucleophilic substitution with 1-fluoro-2,4-dinitrobenzene.

Wu and coworkers prepared a series of de-*O*-sulfonated sulfonium salts from D-arabinose via a coupling reaction between chiral thiols and a diiodide D-arabinose derivative (Scheme 18) [47]. The intermolecular nucleophilic substitution reaction between the above thiol and the diiodide counterpart followed by a diastereoselective intramolecular alkylation provided a chiral five-member sulfonium salt structure. And this kind of de-*O*-sulfonated sulfonium salts can be varied upon using different thiols.

Synthesis of Supported Sulfonium ILs

Supported sulfonium ILs refer to those sulfonium ILs that are tethered to a solid carrier, in which the ILs are tightly bonded to a support surface and show a combined advantage of IL and solid material. In comparison to the ammonium and phosphonium ILs which are stable enough to perform an immobilization operation, the sulfonium ILs have rarely been used to fabricate supported ILs due to their relatively lower stability. Nonetheless, the supported sulfonium salts can be accessed via the alkylation of halogenoalkyl-funtionalized support with thioethers. For example, Guo and coworkers reported the synthesis of chitosan-supported sulfonium salts via in situ formation of sulfonium bromides on the support (Scheme 19) [48]. The approach was based on the alkylation reaction between the acetbromamide group in chitosan support and dialkylsulfide. The functionalization of chitosan with bromoacetyl chloride followed by alkylation of dialkylsulfide with the acetbromamide-functionalized chitosan produced the chitosan-supported sulfonium IL.

Apart from the in situ formation of sulfonium salts on the support, Guo and coworkers described an ion-exchange strategy to generate polymer-supported sulfonium ILs (Scheme 20) [49]. This approach was based on the ion-exchange reaction between sodium alkylsulfonate and sulfonium halides. The copolymerization of sodium 4-vinylbenzene sulfonate with other monomers generated a polymer support containing sodium benzenesulfonate, after which the ion exchange of the obtained polymer with a pre-synthesized sulfonium IL provided the polymer-supported

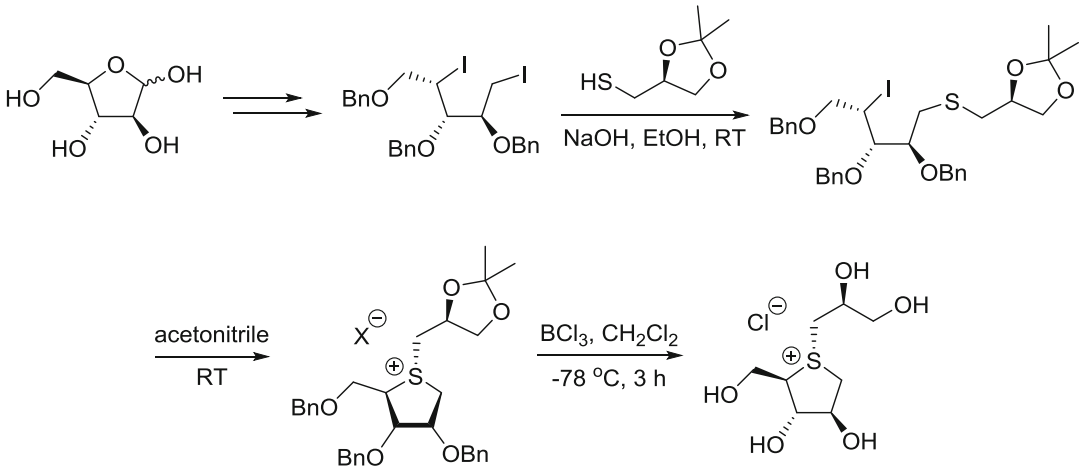

Sulfonium Ionic Liquids, Scheme 18 Synthesis of s chiral sulfonium salts via a coupling reaction between chiral thiol and a diiodide D-arabinose derivative

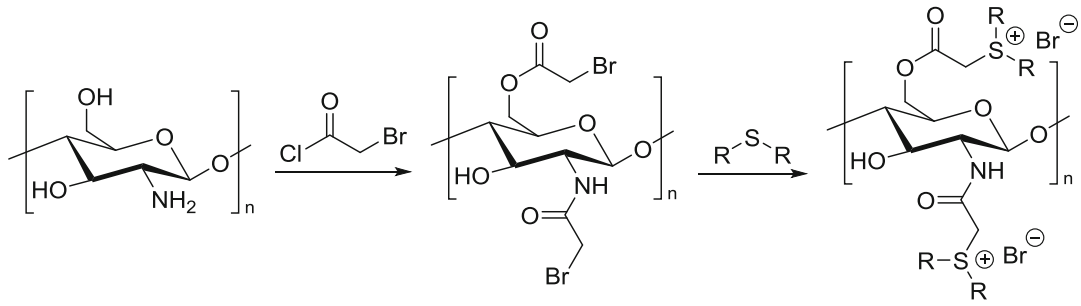

Sulfonium Ionic Liquids, Scheme 19 Synthesis of chitosan-supported sulfonium salts via in situ formation of sulfonium bromides

sulfonium IL. Upon varying sulfonium ILs, a series of supported sulfonium ILs could be obtained.

Synthesis of Sulfonium-Based Polymeric ILs

Sulfonium-based polymeric ILs combine the advantages of sulfonium IL and polymer. Unlike the polymer-supported sulfonium ILs in which the IL moiety is covalently bonded to a polymer surface, the sulfonium ILs in the latter are uniformly built in the polymer skeleton. This is commonly achieved by the polymerization of a vinyl-functionalized sulfonium IL with or without other monomers. For instance, Emrick's group prepared two vinyl-functionalized sulfonium ILs via alkylation of vinyl-functionalized thioether with 1,3-propane sultone [50]. The polymerization of the as-prepared vinyl-functionalized sulfonium ILs furnished the polymeric sulfonium sulfonates in the presence of a chain-transfer agent and initiator (Scheme 21).

Alternatively, the alkylation of a polymeric thioether with alkylation reagent can also lead to the formation of polymeric sulfonium ILs (Scheme 22) [51]. Here, the polymeric thioethers were prepared by the polymerization of vinyl-functionalized thioethers using a similar method with that of the vinyl-functionalized sulfonium ILs.

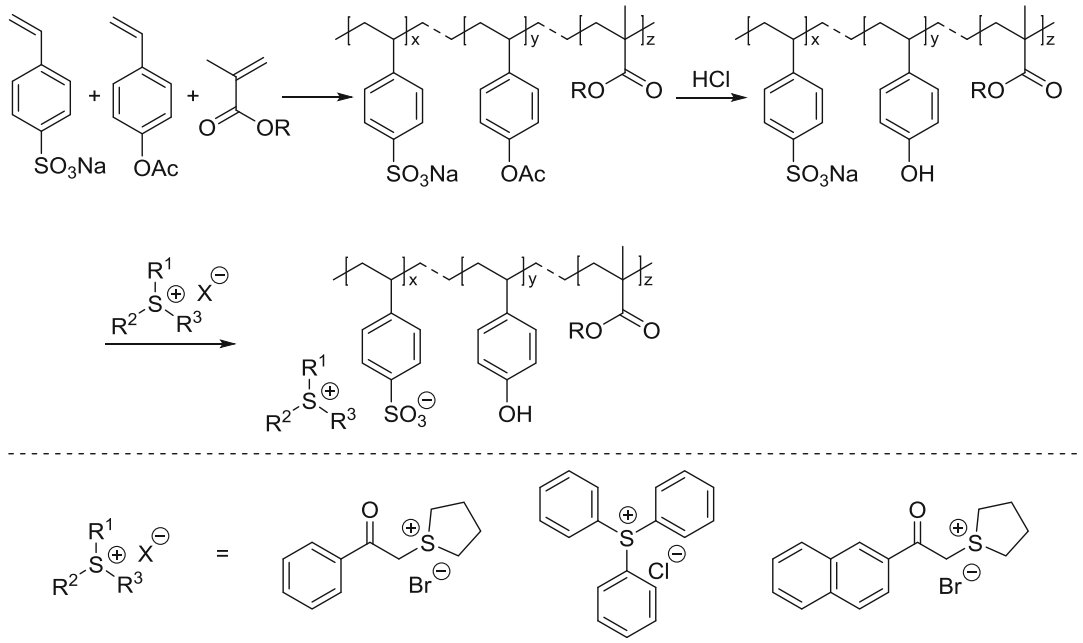

Sulfonium Ionic Liquids, Scheme 20 Synthesis of polymer-supported sulfonium salts via ion-exchange strategy

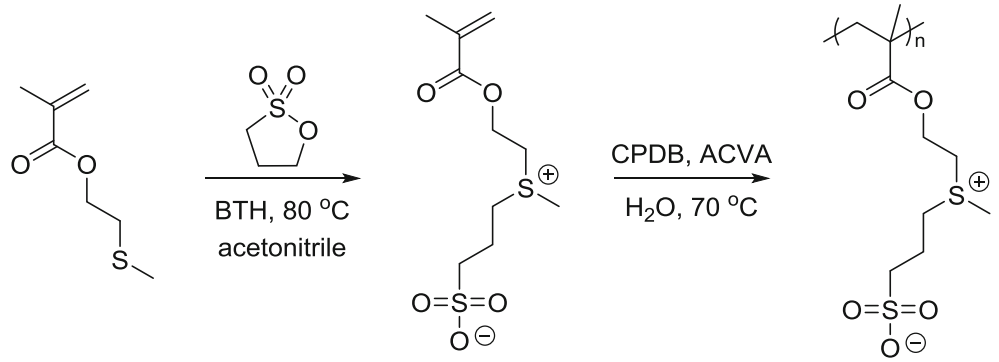

Sulfonium Ionic Liquids, Scheme 21 Synthesis of polymeric sulfonium ILs via polymerization of the vinyl-functionalized sulfonium ILs

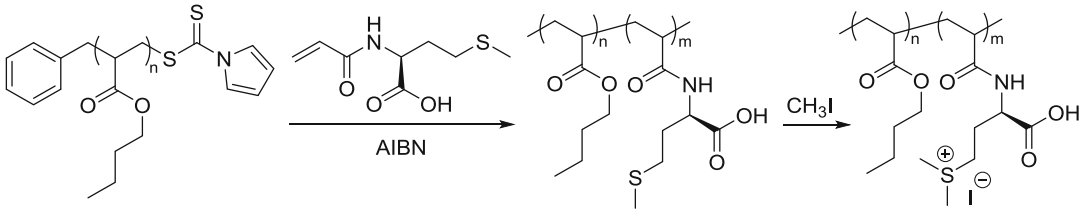

Sulfonium Ionic Liquids, Scheme 22 Synthesis of polymeric sulfonium ILs via alkylation of a polymeric thioether

Characterization of Sulfonium ILs

The standard techniques to characterize molecular sulfonium ILs are mass spectrometry (MS), nuclear magnetic resonance (NMR) spectroscopy, elemental analysis (EA), and Fourier transform infrared spectroscopy (FT-IR). Take triethylsulfonium bromide as an example, it can be detected using electrospray ionization-mass spectrometry (EI-MS), in which the m/z of triethylsulfonium cation would produce a peak in positive-ion mode at 119.1 while Br^- would produce a peak in the negative-ion mode at 78.9. Besides, NMR spectroscopy is employed to determine the structure of ILs. Both ^1H and ^{13}C NMR spectroscopy are often used to confirm the successful alkylation of the thioether with alkyl halide. Apparently, a slight downfield shift in the spectrum of the sulfonium cation would be observed when compared to the unreacted thioether. Elemental analysis (EA) provides C/H/N/S combustion analyses of sulfonium ILs which directly gives the relative content of C, H, N, and S in IL. On the other hand, FT-IR spectroscopy gives an observation of the structural change in the process of the formation of a sulfonium cation from thioether and alkyl halide, especially the formation of a functionalized sulfonium cation which contains a functional group (e.g., hydroxyl, carboxyl, amino) that has characteristic absorption peaks.

Separately, solid-state nuclear magnetic resonance (SSNMR), thermogravimetric analysis (TGA), elemental analysis (EA), and FT-IR are usually employed to characterize the supported and polymeric sulfonium ILs. SSNMR and FT-IR provide direct evidence for the successful incorporation of sulfonium ILs into solid materials based on the appearance of characteristic signals in the spectrum belonging to sulfonium ILs. EA and TGA are used to determine the loading amount of sulfonium ILs in solid materials. Besides, other common testing measures involving in solid material characterization, such as scanning/transmission electron microscope (SEM/TEM), X-ray diffraction (XRD), X-ray photoelectron spectroscopy (XPS), and energy-dispersive X-ray spectroscopy (EDS), are also used here to analyze the structural changes of the materials after being integrated with sulfonium ILs.

Summary

This chapter has summarized some of the recent achievements in the synthesis of sulfonium ILs. We have described the typical synthetic approaches to different sulfonium-based ILs including conventional phosphonium ILs, functionalized sulfonium ILs, supported sulfonium ILs, and polymeric sulfonium ILs. The alkylation of the thioethers with alkylating agents readily delivers the corresponding sulfonium salts. Besides, the structural diversity and designability of sulfonium cation and anion facilitate the fabrication of functionalized ILs which are capable of specific applications. Moreover, the alkylation of thioethers with halogenoalkyl-functionalized solid support and the ion exchange of sodium polystyrene sulfonate with molecular sulfonium ILs generate the supported sulfonium ILs, and the polymerization of vinyl-functionalized sulfonium ILs produces polymeric sulfonium ILs, broadening their potential applications in other fields. All these synthetic routes provide the basis for subsequent investigation in the function-related physicochemical properties.

Cross-References

- ▶ Design of Amino Acid ILs for Dissolution of Lignocellulosic Biomass
- ▶ Functional Ionic Liquid in Multicomponent Reaction, a Powerful Tool for C–C Bond Formation
- ▶ Immobilization of Ionic Liquids, Types of Materials, and Applications
- ▶ Ionic Liquid-Based Nano-Materials for Drug Delivery
- ▶ Metal Ion-Containing Ionic Liquid Catalysts on Solid Supports for Organic Reactions
- ▶ Task-Specific Ionic Liquids: Design, Properties, and Applications

References

1. Watanabe M, Thomas ML, Zhang S, Ueno K, Yasuda T, Dokko K (2017) Application of ionic liquids to energy storage and conversion materials and devices. Chem Rev 117:7190–7239
2. Armand M, Endres F, Macfarlane DR, Ohno H, Scrosati B (2009) Ionic-liquid materials for the electrochemical challenges of the future. Nat Mater 8:621–629
3. Navarra MA (2013) Ionic liquids as safe electrolyte components for li-metal and li-ion batteries. MRS Bull 38:548–553
4. Macfarlane DR, Tachikawa N, Forsyth M, Pringle JM, Howlett PC, Elliott GD, Davis JH, Watanabe M, Simon P, Angell CA (2014) Energy applications of ionic liquids. energy environ Sci 7:232–250
5. Sun H, Zhu G, Zhu Y, Lin M-C, Chen H, Li Y-Y, Hung WH, Zhou B, Wang X, Bai Y, Gu M, Huang C-L, Tai H-C, Xu X, Angell M, Shyue J-J, Dai H (2020) High-safety and high-energy-density lithium metal batteries in a novel ionic-liquid electrolyte. Adv Mater n/a:2001741
6. Martin S, Pratt Iii HD, Anderson TM (2017) Screening for high conductivity/low viscosity ionic liquids using product descriptors. Mol Inform 36:1600125
7. Buzzeo MC, Evans RG, Compton RG (2004) Non-haloaluminate room-temperature ionic liquids in electrochemistry—A review. ChemPhysChem 5:1106–1120
8. Gerhard D, Alpaslan SC, Gores HJ, Uerdingen M, Wasserscheid P (2005) Trialkylsulfonium Dicyanamides - A new family of ionic liquids with very low viscosities. Chem Commun 40:5080–5082
9. Luo S, Zhang Z, Yang L (2008) Lithium secondary batteries using an asymmetric sulfonium-based room temperature ionic liquid as a potential electrolyte. Chin Sci Bull 53:1337–1342
10. Zhang Q, Liu S, Li Z, Li J, Chen Z, Wang R, Lu L, Deng Y (2009) Novel cyclic sulfonium-based ionic liquids: Synthesis, characterization, and physicochemical properties. Chem Eur J 15:765–778
11. Orita A, Kamijima K, Yoshida M, Yang L (2010) Application of sulfonium-, thiophenium-, and thioxonium-based salts as electric double-layer capacitor electrolytes. J Power Sources 195:6970–6976
12. Guo L, Pan X, Zhang C, Wang M, Cai M, Fang X, Dai S (2011) Novel hydrophobic cyclic sulfonium-based ionic liquids as potential electrolyte. J Mol Liq 158:75–79
13. Matsumoto H, Matsuda T, Miyazaki Y (2000) Room temperature molten salts based on trialkylsulfonium cations and bis(trifluoromethylsulfonyl)imide. Chem Lett 29:1430–1431
14. Kaiser D, Klose I, Oost R, Neuhaus J, Maulide N (2019) Bond-forming and -breaking reactions at sulfur(IV): Sulfoxides, sulfonium salts, sulfur ylides, and sulfinate salts. Chem Rev 119:8701–8780
15. Wang D, Yu M, Liu N, Lian C, Hou Z, Wang R, Zhao R, Li W, Jiang Y, Shi X, Li S, Yin F, Li Z (2019) A sulfonium tethered peptide ligand rapidly and selectively modifies protein cysteine in vicinity. Chem Sci 10:4966–4972
16. Li Y, Lian C, Hou Z, Wang D, Wang R, Wan C, Zhong W, Zhao R, Wang Y, Li S, Yin F, Li Z (2020) Intramolecular methionine alkylation constructs sulfonium tethered peptides for protein conjugation. Chem Commun 56:3741–3744
17. Anaya LMB, Petitdemange R, Rosselin M, Ibarboure E, Garbay B, Garanger E, Deming TJ, Lecommandoux S (2020) Design of thermoresponsive elastin-like glycopolypeptides for selective lectin binding and sorting. Biomacromolecules. https://doi.org/10.1021/acs.biomac.0c00374
18. Arvai R, Toulgoat F, Langlois BR, Sanchez J-Y, Médebielle M (2009) A simple access to metallic or onium bistrifluoromethanesulfonimide salts. Tetrahedron 65:5361–5368
19. Yang L, Zhang Z, Gao X, Zhang H, Mashita K (2006) Asymmetric sulfonium-based molten salts with TFSI− or PF6− anion as novel electrolytes. J Power Sources 162:614–619
20. Guo L, Pan X, Wang M, Zhang C, Fang X, Chen S, Dai S (2011) Novel hydrophobic ionic liquids electrolyte based on cyclic sulfonium used in dye-sensitized solar cells. Sol Energy 85:7–11
21. Deyab MA (2019) sulfonium-based ionic liquid as an anticorrosive agent for thermal desalination units. J Mol Liq 296:111742
22. Lee C-P, Peng J-D, Velayutham D, Chang J, Chen P-W, Suryanarayanan V, Ho K-C (2013) Trialkylsulfonium and tetraalkylammonium cations-based ionic liquid electrolytes for quasi-solid-state dye-sensitized solar cells. Electrochim Acta 114:303–308
23. Han H-B, Nie J, Liu K, Li W-K, Feng W-F, Armand M, Matsumoto H, Zhou Z-B (2010) Ionic liquids and plastic crystals based on tertiary sulfonium and bis(fluorosulfonyl)imide. Electrochim Acta 55:1221–1226
24. Vasudevamurthy MK, Weatherley LR, Lever M (2005) enzyme stabilization using synthetic compensatory solutes. Biocatal Biotransformation 23:285–291
25. Baggiolini EG, Hennessy BM, Iacobelli JA, Uskokovic MR (1987) Stereospecific synthesis of the lythgoe's ring a aldehyde for the preparation of 1α-hdroxylated tachysterols and calciferols. Tetrahedron Lett 28:2095–2098
26. Nikolaev DN, Klimenicheva YS, Davidovich PB, Piotrovskii LB (2012) The use of solid phase synthesis for the preparation of monoadducts of fullerene C60. Russ Chem B+ 61:853–857
27. Zhao D, Fei Z, Ang WH, Dyson PJ (2007) Sulfonium-based ionic liquids incorporating the allyl functionality. Int J Mol Sci 8:304–315
28. Mei X, Yue Z, Tufts J, Dunya H, Mandal BK (2018) Synthesis of new fluorine-containing room temperature ionic liquids and their physical and electrochemical properties. J Fluor Chem 212:26–37
29. Coadou E, Goodrich P, Neale AR, Timperman L, Hardacre C, Jacquemin J, Anouti M (2016) Synthesis and thermophysical properties of ether-functionalized sulfonium ionic liquids as potential electrolytes for

electrochemical applications. ChemPhysChem 17:3992–4002
30. Lee SH, Lim YD, Seo DW, Hossain MA, Jang HH, Lee HC, Kim WG (2013) Novel cyclic sulfonium iodide containing siloxane high performance electrolyte for dye-sensitized solar cell. J Ind Eng Chem 19:322–326
31. Venker A, Vollgraff T, Sundermeyer J (2018) Ferrocenyl-sulfonium ionic liquids – synthesis, characterization and electrochemistry. Dalton T 47:1933–1941
32. Nakata T, Nakatani M, Takahashi M, Okai J, Kawaoka Y, Kouge K, Okai H (1996) Properties and reactivities of (p-hydroxyphenyl)benzylmethylsulfonium salts for direct benzyl esterification of n-acylpeptides. Bull Chem Soc Jpn 69:1099–1106
33. Jin M, Wu X, Malval JP, Wan D, Pu H (2016) Dual roles for promoting monomers to polymers: A conjugated sulfonium salt photoacid generator as photoinitiator and photosensitizer in cationic photopolymerization. J Polym Sci Polym Chem 54:2722–2730
34. Li L, Jia D, Wang H, Chang C, Yan J, Zhao ZK (2020) Synthesis of sulfonium N-chloramines for antibacterial applications. New J Chem 44:303–307
35. Yang J, Jiang M, Jin Y, Yang H, Fu H (2017) Visible-light photoredox difluoromethylation of phenols and thiophenols with commercially available difluorobromoacetic acid. Org Lett 19:2758–2761
36. Xu P, Zhao D, Berger F, Hamad A, Rickmeier J, Petzold R, Kondratiuk M, Bohdan K, Ritter T (2020) Site-selective late-stage aromatic [18F]Fluorination via aryl sulfonium salts. Angew Chem Int Ed 59:1956–1960
37. Huang C, Feng J, Ma R, Fang S, Lu T, Tang W, Du D, Gao J (2019) Redox-neutral borylation of aryl sulfonium salts via C–S activation enabled by light. Org Lett 21:9688–9692
38. Tian Z-Y, Zhang C-P (2019) Ullmann-type N-arylation of anilines with alkyl(aryl)sulfonium salts. Chem Commun 55:11936–11939
39. Varga B, Gonda Z, Tóth BL, Kotschy A, Novák Z (2020) A Ni–Ir dual photocatalytic liebeskind coupling of sulfonium salts for the synthesis of 2-benzylpyrrolidines. Eur J Org Chem 2020:1466–1471
40. Kumar A, Gupta AK, Devi M, Gonsalves KE, Pradeep CP (2017) Engineering multifunctionality in hybrid polyoxometalates: Aromatic sulfonium octamolybdates as excellent photochromic materials and self-separating catalysts for epoxidation. Inorg Chem 56:10325–10336
41. Taniki R, Matsumoto K, Hagiwara R (2012) Trialkylsulfonium fluorohydrogenate giving the highest conductivity in room temperature ionic liquids. Electrochem Solid-State Lett 15:F13
42. Maji T, Banerjee S, Bose A, Mandal TK (2017) A stimuli-responsive methionine-based zwitterionic methacryloyl sulfonium sulfonate monomer and the corresponding antifouling polymer with tunable thermosensitivity. Polym Chem 8:3164–3176
43. Mcauliffe CA, Perry WD (1974) Transition metal complexes of the zwitterionic amino acid DL-methylsulfoniummethioninate and of the amido acid derived from it by facile amine deprotonation. Inorg Chim Acta 10:215–220
44. Forbes DC, Standen MC, Lewis DL (2003) Sulfur ylides via decarboxylation of carboxymethylsulfonium betaines: A novel and mild protocol for the preparation of oxiranes. Org Lett 5:2283–2286
45. Lu L, Li X, Yang Y, Xie W (2019) Frontispiece: recent progress in the construction of natural de-o-sulfonated sulfonium sugars with antidiabetic activities. Chem Eur J 25:13458–13471
46. Trottmann F, Ishida K, Franke J, Stanišić A, Ishida-Ito M, Kries H, Pohnert G, Hertweck C (2020) Sulfonium acids loaded onto an unusual thiotemplate assembly line construct the cyclopropanol warhead of a burkholderia virulence factor. Angew Chem Int Ed 59:1–6
47. Huang Y, Gao Y, He W, Wang Z, Li W, Lin A, Xu J, Tanabe G, Muraoka O, Wu X, Xie W (2019) Practical route to neokotalanol and its natural analogues: sulfonium sugars with antidiabetic activities. Angew Chem Int Ed 58:6400–6404
48. Sun X, Zhang J, Chen Y, Mi Y, Tan W, Li Q, Dong F, Guo Z (2019) Synthesis, characterization, and the antioxidant activity of carboxymethyl chitosan derivatives containing thiourea salts. Polymers 11:1810
49. Wang Q, Zhang C, Yan C, You F, Wang L (2019) One-component chemically amplified resist composed of polymeric sulfonium salt pags for high resolution patterning. Eur Polym J 114:11–18
50. Santa Chalarca CF, Emrick T (2017) Reactive polymer zwitterions: Sulfonium sulfonates. J Polym Sci Polym Chem 55:83–92
51. Imamura R, Mori H (2019) Protein-stabilizing effect of amphiphilic block copolymers with a tertiary sulfonium-containing zwitterionic segment. ACS Omega 4:18234–18247

Supported Ionic Liquids

Wentao Bi[1] and Hongdeng Qiu[2]
[1]Jiangsu Collaborative Innovation Center of Biomedical Functional Materials, Jiangsu Key Laboratory of Biomedical Materials, College of Chemistry and Materials Science, Nanjing Normal University, Nanjing, China
[2]CAS Key Laboratory of Chemistry of Northwestern Plant Resources and Key Laboratory for Natural Medicine of Gansu Province, Lanzhou Institute of Chemical Physics, Chinese Academy of Sciences, Lanzhou, China

Introduction

Supported ionic liquids (SILs) consist of two components: the support material and the ionic liquid (IL), and there are various types of each.

SIL preparation can be divided into two strategies according to the interactions between the IL and support. The first method is a noncovalent preparation strategy, where ILs adsorb onto either the surface or pores of a support with a high specific surface area. In this case, there are only weak interactions, such as van der Waals forces, hydrogen bonding, and π-π interactions, between the support and the IL. Such materials are greatly affected by the surrounding environment, and their reusability is not ideal. The second method is referred to as a covalent preparation strategy, where the support and IL are connected by covalent bonds. The SILs prepared by this strategy have higher stability and better reusability than those prepared by the first method, but this second preparation process is more complicated. SIL preparation methods vary widely depending on the support being used, especially in covalent preparation methods. This entry focuses on SIL preparation strategies, and their corresponding characterization methods, based on commonly used supports: silica, polymers, carbon nanomaterials, metal-organic frameworks (MOFs), and clays.

Synthesis of Supported ILs

Silica-Supported ILs (SSILs)

Most supports used in SILs are porous silica gels and silica-based materials because they have large specific surface areas that allow them to carry more ILs. Various methods have been developed for preparing these silica-supported ILs. The simplest of these is a noncovalent method where the SSILs are fabricated by adsorption of the ILs to the silica surface. Alternatively, they can be prepared by a covalent method, where the ILs are anchored to the surface through bonding or grafting.

Noncovalent Preparation of SSILs

Generally, a specific ratio of the IL and silica support is mixed in a suitable solvent, and then the solvent is removed by evaporation or freeze-drying to obtain the SSIL. However, this method has some shortcomings, the most prominent being that the ILs on the prepared surface are easily lost when the SSILs are used. Unfortunately, this is a problem that most noncovalently prepared SSILs encounter. Additional issues arise when the solvent used in this process forms azeotropes or eutectic solutions with the ILs, which results in the solvent not being completely removed that subsequently impedes any research. However, large quantities of SSILs can be achieved using fluidized bed spray-coating technology, where the silica supports are fluidized by a temperature-controlled gas flow (such as air, nitrogen, or argon), and then the IL solution is added, where it passes through the nozzle and is sprayed onto the material (Scheme 1) [1]. Simultaneously, the gas flow ensures that the solvents are rapidly evaporated. Silica-based materials with three-dimensional mesoporous structures can also be fabricated by a strategy known as the "ship-in-bottle" method. This method mixes alkyl imidazoles (or similar compounds), haloalkanes, and three-dimensional mesoporous materials (such as SBA-16 and MCM-48), where they are heated and react to generate the ILs. The molecular size of the produced ILs is made to be larger than the pore size, which traps them in the holes. Furthermore, this method successfully solved the problem of IL leaching in noncovalently prepared SSILs.

Nitrogen adsorption is commonly measured when characterizing these SSILs because it can indicate any decrease in the surface area and pore size of the prepared SSILs compared to those of the original porous silica material, which only occurs when the ILs are covering the silica surface. In addition, the compositions of ILs and silica are quite different; therefore, their characteristic peaks can be identified by infrared (IR) and solid nuclear magnetic resonance (NMR) spectroscopy methods to determine if the SSILs were successfully prepared. Scanning electron microscopy (SEM) can also be used to directly observe SSILs, and due to the conductivity of ILs, no electric local charge is formed, which is helpful when using this type of instrumentation. Thermogravimetric analysis (TGA) is also a powerful characterization method, because silicon dioxide is stable at high temperatures while ILs decompose. This reduces the weight of the SSILs, and the amount of ILs that had been

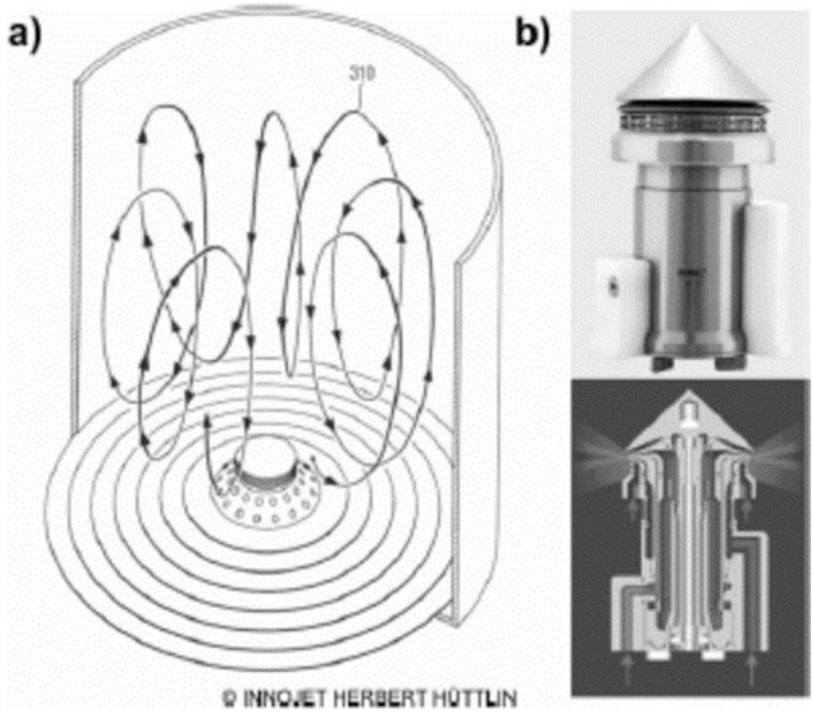

Supported Ionic Liquids, Scheme 1 (**a**) Schematic drawing of the toroidal movement of particles in the Aircoater IAC5; (**b**) photograph of the spraying nozzle (top) and cross-section of the nozzle, indicating the two flows (bottom) [1]

loaded on the surface can be estimated by this mass reduction. Elemental analysis can also be used to quantitatively analyze the IL loading amount by analyzing the amount of nitrogen in the SSILs. Since silica contains no nitrogen and most of the ILs do, the amount of ILs can be calculated.

Covalent Preparation of the SSILs

For all covalently prepared IL-modified silica gels, the first step requires a strong acidic aqueous solution (usually nitric acid or hydrochloric acid) to activate the silica particles. This increases the silanol group content on the silica surface and eliminates metal oxides and nitrogen-containing impurities. Next, these activated silica particles can be reacted with a silane coupling agent, such as 3-chloropropyltrimethoxysilane or 3-chloropropyltriethoxysilane, in dry toluene to obtain chloropropyl silica, which would be subsequently reacted with an alkyl imidazole or other similar compound to produce the SSILs [2]. The reaction efficiency when using a trimethoxysilane coupling agent is higher than when a triethoxysilane agent is used, which is due to the smaller steric hindrance of the former. The chloride ions of the ILs can then undergo ion-exchange with anions on the silica surface to obtain the desired surface-confined ILs. Alternatively, the silane coupling agent and imidazole (or any imidazole derivative) can be reacted first, and then the generated ILs can react with the activated silica particles. However, the reaction conditions and purity of the synthesized IL silane coupling reagent should be strictly controlled. Another option is to first bond the IL anions to the silica gel surface and then connect the IL cations through ionic interactions. For example, acidic $[Al_2Cl_7]$ anions would react with the free hydroxyl groups on the surface to form an anionic solid surface, which is then connected to the IL cation. The disadvantage of this route is that the material is relatively unstable in ionic solutions. For all three of these methods, the bonding density of the imidazolium silica decreased as the chain length of the alkyl branches of the imidazoles

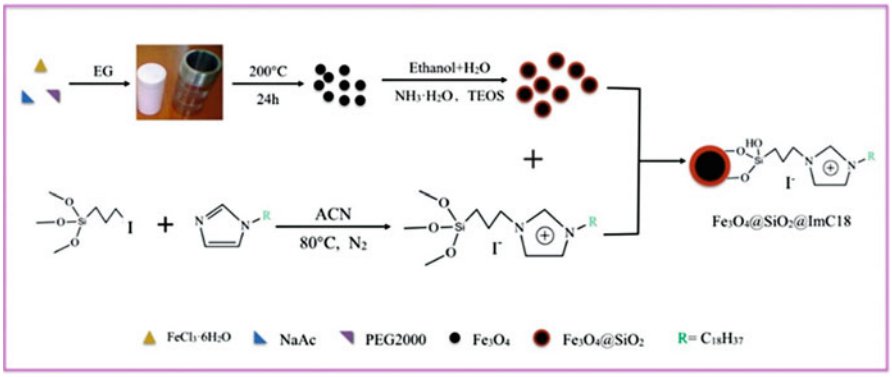

Supported Ionic Liquids, Scheme 2 Schematic diagrams of $Fe_3O_4@SiO_2@ImC18$ synthesis procedure and adsorption process [3]

increased, which could be ascribed to the steric hindrance caused by this chain lengthening. Furthermore, these methods can be used to modify the surface of magnetic material covering the silica shell (Scheme 2) [3].

The use of ordered mesoporous silica materials for covalent SSIL preparations has gradually increased in recent years, owing to their adjustable pore size. Similar to IL-modified silica gel, these mesoporous silica materials can also be modified by the three aforementioned covalent methods. However, unlike silica gel, mesoporous silica-based SSILs can be prepared by in situ condensation of an IL silane coupling reagent and tetraethoxysilane by the gel-gel method. However, the addition of the ILs will affect the surfactant template performance for preparing mesoporous silica, and thus the pore size, so the reaction conditions should be regulated.

Poly(ionic liquid) (PIL)-modified silica is another important SSIL that overcomes an issue faced by other silica-based materials: the lack of functional groups on the silica surface. For preparing this kind of material, in situ, free radical polymerization is commonly used. This method usually requires the sulfhydryl or unsaturated double bond groups on the silica surface to be modified to achieve covalent connection between the PILs and the silica (Scheme 3) [4]. The characterization methods of covalently prepared SSILs are similar to those used to characterize noncovalently prepared SSILs. Although it is theoretically necessary to verify the covalent bond between the IL and the silica-based materials, most of these bonds are Si-O bonds, which are difficult to be characterized.

Polymer-Supported Ionic Liquids (PSILs)

Combining ILs with polymers, PSILs can be prepared and used in organic catalytic reactions, membrane and chromatographic separations, and battery electrolytes. There are two kinds of methods to prepare PSILs: noncovalent and covalent. Covalent methods attach ILs on polymers through covalent bonds, whereas noncovalent methods load the polymers by adsorption. Compared with the covalent methods, noncovalent methods have some disadvantages, such as poor stability and easy loss of ILs during use [5].

Noncovalent Preparation of PSILs

PSILs prepared by noncovalent methods are usually used for membrane separation. Generally, the preparation process involves placing the porous membrane in a vacuum dryer to remove any water and air from the holes, then adding the ILs into the membrane or loading the ILs on the membrane under pressurized or vacuum conditions, and finally wiping off any excess ILs on the membrane surface with a thin paper. Most of the ILs used are hydrophobic ILs with hexafluorophosphate or bis (trifluoromethylsulfonimide) anions, whereas the membranes are mainly hydrophobic ones such as polyfluoroethylene, hydrophobic nylon, and

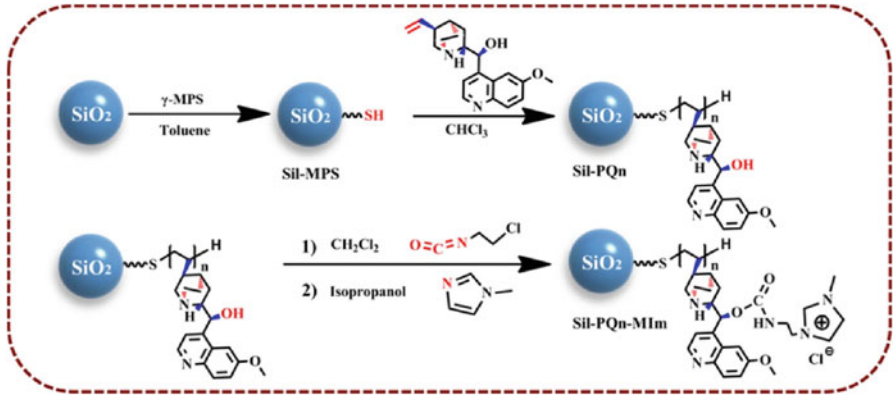

Supported Ionic Liquids, Scheme 3 Schematic diagram for the preparation of Sil-PQn and Sil-PQn-MIm [4]

polypropylene fiber membranes. Although IR, NMR, UV-vis, and SEM can be used for the characterization of these materials, most of the papers have less complete characterization [6].

Covalent Preparation of PSILs

PSILs prepared by covalent methods are also known as poly(ionic liquid)s (PILs). PILs are composed of covalently linked IL species and have the characteristics of macromolecules, thus cleverly combining some of the unique properties and functions of ILs with those of polymers (such as ease of processing and shape durability). There are generally two strategies for synthesizing PILs: synthesis of PILs with cationic moieties in the polymer backbone, and synthesis of PILs with anionic moieties in the polymer backbone (Scheme 4) [7]. For the first strategy, the most commonly used method is to synthesize polymer backbones with IL cations by a chain-growth polymerization method and then to change the anions of the PILs by ion exchange. A large variety of cations and anions in IL chemistry can be used for the polymers. Cations such as imidazolium, pyridinium, pyrrolidinium, ammonium, and phosphonium have been used, and the utilized anions can be categorized into carboxylates, sulfonates, sulfonamides, and inorganic types. In addition to the traditional free radical polymerization method for the polymerization of IL cations with double bonds, these PILs can be synthesized by using methods such as atom transfer radical, reversible addition-fragmentation transfer, ring-opening, and ring-opening metathesis polymerizations. Most PILs are polymerized in bulk or in solution. PILs can also be synthesized in emulsions or dispersion media. In addition to linear homopolymers, bi- or trifunctional acrylic or styrene-based IL monomers can be added to synthesize PILs with cross-linked networks by free radical polymerization. PILs with three-dimensional cross-linked networks can also be synthesized by using alkoxysilane-functionalized IL monomers in acid- or base-catalyzed sol–gel polycondensation reactions. Although these methods of synthesizing the IL monomer first and then generating the polymer have many advantages, they involve a number of organic synthesis and purification steps at the monomer level and require the polymerization conditions of each individual monomer to be controlled. Therefore, postsynthetic methods have been used to prepare PILs; that is, polymer backbones containing imidazole or pyridine were first synthesized and then treated with halogenated alkanes to generate the PILs, or polymer backbones with halogenated alkyl functional groups were synthesized and then treated with imidazole or pyridine to form PILs (Scheme 5) [8]. This method reduces the difficulty of monomer preparation, but it still cannot be guaranteed that all imidazole or pyridine moieties in the polymer will be converted into ILs. Far fewer PILs have been synthesized with the second synthesis method than with the first. This may be a result of the difficulty in synthesizing anionic monomers

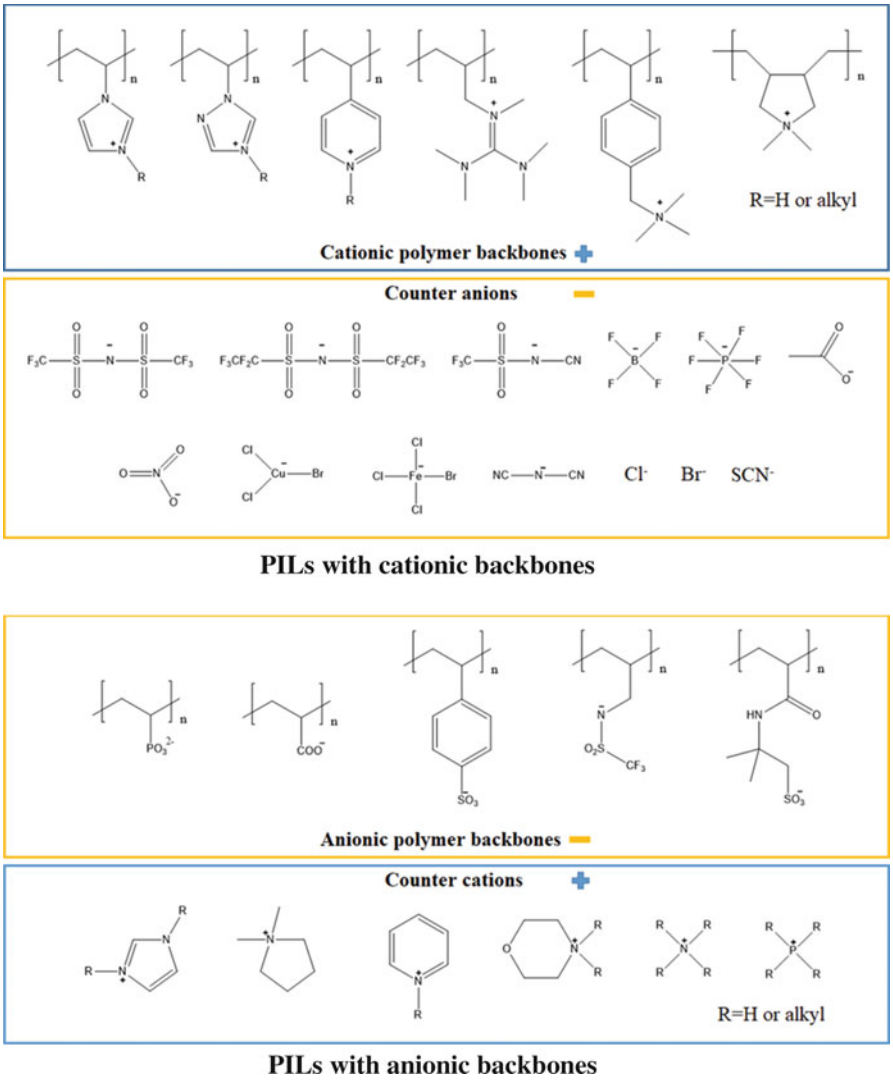

Supported Ionic Liquids, Scheme 4 Typical chemical structures of PILs

that can be used to form ILs. The PILs have backbones such as poly(vinyl sulfonate), poly (acrylamido)-2-methylpropane sulfonate, poly (styrene sulfonate), poly(acrylic acid), and poly (phosphonic acid), and the counter cations combined with them to form ILs are mainly of the alkylimidazole, alkylpyridine, or tetra-alkylammonium type. On the basis of these two strategies, ILs can be polymerized with other functional monomers, or IL cationic and anionic monomers can be polymerized to form random and block polymers, thereby improving their performance.

Infrared (IR) spectroscopy is the most commonly used method for characterizing PILs, and the characteristic peaks of the ILs can be observed. X-Ray diffraction (XRD), scanning electron microscopy (SEM), and transmission electron microscopy (TEM) are mostly used to observe the morphology of PILs. Differential scanning calorimetry (DSC) and thermogravimetric analysis (TGA) can be used to study the thermal performance of the PILs. If only the ILs in the polymer contain N, S, and O, elemental analysis can also be used to characterize PILs. For the synthesis of PILs by using the first method, the

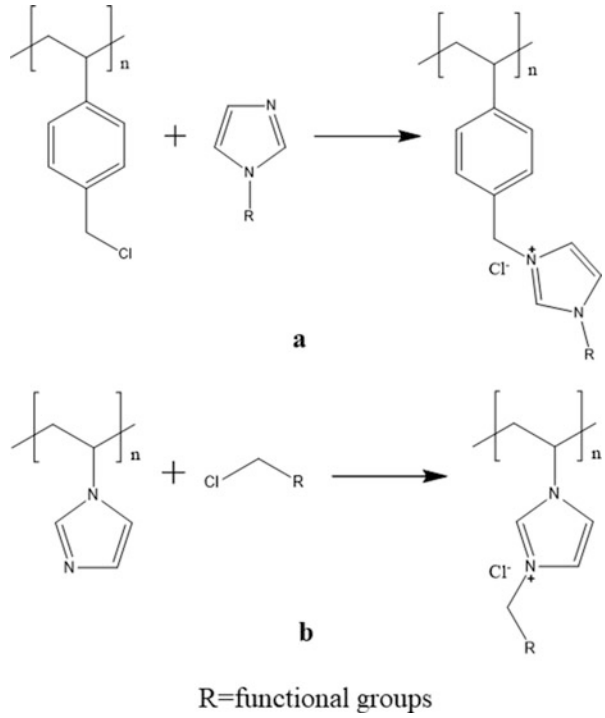

Supported Ionic Liquids, Scheme 5 Postsynthetic methods for preparation of PILs

IL monomers used should be characterized by 1H and 13C NMR spectroscopy to confirm their successful synthesis and purity [9]. Size exclusion chromatography can be used to measure the molecular weight of PILs, but this method cannot be used to measure the molecular weight of cross-linked PILs.

Carbon Nanomaterials Supported ILs (CNMSILs)

Carbon nanomaterials (CNMs: carbon nanotubes, graphene, and graphene oxide) have unique structures on the nanometer scale, with large specific surface areas and unique thermal, mechanical, or electronic properties. Owing to these structural and performance characteristics, CNMs are widely used in the fields of adsorption, catalysis, and electrochemistry. In addition, there are strong interactions (such as π–π interactions, van der Waals forces, and hydrophobic interactions) within the CNMs and with their target compounds; however, this also makes them difficult to disperse in some solvents, which limits their application. ILs possess the characteristics of miscibility, electrical conductivity, and high thermal stability, and their inherent properties (such as hydrophobicity, hydrophilicity, and polarity) can be changed by selection of the cation and anion components. Therefore, the combination of CNMs with ILs can compensate for the CNM defects, enhance the physical and chemical properties, and increase the scope of application. Generally, according to reports in the literature, the preparation of CNMSILs can be also divided into two types, noncovalent and covalent, according to the interactions between them (Scheme 6) [10].

Noncovalent Preparation of CNMSILs

Noncovalent preparation modifies the surface of CNMs through physical action and is simple and nondestructive. The main mechanism is cation–π, π–π, or dipole–π interactions between the imidazolium cations of the ILs and the π network of the CNMs. The interactions between the CNMs and ILs are weak, and the ILs will gradually be lost when they are used, but this method provides

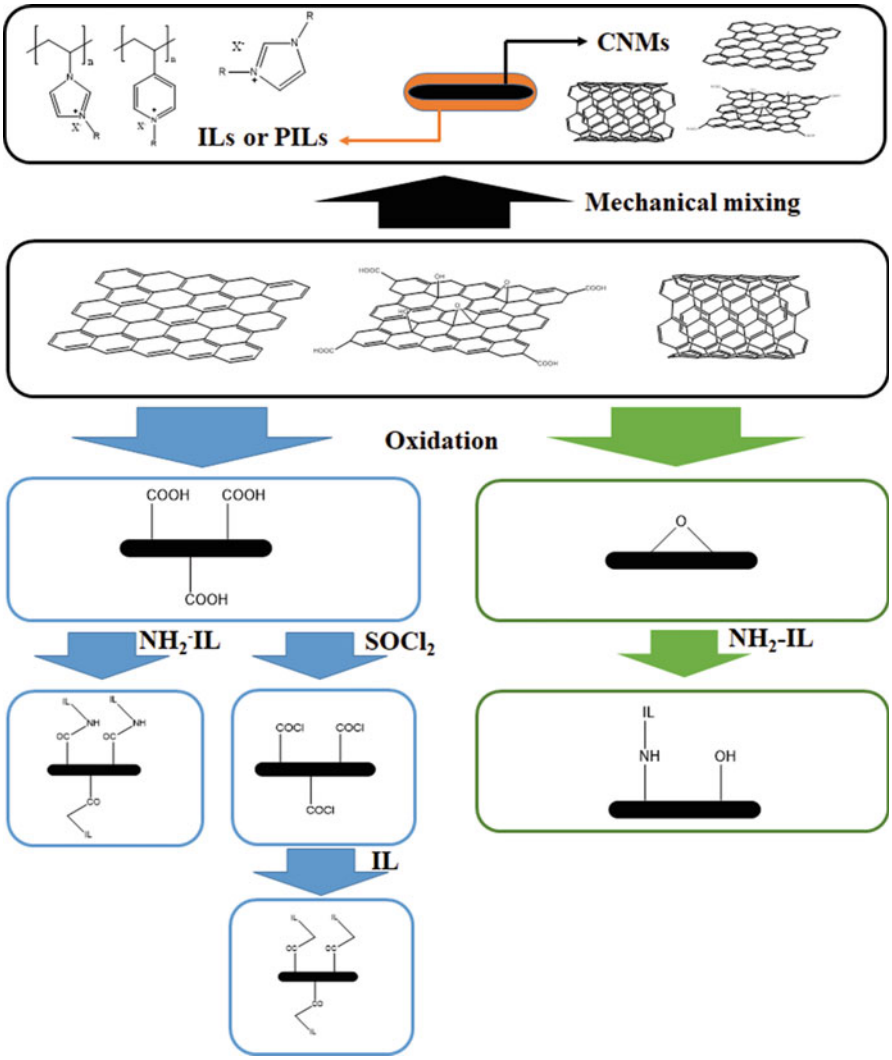

Supported Ionic Liquids, Scheme 6 Scheme of functionalization of CNMs with ILs

a convenient method for surface modification of CNMs without destruction of the chemical structure. Generally, CNMs and ILs are mixed in an appropriate ratio, and the mixture is sonicated or vigorously stirred in a mortar until a uniform material is obtained. It was first reported that imidazolium-based ILs and single-walled carbon nanotubes (SWCNTs) were ground to form thermally stable gels (so-called "bucky gels") [11]. In these gels, the bundles of severely entangled nanotubes were stripped into thinner bundles or even individual tubes. The interactions between the ILs and SWCNTs improved the dispersion of the SWCNTs in the ILs. According to the phase transition and rheological properties of the gels, it is speculated that bucky gels are formed by physical cross-linking of the SWCNTs, mediated by the local molecular order of the ILs. Composite materials of graphene (G)/graphene oxide (GO) and ILs can also be formed by grinding their mixtures. ILs can be adsorbed on the surface through noncovalent interactions with G or GO. Moreover, similar to that of CNTs, the dispersibility of G/Go in ILs is enhanced as a result of interactions between G/Go and ILs. Therefore, this method can also be used to

exfoliate graphite into graphene sheets or to prepare graphene-based dispersions by using ILs [12]. Although the mechanic method is very simple and the CNMILs prepared are thermally stable, these composite materials are prone to leaching and morphological changes during using.

Functionalization of CNMs with PILs instead of ILs can improve their stability, processability, and durability. PIL and CNM composites can be prepared by in situ polymerization or solution mixing [13]. The first method involves mixing CNMs and IL monomers and using 2,2-′-azobisisobutyronitrile as an initiator to perform in situ free radical polymerization of IL monomers on the surface of the CNMs. The second method is to directly and mechanically mix CNMs with presynthesized PILs. This method is similar to the above method for preparing CNM-supported ILs, except that PILs are used instead of ILs. For the combination of noncovalently functionalized multiwalled carbon nanotubes (MWCNTs) with PILS, it was found that in situ polymerization can form a uniform polymer coating on the MWCNT surface, which makes the nanotubes disperse better, whereas the solution mixing method does not achieve uniform functionalization on the MWCNT surface. This is because PILs with larger volumes and molecular weights do not disperse well in solution with the MWCNTs, and the PILs also have larger steric hindrance, which affects the functionalization of the MWCNTs. These preparation methods can also be used to modify SWCNTs and graphene sheets with PILs. In addition, through functional group modification of the PILs and CNMs, new noncovalent forces, such as hydrogen bonding and electrostatic forces, can be generated to improve the modification of the CNMs with PILs. Tunable changes in hydrophobicity or hydrophilicity of CNM-supported PILs can be realized by anion-exchange reactions with PILs on the surface of CNMs.

The amount of ILs or PILs grafted onto the CNMs can be determined by TGA in air and an inert atmosphere. The thermal decomposition of ILs and PILs in air is basically complete below 500 °C, whereas the thermal stability of CNMs is better at this temperature. When ILs or PILs are attached to CNMs, the thermal stability of the CNMs decreases. ILs and CNMs are prepared by noncovalent interactions, so SEM and TEM can be used to observe directly whether CNMs have been successfully modified with ILs or PILs. Energy-dispersive X-ray spectroscopy (EDX) with a copper grid as a substrate can also provide strong support. The N peaks in the EDX spectrum of the functionalized CNMs are caused by ILs or PILs.

Covalent Preparation of CNMSILs

As mentioned before, owing to the weak interactions, CNMs noncovalently functionalized with ILs often encounter leaching problems when exposed to solvents. To solve this problem, a covalent functionalization method has been developed. Unlike noncovalent functionalization, covalent attachment reduces the loss of ILs during use and leads to high thermal and chemical stability, as well as excellent durability. However, this method requires several functional steps, which destroy the CNM structure, interrupt the π network of the CNMs, and reduce the CNM mechanical and electrical performance. It is controversial whether the ILs are still real liquids once they are chemically combined with the CNMs. However, the unique properties of the ILs and CNMs remain in the CNMSILs. Generally, covalent functionalization oxidizes the surfaces of the CNMs and connects the ILs to the surfaces through chemical reactions. Surface oxidation of CNMs produces a large number of functional groups, such as hydroxy, carboxyl, and epoxy groups, through strongly oxidizing acid treatment. Thereafter, ILs are introduced onto the surface of oxidized CNMs through chemical bonds. Covalent functionalization of CNMs and ILs can usually be achieved through condensation and nucleophilic ring-opening reactions.

Condensation functionalization can be performed in two ways: ILs can be directly grafted onto the surface of CNMs, or they can be generated on the surface of CNMs after imidazole grafting [14]. For the first method, amine- and hydroxy-terminated ILs are first prepared, and then the functional groups on the surface of the CNMs are oxidized to carboxyl functional

groups. However, the two cannot react directly. Only when the carboxylic acid group on the surface of the CNM is activated by thionyl chloride or *N*,*N*′-dicyclohexylcarbodiimide in *N*, *N*-dimethylformamide, can the condensation reaction occur. In the second method, imidazoles are partially grafted onto the surface of the CNMs with covalent bonds and then treated with alkyl halides or compounds containing halogenated alkyl groups to generate the corresponding CNM-supported ILs. This method avoids the purification of ILs, and the reproducibility is better than that of the first method. Nucleophilic ring-opening reactions can be achieved by attack of the epoxy group of GO with amine-terminated ILs. Compared with the other methods, this reaction occurs easily. Because GO has a large number of reactive epoxy groups, this method is mostly used to introduce ILs into GO. In general, condensation reactions can be applied to the covalent functionalization of most CNMs, whereas nucleophilic ring-opening reactions are mainly used for GO.

XRD analysis can be carried out to characterize the CNMSILs. It is worth noting that no obvious peaks attributed to CNMs could be found for IL-functionalized CNMs. In addition to the characterization methods for noncovalently prepared CNMSILs, IR spectroscopy and X-ray photoelectron spectroscopy (XPS) can also be used to determine whether CNMs modified with ILs generate new IL characteristic peaks [15].

MOF-Supported ILs (MSILs)

To make ILs widely applicable, the concept of impregnating porous supports with ILs has been proposed. As a new host material for ILs, metal–organic frameworks (MOFs) have great potential for tuning the properties of ILs through interactions between the host and guest. The preparation of such materials can be divided into noncovalent and covalent methods.

Noncovalent Preparation of MSILs

Combinations of MOFs and ILs were first obtained from ionthermal syntheses in which ILs were used as solvents. Ionthermally synthesized MOFs usually have a negatively charged framework, and the IL cations remain in the MOF as counter ions to maintain electrical neutrality. Owing to strong host–guest interactions, the cations are embedded in the MOFs in an ordered structure. However, because the IL cations strongly bind to the MOFs, these cations in synthetic MOFs are not considered to have the same useful properties as the original ILs. In addition, the choice of ILs and MOFs that can be used for ionthermal synthesis is limited, which restricts the widespread use of these MSILs [16].

In addition to this in situ impregnation method, several strategies for postsynthesis impregnation have been developed. For MOFs with coordinated unsaturated sites, IL-modified MOFs can be prepared by mixing alkaline ILs with them. Taking HKUST-1 as an example, the amino-functionalized IL ([AIL][OH]) and HKUST-1 powder were mixed in [AIL][OH] ethanol solution and stirred at room temperature. HKUST-1 has coordinated unsaturated sites, which cause the [AIL][OH] ions to be pinned by the lewis acid. Excess [AIL][OH] can be removed by filtration and solvent washing. Another strategy is tandem postsynthesis modification. This ship-in-bottle process can effectively confine ILs to the channels of MOFs. In this way, brønsted acidic ILs have been confined in the mesopores of Cr-MIL-101. N–Cr coordination occurs between coordinated unsaturated sites of Cr-MIL-101 and N-heterocyclic compounds containing two nitrogen atoms (triethylenediamine or imidazole). Subsequently, 1,4-butane sultone was added to react with the N-heterocyclic compounds to generate the ILs. Finally, after addition of H_2SO_4, the anions of the ILs are exchanged with HSO_4^-. In a third strategy, ILs are introduced into the pores of MOFs by capillary action. This method only requires the ILs to be mixed with the MOFs; the ILs enter the pores of the MOFs through physical action, and diffusion is enhanced by capillary action. The advantage of this strategy is that it can be widely used with various types of ILs and MOFs, but the obvious disadvantage is that the ILs are easily leached from the MOFs during use [16].

Nitrogen adsorption or IR absorption measurements were performed to confirm the presence of ILs in the pores of MOFs after impregnation by

using these strategies. Nitrogen adsorption isotherms and pore-size distributions indicate that the pore volumes of the MOFs decrease after the addition of ILs, indicating that IL molecules are present in the pores of the MOFs. In addition, the observed IR spectrum shows C=N, C=C, and C–N stretching bands, which can also indicate the presence of nitrogen heterocycles in ionic liquids. However, this characterization method is not very accurate because these stretching bands may also exist in the MOFs. Beside these characterization techniques, analysis of the observed XRD patterns by the maximum entropy method (MEM) and Rietveld refinement is a useful characterization technique. MEM analysis enables visualization of the electron density of guest molecules included in porous materials from the observed XRD patterns. Before the introduction of the ILs, there is no obvious charge density in the pores of the MOFs, indicating that the MOFs do not contain guest molecules. By contrast, apparent electron density peaks appeared in the pores of the MOFs after the introduction of the ILs, indicating that the ILs have successfully entered the pores of the MOFs.

Covalent Preparation of MSILs

To immobilize ILs on MOFs, it is usually necessary to prepare MOFs (such as UiO-66, and MIL-101) with amino groups (NH2-MOFs) by a mild hydrothermal process. The ILs can then be directly grafted onto the NH2-MOFs (Scheme 7), or they can be generated on the NH2-MOFs after imidazole grafting (Scheme 8) [17]. In the first method, the NH2-MOFs react directly with ILs containing carbonyl groups through coupling reactions. Fourier-transform IR spectroscopy and XPS analysis were used to monitor the molecular interactions and functionalization of the material. By comparison with those in NH2-MOFs, the characteristic peaks of imidazole, C=N, and N–H bonds in IL-MOFs after impregnation can confirm the coupling of ILs with the NH2-MOFs. In addition, the presence or absence of characteristic peaks corresponding to the IL anions can also be observed after synthesis. TGA of IL-MOFs showed an initial weight loss of around 150 °C, which was ascribed to loss of the ILs and confirms the presence of covalently bound ILs on the MOFs. For 1H NMR spectroscopic analysis, IL-MOFs can be digested in D2SO4 with

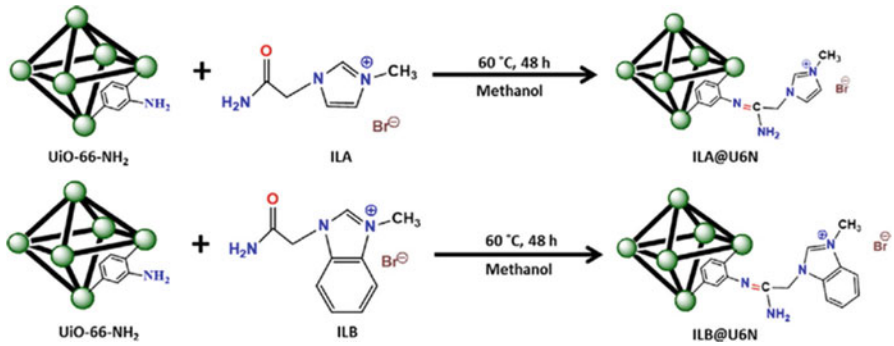

Supported Ionic Liquids, Scheme 7 Synthesis of MILs based on UiO-66 [18]

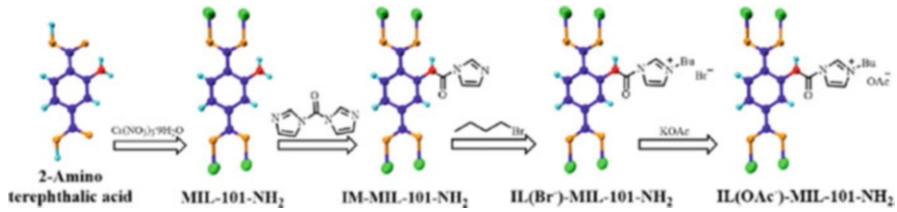

Supported Ionic Liquids, Scheme 8 Synthesis of MILs based on MIL-101 [19]

sonication, and the peaks of the ILs in the 1H NMR spectra indicated that the ILs were successfully anchored on the MOFs [18]. For the second method, imidazole-modified MOFs (IM-MOFs) were prepared by the reaction of *N*, *N*-carbonyldiimidazole with the amino groups of NH2-MOFs. The IL-MOFs were then prepared by alkylation of an alkyl halide with the imidazolyl moiety of the IM-MOFs. Nitrogen adsorption isotherms can also be used to confirm the immobilization of MOFs with ILs. The decreasing total pore volume, pore size, and Brunauer–Emmett–Teller surface area can be attributed to the incorporation of ILs inside the pores of the MOFs. In addition, if the anions of ILs have special UV absorption, UV–visible spectroscopy can be used to determine whether the ILs have been successfully attached to the MOFs [19].

Clay-Supported ILs (CSILs)

The various advantages of ILs have led researchers to investigate their potential use for the modification of clay minerals (sepiolite, palygorskite, smectites, halloysites, kaolinites, etc.), thereby improving the physical and chemical properties of the latter. The resulting hybrid materials have been successfully applied in various fields, including catalysis, energy production, and depollution. Methods for the preparation of clay-supported ILs (CSILs) can be classified as noncovalent and covalent, similar to those for other IL-modified materials. Although there are many types of clay, their preparation methods are similar; hence, kaolinite is used as the representative material for the description herein [20].

Noncovalent Preparation of CSILs

Kaolinite is a layered clay mineral, and intercalation is a common method for the noncovalent preparation of CSILs. The preparation involves mixing and heating the ILs (imidazolium and pyridinium ILs) and kaolinite under nitrogen protection in DMSO (for preintercalation), followed by washing off the excess ILs thoroughly with the solvent (Scheme 9). In addition to DMSO, urea and other polar compounds can be used for preintercalation [20]. The synthesis of pyrrolidinium ILs is similar to that of ILs based on imidazole and pyridine. However, pyrrolidinium ILs can intercalate with kaolinite in the absence of a solvent and preintercalation reagent. The choice of washing solvent is crucial because it should remove only the ILs adsorbed on the surface but should not have sufficient polarity to prevent intercalation. In this regard, isopropanol is the ideal solvent. Moreover, the larger the particle size of the ILs, the smaller is the amount of organic compounds between the clay mineral layers. Besides, unlike montmorillonite intercalation, it shows more than one layer of modifier in the interlayer space. In the case of kaolinite modified by ILs, only one layer is stable. The strong dipole between adjacent layers (along the c-axis direction) can explain this phenomenon. The strong electrostatic attraction will inevitably prevent the formation of multilayer films of less stable ILs in the interlayer space. Because of their large size, it is difficult to use PILs for the intercalation of kaolinite; hence, they are mainly used for the exfoliation of kaolinite.

Kaolinite intercalated with ILs can be characterized by XRD in addition to traditional

Supported Ionic Liquids, Scheme 9 Process of intercalation of IL in the interlamellar spaces of kaolinite [21]

characterization methods. For example, in 1-ethylpyridine chloride intercalated kaolinite, the resulting IL intercalated kaolinite was completely replaced by 1-ethylpyridine chloride in DMSO [21]. The d001 value increased from 0.71 nm for the original kaolinite to 1.10 nm for the kaolinite with DMSO, eventually reaching 1.35 nm. The increase in d001 (0.64 nm) is consistent with the size of the organic cation inclined by 30° relative to the a, b planes of kaolinite.

Covalent Preparation of CSILs

Kaolin has a large number of aluminol groups. Hence, ILs with hydroxyl groups (imidazolium and pyridinium ILs) can be functionalized with aluminol during the synthesis. In contrast, the synthesis of kaolinite functionalized with alkylammonium ILs requires two steps. In the first step, the hydroxyl group in the alkylammonium derived from diethanolamine and triethanolamine can form a covalent bond with the aluminol group. In the second step, haloalkanes are used for quaternization. During the synthesis, haloalkanes of different sizes can be used to adjust the properties of the resulting compounds. XRD also plays an important role in the characterization of CSILs prepared by covalent methods. The XRD results revealed that despite the difference in lengths of the haloalkanes added for the quaternization of amino alcohols, the resulting materials showed short basal spacing distances (between 1.10 and 1.13 nm). This phenomenon could be attributed to the preferred orientation of the grafted organic cations in the interlayer space.

Summary

This chapter summarized the recent developments in supported ionic liquids, especially in the novel preparation strategies and characterization methods. Generally, based on the interaction between the supporting material and ionic liquid, the preparation strategies of supported ionic liquids are divided into two groups, which are noncovalent and covalent preparation methods. We have described the preparation strategies and the corresponding characterization methods of supported ionic liquids with five commonly used supports: silica, polymers, carbon nanomaterials, metal-organic frameworks (MOFs), and clays. The synthetic strategies and characterization methods discussed in this entry not only provide strategies in the synthesis of custom-designed supported ionic liquids, but also present important information in the understanding of molecular structure of supported ionic liquids.

Cross-References

- ▶ Immobilization of Ionic Liquids, Types of Materials, and Applications
- ▶ Ionic Liquid Materials for the Adsorption of Toxic Gases
- ▶ Ionic Liquid-Based Adsorbents for the Removal of Toxic Dyes from Wastewater
- ▶ Ionic Liquid-Based Microextraction and Determination of Components in Food-Related Products
- ▶ Magnetic/Ionic Liquids for the Extraction of Phenolic Compounds from Aqueous Medium
- ▶ Task-Specific Ionic Liquids: Design, Properties, and Applications

References

1. Werner S, Szesni N, Kaiser M, Haumann M, Wasserscheid P (2012) A scalable preparation method for SILP and SCILL ionic liquid thin-film materials. Chem Eng Technol 35(11):1962–1967
2. Bi W, Zhou J, Row KH (2010) Separation of xylose and glucose on different silica-confined ionic liquid stationary phases. Anal Chim Acta 677(2):162–168
3. Liu H, Li Z, Takafuji M, Ihara H, Qiu H (2017) Octadecylimidazolium ionic liquid-modified magnetic materials: preparation, adsorption evaluation and their excellent application for honey and cinnamon. Food Chem 229:208–214
4. Zhou H, Chen J, Li H, Quan K, Zhang Y, Qiu H (2020) Imidazolium ionic liquid-enhanced poly(quinine)-modified silica as a new multi-mode chromatographic stationary phase for separation of achiral and chiral compounds. Talanta 211:120743
5. Zhou X, Weber J, Yuan J (2019) Poly(ionic liquid)s: platform for CO_2 capture and catalysis. Curr Opin Green Sustain Chem 16:39–46
6. Branco LC, Crespo JG, Afonso CAM (2002) Highly selective transport of organic compounds by using

supported liquid membranes based on ionic liquids. Angew Chem Int Ed 41(15):2771–2773
7. Mecerreyes D (2011) Polymeric ionic liquids: broadening the properties and applications of polyelectrolytes. Prog Polym Sci 36(12):1629–1648
8. Mehnert CP (2005) Supported ionic liquid catalysis. Chem Eur J 11(1):50–56
9. Zhang Y, Shen Y, Yuan J, Han D, Wang Z, Zhang Q, Niu L (2006) Design and synthesis of multifunctional materials based on an ionic-liquid backbone. Angew Chem Int Ed 45(35):5867–5870
10. Jon C-S, Meng L-Y, Li D (2019) Recent review on carbon nanomaterials functionalized with ionic liquids in sample pretreatment application. Trends Anal Chem 120:115641
11. Fukushima T, Kosaka A, Ishimura Y, Yamamoto T, Takigawa T, Ishii N, Aida T (2003) Molecular ordering of organic molten salts triggered by single-walled carbon nanotubes. Science 300(5628): 2072–2074
12. Zhang B, Ning W, Zhang J, Qiao X, Zhang J, He J, Liu C-Y (2010) Stable dispersions of reduced graphene oxide in ionic liquids. J Mater Chem 20(26):5401–5403
13. Tunckol M, Fantini S, Malbosc F, Durand J, Serp P (2013) Effect of the synthetic strategy on the non-covalent functionalization of multi-walled carbon nanotubes with polymerized ionic liquids. Carbon 57:209–216
14. Xin B, Hao J (2014) ChemInform abstract: imidazolium-based ionic liquids grafted on solid surfaces. ChemInform 45(50)
15. Yang H, Shan C, Li F, Han D, Zhang Q, Niu L (2009) Covalent functionalization of polydisperse chemically-converted graphene sheets with amine-terminated ionic liquid. Chem Commun (26):3880–3882
16. Safaei M, Foroughi MM, Ebrahimpoor N, Jahani S, Omidi A, Khatami M (2019) A review on metal-organic frameworks: synthesis and applications. Trends Anal Chem 118:401–425
17. Fujie K, Kitagawa H (2016) Ionic liquid transported into metal–organic frameworks. Coord Chem Rev 307:382–390
18. Kurisingal JF, Rachuri Y, Pillai RS, Gu Y, Choe Y, Park D-W (2019) Ionic-liquid-functionalized UiO-66 framework: an experimental and theoretical study on the Cycloaddition of CO_2 and epoxides. ChemSusChem 12(5):1033–1042
19. Chong SY, Wang TT, Cheng LC, Lv HY, Ji M (2019) Metal–organic framework MIL-101-NH2-supported acetate-based Butylimidazolium ionic liquid as a highly efficient heterogeneous catalyst for the synthesis of 3-Aryl-2-oxazolidinones. Langmuir 35(2):495–503
20. Dedzo GK (2019) Kaolinite clay mineral reactivity improvement through ionic liquid functionalization. Isr J Chem 59(9):778–788
21. Letaief S, Detellier C (2005) Reactivity of kaolinite in ionic liquids: preparation and characterization of a 1-ethyl pyridinium chloride–kaolinite intercalate. J Mater Chem 15(44):4734–4740

Surface Tension of Ionic Liquids

Dawei Fang and Jie Wei
Institute of Rare and Scattered Elements, College of Chemistry, Liaoning University, Shenyang, P. R. China

Introduction

Among the unique properties of ionic liquids, surface tension plays a special and crucial role. Since the ionic nature of ILs makes it extremely difficult to accurately measure the cohesive forces present in the liquid, in view of this situation, the corresponding states principles and other powerful correlation techniques are often applied to solve the issue, which is also still a challenge. So it is found that surface tension value is an effective way to avoid this problem, and it is possible to access at the liquid-vacuum boundary. Surface tension is a measure of cohesive forces between liquid molecules present at the surface, and it represents the quantification of force per unit length of free energy per unit area. Thus, the measurement of surface tension of ionic liquids is one of the most effective ways to (indirectly) access the intrinsic energetics that are involved in the interactions between the ions [1]. In addition, surface tension data are also a powerful means to explore the different types of segregation/orientation that occur at ionic/molecular level and how these influence the interactions with other molecules [1, 2]. Finally, it must be stressed that surface tension data are core in colloid and interface sciences, including the use of ionic liquids and their mixtures in the chemical industry and are extremely important in mass-transfer operations, such as in distillation, extraction, absorption, and adsorption [3]. Here, this entry tries to give the surface tension-related information including the definition of surface tension, measurements methods, factors affecting, and surface properties, which will make it easily understood.

Definition of Surface Tension

As one of the important physicochemical properties, surface tension is caused by the cohesive forces among liquid molecules due to the fact that each molecule is pulled equally in every direction by neighboring liquid molecules, obtaining a net force equal to zero. As the molecules at the surface of liquid do not have the same molecules on all sides of them, they are pulled inward, creating an internal pressure, forcing at liquid surface to contract in a minimal area [4]. In other words, surface tension is the energy that must be supplied to increase the surface area by one unit by performing like energy necessary to create surfaces in physical chemistry. Thus, surface tension can manifest itself in forms of both surface force and surface energy, and so it can affect the mass and heat transfer on the interface and provide information about the structure relationship between two phases [4].

Measurement Methods for Surface Tension

There are mainly two approaches to obtain surface tension: experimental methods and estimation.

Experimental Methods

The most common methods for measuring surface tension may be grouped into the five following classes [1]: (i) methods based on drop/meniscus shape: capillary rise (CR) [5] and pendant drop (PD) [6]; (ii) detachment methods: du Noüy ring (DNR) [7] and Wilhelmy plate (WP) [8]; (iii) methods based on menisci at the stability limit: drop weight/volume (DW or DV) [9] and maximum bubble pressure (BP) [10]; (iv) spinning drop method (SD) [11]; and (v) dynamic light scattering methods (DLS) [12]. And the above experimental techniques have been usually used to determine the surface tension of ionic liquids from ambient atmosphere to highly controlled environments, at various temperatures.

Estimation

However, at present, it is faced with the lack of resources of surface tension owing to the increasing number of ionic liquids, and its determination could be a huge challenge; also new estimation methods of the surface tension of ionic liquids based on simple calculation and properties are highly desirable, that is, surface tension can be also obtained from molecular dynamic simulations [13], quantitative structure-property relationship (QSPR) methods [14], parachor and ionic parachor [15], group-contribution methods [16], molar surface Gibbs free energy methods [17], corresponding states theory method [18], and neural network model [19].

Factors Affecting

Effect of the Cation

Based on the cation, the available ionic liquids have been divided into five families: imidazolium, pyridinium, ammonium, phosphonium, and guanidinium. Take imidazolium-based ionic liquids $[C_nC_1Im][Tf_2N]$ series as an example; as one of the most common ionic liquids, it is reported that the surface tension for $[C_nC_1Im][Tf_2N]$ series strongly decreases with increasing alkyl chain for the short alkyl chains ($n \leq 8$), which is in agreement with the reported values [20–22], and increasing the chain length further from $[C_8C_1Im][Tf_2N]$ to $[C_{12}C_1Im][Tf_2N]$ does not have any further effect on the surface tension [23], and the same trend is observed by many groups [24]; simulations have confirmed these experimental findings [25]. Different anions based on imidazolium-based ionic liquids, such as $[BF_4]^-$, $[PF_6]^-$, are still the same phenomenon [5, 21]. In addition, the functional groups in their side chains also have an effect on the surface tension, for example, the surface tension of $[Me(EG)_2C_1Im][Tf_2N]$ and $[C_6C_1Im][Tf_2N]$ are 36.5 ± 0.7 mN m^{-1} and 30.2 ± 0.6 mN m^{-1}, respectively [23].

Effect of Cationic Head Group

Generally, the surface tension of imidazolium-based IL is compared with the pyrrolidinium-based IL, and it is shown in Table 1.

From the table, it is found that surface tension is higher for the pyrrolidinium ILs than for the imidazolium ILs; besides that, there are also

Surface Tension of Ionic Liquids, Table 1 Surface tension of imidazolium IL and pyrrolidinium IL from the references

Imidazolium ILs	Surface tension/mN·m^{-1}	Pyrrolidinium ILs	Surface tension/mN·m^{-1}
$[C_4C_1Im][Tf_2N]$ [23]	30.7 ± 0.6	$[C_4C_1Pyrr][Tf_2N]$ [23]	32.3 ± 0.7
$[C_4C_1Im][SCN]$ [26]	45.9 ± 0.2	$[C_4C_1Pyrr][SCN]$ [26]	49.8 ± 0.1
$[C_4C_1Im][N(CN)_2]$ [24]	48.6 ± 0.1	$[C_4C_1Pyrr][N(CN)_2]$ [24]	55.8 ± 0.2

ammonium, phosphonium, and guanidinium ionic liquids, and it means that the surface tension has a great relationship with the cationic head group.

Effect of the Anion

Like the cationic group, the anion also influences on the surface tension, but the change trends are unfixed. There are a variety of anions sizes containing small (e.g. halides, $[NO_3]^-$, and $[BF_4]^-$), medium-sized (e.g. $[PF_6]^-$, $[B(CN)_4]^-$, and $[MeOSO_3]^-$), and large (e.g. $[TfO]^-$), however, it is found that the surface tension either increases or decreases with increasing anion size, or that there is no dependence at all [26, 27]. When the selected anions can be seen as more or less of spherical shape, such as $[BF_4]^-$, $[PF_6]^-$, and $[B(CN)_4]^-$, it can be seen as one group, and the surface tension increases with anion size; it is obvious that the order is $[BF_4]^- < [PF_6]^- < [B(CN)_4]^-$ [23].

Effect of Temperature

Most of the studies dealing with the effect of temperature on the surface tension of ionic liquids are restricted to a relatively narrow temperature range, typically from around room temperature (280–300 K) up to around 350 K [1]. For most of the ionic liquids studied, a 20 K increase in temperature corresponds to a 1–2 mN m^{-1} drop in surface tension [1]. Only a few reports are available in which the upper temperature limit was extended beyond 370 K [5, 28], such as the surface tension of different imidazolium-based ionic liquids up to 395 K [5]; the surface tension of 1-alkyl-3-methylimidazolium bistriflamide $[C_nC_1im][Ntf_2]$(n = 2–14), ionic liquids up to 530 K [28], which is quite close to the onset of decomposition temperature; and the surface tension of 1-ethanol-3-methylimidazolium tetrafluoroborate $[(OH)C_2C_1im][BF_4]$, and 1-octyl-3-methylimidazolium tetrafluoroborate $[C_8C_1im][BF_4]$, up to 455 K using the drop-shape analysis method equipped with a thermostatic chamber [29].

It is obvious that temperature has an important influence on the surface tension, generally, it decreases with the increasing of temperature (see Table 2). For most ionic liquids, the surface tension decreases linearly with the increasing temperature. In addition, the Guggenheim or Eötvos equations can be used to present the surface tension of ionic liquids with temperature and their use in extrapolation schemes that allow for the estimation of the hypothetical critical and normal boiling temperatures of ionic liquids [6], which is introduced in detail as follows. The general trend for some reported ILs is $[C_npy][NTf_2]$(n = 2,4,6) [30], $[C_nmim][Tf_2N]$ (n = 2,3,4,5,6,7,8,10) [31]; $[C_nmim][Ala]$ (n = 2–6) [21], $[H_2N{-}C_nmim][PF_6]$(n = 2,3) [32]; that the surface tension decreases with increasing temperature is observed and shown in Fig. 1.

Effect of Water Contents and Other Impurities

It is reported that there are crucial discrepancies in the values of surface tension data which can be partially explained by the ionic liquids with different amounts of water or other impurities, e.g., halides. And in addition, hygroscopic ionic liquids could absorb water when exposed to air; as a matter of fact, the water content of the samples could increase continuously. Huddleston et al. [7] show that the values of surface tension are reduced with the increasing of water contents or other impurities, and this is in accordance with Yang et al. [33, 34]. However, Malham et al. [35] hold a view that the influence of water on surface tension values is almost negligible. Rebelo et al. [1] have summarized that water and halide content on the surface tension of some selected imidazolium-based ionic liquids, and it is found

Surface Tension of Ionic Liquids, Table 2 Surface excess entropy S_a and surface excess energy E_a of some reported ionic liquids

ILs	$10^3 S_a$ / mJ·K^{-1}·m^{-2}	E_a / mJ·m^{-2}	ILs	$10^3 S_a$ / mJ ·K^{-1}·m^{-2}	E_a / mJ·m^{-2}
[C_2mim][Ala] [21]	70.3	73.7	[H_2N-C_2mim][PF_6] [32]	66.9 ± 1.8	75.3 ± 0.6
[C_3mim][Ala] [21]	70.5	71.1	[H_2N-C_3mim][PF_6] [32]	43.5 ± 2.2	63.8 ± 0.7
[C_4mim][Ala] [21]	70.7	68.8	[C_2mim][ReO_4] [33]	62.7	67.8
[C_5mim][Ala] [21]	70.8	67.1	[C_4mim][ReO_4] [33]	61.5	63.1
[C_6mim][Ala] [21]	71.0	64.6	[C_5mim][ReO_4] [33]	61.3	61.0
			[C_6mim][ReO_4] [33]	60.5	59.5

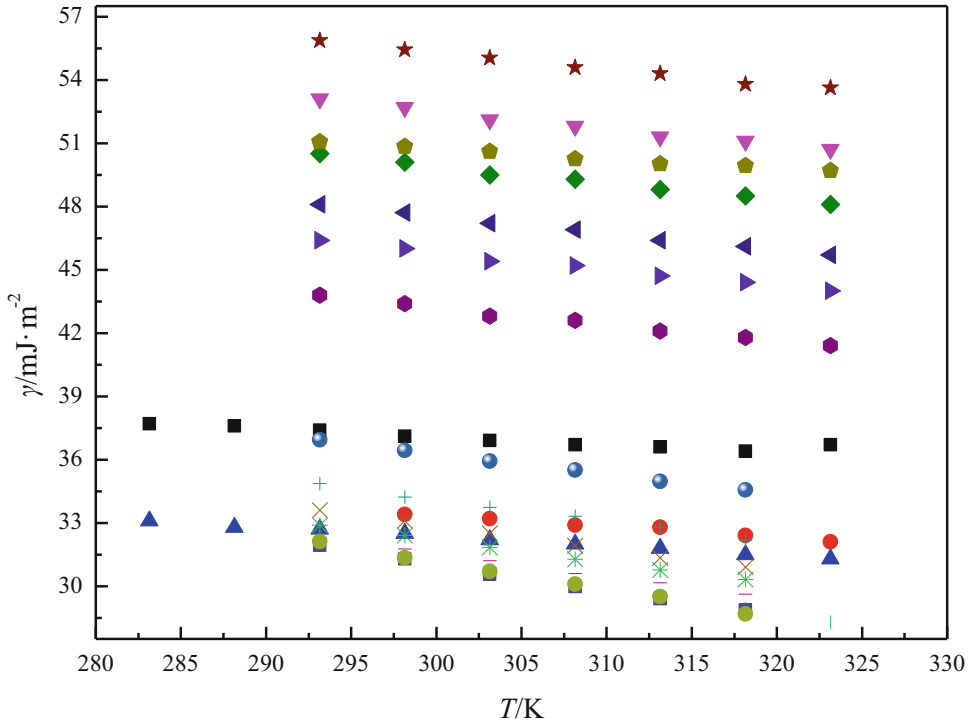

Surface Tension of Ionic Liquids, Fig. 1 The surface tension of some reported ILs is varied with temperatures. (■ [C_2py][NTf_2]; ● [C_4py][NTf_2]; ▲ [C_6py][NTf_2]; ▼ [C_2mim][Ala]; ◆ [C_3mim][Ala]; ◀ [C_4mim][Ala]; ▶ [C_5mim][Ala]; ⬢ [C_6mim][Ala]; ★ [H_2N−C_2mim][PF_6]; × [H_2N–C_3mim][PF_6]; ● [C_2mim][Tf_2N]; + [C_3mim][Tf_2N]; × [C_4mim][Tf_2N]; ✳ [C_5mim][Tf_2N]; – [C_6mim][Tf_2N]; | [C_7mim][Tf_2N]; ■ [C_7mim][Tf_2N]; ● [C_{10}mim][Tf_2N])

that that due to different water and halide contents in each measurement, there is no obvious trend between the reported amounts of water present in the samples and the magnitude of the surface tension values. So, it is obvious that proper sample handling and experimental methods are one of effective ways to reconcile conflicting views [36]. The values of surface tension are reduced with the increasing of the temperatures, and it is a linear relationship between surface tension and temperature as reported in references [32–34]; in addition, water contents of ionic liquids have also an effect on the surface tension, and it is shown in Fig. 2, especially for the hydrophilic ionic liquids, e.g., [$C_n$mim][OAc](n = 2–6) [34], [$C_n$mim][Pro] (n = 2–6) [37].

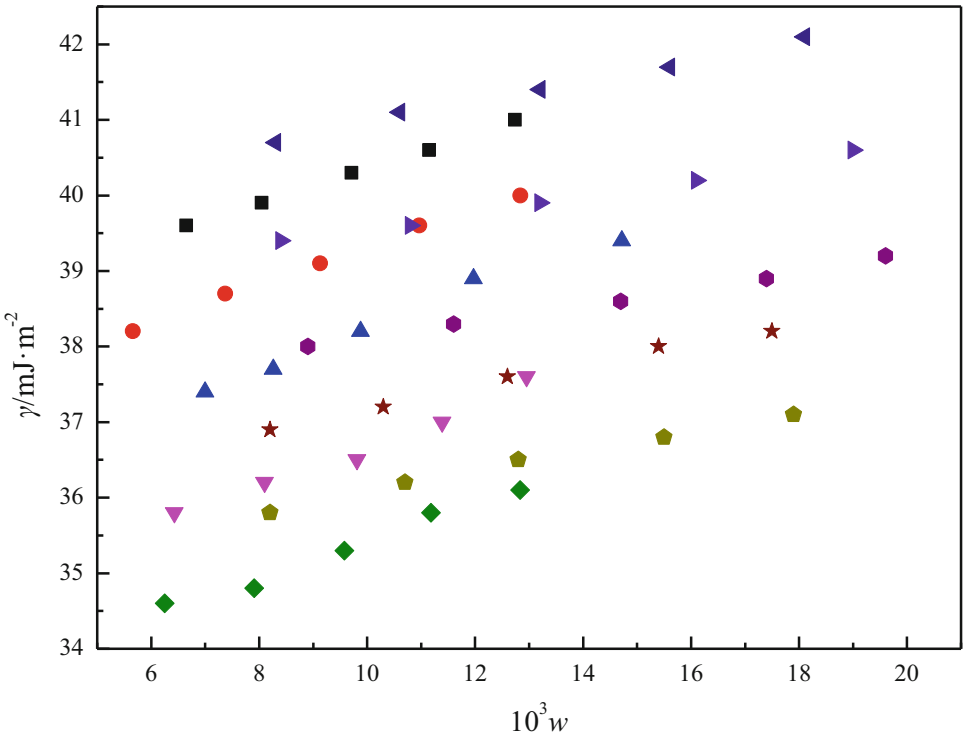

Surface Tension of Ionic Liquids, Fig. 2 Experimental values of surface tension change with the water contents of ionic liquids. (■ [C_2mim][OAc]; ● [C_3mim][OAc]; ▲ [C_4mim][OAc]; ▼ [C_5mim][OAc]; ◆ [C_6mim][OAc]; ◀ [C_2mim][Pro]; ▶ [C_3mim][Pro]; ⬢ [C_4mim][Pro]; ★ [C_5mim][Pro]; ⬟ [C_6mim][Pro])

Surface Tension of Ionic Liquid Mixtures or Solutions

Water and other molecular solvents such as alcohols, n-alkanes, 1-octene, and benzene are mixed with ionic liquids, and ionic liquid solutions or mixtures are formed, and the determination of the surface tension is well carried out aiming to establish the critical micelle concentration of surfactant-like ionic liquids [1]. Additional studies have addressed the surface tensions of mixtures of ionic liquids combining both imidazolium-ammonium-, ammonium-ammonium-, and imidazolium-imidazolium-based pairs of ionic liquids [36, 38]; the surface tension of mixtures of ionic liquids can provide valuable information on the preferential migration and organization of ionic liquids at the surface [1]. And it is not easily correlated with the surface tension of the pure components. The local composition at a binary mixture interface differs from that in the bulk due to the preferential adsorption of one of the components (usually the compound with lower surface tension). This means that adding an ionic liquid to water leads to a decrease of the surface tension, while adding it to an organic solvent has the opposite effect. There is no simple definition for an ideal mixture in terms of its surface, but, for the sake of convenience, it is common practice to consider ideality as the linear dependence of the surface tensions of a binary mixture:

$$\gamma = x_1\gamma_1^* + x_2\gamma_2^* \quad (1)$$

where x_i is the molar fraction of pure component i and γ_i^* is its surface tension at the same temperature. The surface tension of mixtures has been predicted; however, its variation with composition is usually required parameters, which are difficult

to obtain. One of the oldest and easiest approaches is the regular solution theory of Guggenheim [39]. The main focus of most studies regarding the surface tension of ionic liquid mixtures has been on the effect of the nature of the ionic liquid or cosolvent and temperature.

Solvent Component Effects

As mentioned above, solvent components are generally divided into water, alcohols, n-alkanes, 1-octene, benzene [7, 22, 35, 40, 41], etc.

Trace of water is usually seen as an impurity in the surface tension of pure ionic liquids, which was discussed in section "Effect of Water Contents and Other Impurities". In this section, we evaluate the effect of water as a general mixture component and compare it with other solvents.

In the year 2001, the effect of water on the physical properties of ionic liquids was rarely carried out [2]. Later, many works reported the results on the surface tension of binary mixtures of hydrophilic ionic liquids and water with different concentrations [35]. It is found that in the water-rich phase, surface tension decreases rapidly for the mixtures between $[C_4C_1C_1im][BF_4]$ or $[C_4C_1im][BF_4]$ and water, in the entire concentration range [35]. With addition of more ionic liquid, the surface tension (which is already quite close to that of the pure ionic liquid) increases slightly until the value for the pure ionic liquid is reached. It is obvious that there is the presence of a minimum around the break point; authors explained this anomalous behavior considering differential surface segregation of anions and cations at different concentration regimes, and cations are primary species at the interface at very low-ionic liquid concentrations; there are further investigations involving aqueous solutions of other ionic liquids [22]; the surface tension of three systems $[C_4C_1im]Cl$, $[C_4C_1im]Br$, and $[C_4C_1im][BF_4]$ with water was also explored, and $[C_4C_1im][BF_4]$ + water system showed a similar trend, that is, it sharply decreases with a weak dependence on increasing ionic liquid concentration, x_{IL}. The other two systems $[C_4C_1im]Cl$ and $[C_4C_1im]Br$ + water exhibited a more regular decrease with increasing x_{IL} [42]. Other results have investigated aqueous solutions of $[C_2C1im][C_2SO_4]$, $[C_4C_1im][Ntf_2]$, $[C_4C_1im][PF_6]$, and $[C_4C_1im][Glu]$; in the ionic-liquid-rich phase, the surface tension decreasing with increasing x_{IL} was regular [21, 22], and it shows a more or less pronounced drop of surface tension at water-rich concentrations and a more subdued decrease with increasing x_{IL} at ionic-liquid-rich concentrations. It must be stressed, however, that the contrast between the two regimes (water-rich side versus ionic-liquid-rich side) is also a consequence of the significant difference between the molar mass and molar volumes of most ionic liquids and that of water (at least one order of magnitude); any diagram plotted as a function of the mixture molar fraction will enhance variations on the water-rich side.

As the second largest class of solvents, alcohols are mixed with ionic liquids which are also a research hotspot; the surface tension of mixtures at 298.15 K was often measured, and a general overview of the effect of alcohol alkyl chain length on the surface tension of (ionic liquid + alcohol) mixtures, which is consistent with the reported results [43]. From the cases, the kind of alcohols has a key influence on the surface tension of ionic liquid + alcohol, that is, the surface tension of mixtures decreases with increasing concentration of alcohol, and the slope is more pronounced (on the ionic-liquid-rich side) when the alkyl chain of the alcohol is longer; interestingly, for very short alkyl chains alcohols, such as methanol, the plot of surface tension as a function of the mixture mole fraction is almost linear. In addition, there are also few publications presenting surface tension values for ternary mixtures composed of ionic liquid + water + β-cyclodextrin [44]. Although it could provide complementary evidence on the formation of inclusion complexes, some general remarks can be made based on the surface tension data.

Temperature Effects

Temperature effects on the surface tension of ionic liquid mixtures can be explored [35], that is in the

usual range from 298 K to 308 K, the surface tension at a given composition decreases with increasing temperature. It was also found that at higher temperatures, the surface tension drop caused by the molecular solvent becomes less significant.

Surface Properties of Ionic Liquids

As mentioned before, surface tension decreases linearly with the increasing temperature, and the slopes of the experimental values of γ against T could be seen as surface excess entropy S_a:

$$S_a = -(\partial\gamma/\partial T)_p \tag{2}$$

Many groups [21, 32, 33] have reported the surface excess entropy S_a of ionic liquids, as listed in Table 2. Compared to a fused salt $NaNO_3$ (S_a = 146 mJ m^{-2}) [45], it is interesting to find that ionic liquids present lower surface entropy, and the surface entropy is much closer to that of an organic compound such as benzene (S_a = 67 mJ m^{-2}) and octane (S_a = 51.1 mJ m^{-2}) [45]. This fact shows that the interaction energy among ions in the studied ionic liquids is less than that in inorganic fused salts because the surface excess energy is dependent on the interaction energy between ions, that is, this means the crystal energy of ionic liquids is much less than that of inorganic fused salts [46–49].

In addition, the values of the surface excess energy E_a likewise could be obtained from the surface tension:

$$E_a = \gamma - T\,(\partial\gamma/\partial T)_p \tag{3}$$

And E_a values for some of the ionic liquids at 298.15 K are also shown in Table 2.

Related Thermodynamic Properties

The parachor, P, is a relatively old concept; generally, it could be obtained by surface tension and density:

$$P = \left(M\gamma^{1/4}\right)/\rho \tag{4}$$

Deetlefs et al. [50] pointed out that it is a remarkably useful tool to predict physicochemical properties of ILs. That is, from the above equation, we can see that parachor is available as a link between the structure, density, and surface tension, and it may become a method to estimate surface tension of ILs from its density.

In addition, interstice volume, v, was obtained based on the interstice model [51].

$$v = 0.6791(k_B T/\gamma)^{3/2} \tag{5}$$

where k_B is the Boltzmann constant.

Thermal expansion coefficient, α, is also derived. For many liquids, the traditional Eötvös equation [51, 52] usually expresses the relationship between surface tension and temperatures, and it shows as follows:

$$\gamma V^{2/3} = k_E\,(T_c - T) \tag{6}$$

where V is molar volume, γ is surface tension of mixtures, and T_c is critical temperature. k_E is the Eötvös empirical and related to polarity of the liquid. And the critical temperature T_c is also obtained, which is one of the most important thermophysical properties because they can be used in many corresponding state correlations regarding the equilibrium and transport properties of fluids.

However, the determination of the IL critical temperatures is a challenging task because ILs are decomposed at temperatures below the critical point. Although these values are hypothetical quantities, their usefulness is unquestionable, as originally shown for ILs in a previous work [10]. IL critical temperatures can typically be estimated using the Eötvös or Guggenheim [53] relation:

$$\gamma = K_{Gug}\left(1 - T/T_{c,Gug}\right)^{11/9} \tag{7}$$

According to the relationship temperature of normal boiling point (NBP) of ionic liquids

$T_b \approx 0.6\ T_c$, for ionic liquids, T_b is also estimated, and it is easy to obtain the values of $\Delta_l{}^g H_m{}^0(T_b)$ by Rebelo's [6]. In addition, according to Kabo's empirical equation [53], the molar enthalpy of vaporization, $\Delta_l{}^g H_m{}^0(298\text{K})$, of ionic liquids can be estimated by the following equation:

$$\Delta_l{}^g H_m{}^0(298\ \text{K}) = 0.01121\gamma V^{2/3} N^{1/3} + 2.4\ \text{kJ}\cdot\text{mol}^{-1} \quad (8)$$

In addition to $\Delta_l{}^g H_m{}^0(298\text{K})$, another thermodynamic parameter, Hildebrand solubility parameter (δ_H), is an effective measure of the strength of molecular interactions between solvent molecules. Thus, it is widely used in predicting the solubility of various chemicals in organic solvents. According to the calculated $\Delta_l{}^g H_m{}^0(298\ \text{K})$ values, δ_H can be estimated by the following equation [54]:

$$\delta_H = \left(\Delta_l{}^g H_m{}^0(298\text{K}) - RT/V_m\right)^{1/2} \quad (9)$$

The traditional Eötvös equation has been improved by the introduction of molar surface Gibbs energy g_s by Tong et al. [55], and it is presented as follows:

$$g_s = \gamma V^{2/3} N^{1/3} = k_E N^{1/3}(T_c - T) = C_0 - C_1 T \quad (10)$$

Although both expressions are empirical equation, each item in equations has not only the energy dimension but also clear physical meaning. From the above related equations, $C_1 = k_E N^{1/3} = -(\partial g_s/\partial T)_p = s$, that is, C_1 represents molar surface entropy, and s, the molar surface entropy, is related to the polarity of the mixtures, and it is a strong positive relationship between the molar surface entropy and the polarity. According to the definition of Gibbs, the molar surface enthalpy, h, was obtained from the table; the molar surface enthalpy is a temperature-independent constant, that is, the process from the bulk to the surface of the mixture is an isocoulombic one [56].

According to the Auerbach relation [57], the speed of sound can be calculated from surface tension and density by the following equation:

$$u/\text{m}\cdot\text{s}^{-1} = \gamma/(0.00063\rho))^{2/3} \quad (11)$$

Cross-References

▶ Surface Tension of Ionic Liquids

References

1. Tariq M, Freire MG, Saramago B, Coutinho JAP, Lopes JNC, Rebelo LPN (2012) Surface tension of ionic liquids and ionic liquid solutions. Chem Soc Rev 41:829–868
2. Lockett V, Sedev R, Harmer S, Ralston J, Horne M, Rodopoulos T (2010) Orientation and mutual location of ions at the surface of ionic liquids. Phys Chem Chem Phys 12:13816–13827
3. Luís A, Shimizu K, Araújo JMM, Carvalho PJ, Lopes-da-Silva JA, Lopes JNC, Rebelo LPN, Coutinho JAP, Freire MG, Pereiro AB (2016) Influence of nanosegregation on the surface tension of fluorinated ionic liquids. Langmuir 32:6130–6139
4. Rivera JL, Molina-Rodríguez L, Ramos-Estrada M, Navarro-Santos P, Lima E (2018) Interfacial properties of the ionic liquid [bmim][triflate] over a wide range of temperatures. RSC Adv 8:10115–10123
5. Ghatee MH, Zolghadr AR (2008) Surface tension measurements of imidazolium-based ionic liquids at liquid–vapor equilibrium. Fluid Phase Equilib 263:168–175
6. Rebelo LPN, Lopes JNC, Esperanc JMSS, Filipe E (2005) On the critical temperature, normal boiling point, and vapor pressure of ionic liquids. J Phys Chem B 109:6040–6043
7. Huddleston JG, Visser AE, Reichert WM, Willauer HD, Broker GA, Rogers RD (2001) Characterization and comparison of hydrophilic and hydrophobic room temperature ionic liquids incorporating the imidazolium cation. Green Chem 3:156–164
8. Berthon L, Nikitenko SI, Bisel I, Berthon C, Faucon M, Saucerotte B, Zorza N, Moisy P (2006) Influence of gamma irradiation on hydrophobic room-temperature ionic liquids [BuMeIm]PF_6 and [BuMeIm]$(CF_3SO_2)_2N$. Dalton Trans 21:2526–2534
9. Kilaru P, Baker GA, Scovazzo P (2007) Density and surface tension measurements of imidazolium-, quaternary phosphonium-, and ammonium-based room-temperature ionic liquids: data and correlations. J Chem Eng Data 52:2306–2314
10. Jin H, O'Hare B, Dong J, Arzhantsev S, Baker GA, Wishart JF, Benesi AJ, Maroncelli M (2008) Physical properties of ionic liquids consisting of the 1-butyl-3-

methylimidazolium cation with various anions and the bis(trifluoromethylsulfonyl)imide anion with various cations. J Phys Chem B 112:81–92
11. Muhammad A, Mutalib MIA, Wilfred CD, Murugesan T, Shafeeq AS (2008) Thermophysical properties of 1-hexyl-3-methyl imidazolium based ionic liquids with tetrafluoroborate, hexafluorophosphate and bis(trifluoromethylsulfonyl)-imide anions. J Chem Thermodyn 40:1433–1438
12. Halka V, Tsekov R, Freyland W (2005) Peculiarity of the liquid/vapour interface of an ionic liquid: study of surface tension and viscoelasticity of liquid $BMImPF_6$ at various temperatures. Phys Chem Chem Phys 7: 2038–2043
13. Shimizu K, Heller BSJ, Maier F, Steinrück HP, Lopes JNC (2018) Probing the surface tension of ionic liquids using the Langmuir principle. Langmuir 34:4408–4416
14. Shang Q, Yan FY, Xia SQ, Wang Q, Ma PS (2013) Predicting the surface tensions of ionic liquids by the quantitative structure property relationship method using a topological index. Chem Eng Sci 101:266–270
15. Gardas RL, Coutinho JAP (2008) Applying a QSPR correlation to the prediction of surface tensions of ionic liquids. Fluid Phase Equilib 265:57–65
16. Gharagheizi F, Ilani-Kashkouli P, Mohammadi AH (2012) Group contribution model for estimation of surface tension of ionic liquids. Chem Eng Sci 78:204–208
17. Pan Y, Zheng L, Xing NN, Ji HG, Guan W (2017) The molar surface Gibbs free energy and estimate of polarity for a new ether-functionalized ionic liquid [$C_2$2O1IM][DCA]. J Chem Thermodyn 112:213–219
18. Wu KJ, Zhao CX, He CH (2012) A simple corresponding-states group-contribution method for estimating surface tension of ionic liquids. Fluid Phase Equilib 328:42–48
19. Atashrouz S, Amini E, Pazuki G (2015) Modeling of surface tension for ionic liquids using group method of data handling. Ionics 21:1595–1603
20. Olea AF, Worrall DR, Wilkinson F, Williamsa SL, Abdel-Shafia AA (2002) Solvent effects on the photophysical properties of 9,10-dicyanoanthracene. Phys Chem Chem Phys 4:161–166
21. Fang DW, Guan W, Tong J, Wang ZW, Yang JZ (2008) Study on physicochemical properties of ionic liquids based on alanine [$C_n$mim][ala] ($n = 2,3,4,5,6$). J Phys Chem B 112:7499–7505
22. Santos CS, Baldelli S (2009) Alkyl chain interaction at the surface of room temperature ionic liquids: systematic variation of alkyl chain length ($R = C_1-C_4, C_8$) in both cation and anion of [RMIM][$R-OSO_3$] by sum frequency generation and surface tension. J Phys Chem B 113:923–933
23. Kolbeck C, Lehmann J, Lovelock KRJ, Cremer T, Paape N, Wasserscheid P, Fröba AP, Maier F, Steinrück HP (2010) Density and surface tension of ionic liquids. J Phys Chem B 114:17025–17036
24. Dzyuba SV, Bartsch RA (2002) Influence of structural variations in 1-alkyl(aralkyl)-3-methylimidazolium hexafluorophosphates and bis(trifluoromethylsulfonyl) imides on physical properties of the ionic liquids. Chem Phys Chem 3:161–166
25. Bhargava BL, Balasubramanian S, Klein ML (2008) Modelling room temperature ionic liquids. Chem Commun 29:3339–3351
26. Sánchez LG, Espel JR, Onink F, Meindersma GW, de Haan AB (2009) Density, viscosity, and surface tension of synthesis grade imidazolium, Pyridinium, and Pyrrolidinium based room temperature ionic liquids. J Chem Eng Data 54:2803–2812
27. Martino W, de la Mora JF, Yoshida Y, Saito G, Wilkes J (2006) Surface tension measurements of highly conducting ionic liquids. Green Chem 8:390–397
28. Tariq M, Serro AP, Mata JL, Saramago B, Esperanc JMSS, Lopes JNC, Rebelo LPN (2010) High-temperature surface tension and density measurements of 1-alkyl-3-methylimidazolium bistriflamide ionic liquids. Fluid Phase Equilib 294:131–138
29. Restolho J, Serro AP, Mata JL, Saramago B (2009) Viscosity and surface tension of 1-Ethanol-3-methylimidazolium Tetrafluoroborate and 1-Methyl-3-octylimidazolium Tetrafluoroborate over a wide temperature rang. J Chem Eng Data 54:950–955
30. Liu QS, Yang M, Yan PF, Liu XM, Tan ZC, Welz-Biermann U (2010) Density and surface tension of ionic liquids [$C_n$py][NTf_2] ($n = 2, 4, 5$) J. Chem Eng Data 55:4928–4930
31. Carvalho PJ, Freire MG, Marrucho IM, Queimada AJ, Coutinho JAP (2008) Surface tensions for the 1-Alkyl-3-methylimidazolium bis(trifluoromethylsulfonyl)-imide ionic liquids. J Chem Eng Data 53:1346–1350
32. Kurnia KA, Abdul Mutalib MIA, Man Z, Bustam MA (2012) Density and surface tension of ionic liquids [$H_2N–C_2$mim][PF_6] and [$H_2N–C_3$mim][PF_6]. J Chem Eng Data 57:2923–2927
33. Fang DW, Wang H, Yue S, Xiong Y, Yang JZ, Zang SL (2012) Physicochemical properties of air and water stable rhenium ionic liquids. J Phys Chem B 116: 2513–2519
34. Guan W, Ma XX, Li L, Tong J, Fang DW, Yang JZ (2011) Ionic Parachor and its application in acetic acid ionic liquid homologue 1-Alkyl-3-methylimidazolium acetate {[$C_n$mim][OAc]($n = 2,3,4,5,6$)}. J Phys Chem B 115:12915–12920
35. Malham IB, Letellier P, Turmine M (2006) Evidence of a phase transition in Water-Butyl-3-methylimidazolium Tetrafluoroborate and Water-1-Butyl-2,3-dimethylimidazolium Tetrafluoroborate mixtures at 298 K: determination of the surface thermal coefficient, $b_{T,P}$. J Phys Chem B 110:14212–14214
36. Li N, Zhang SH, Zheng LQ, Dong B, Li XW, Yu L (2008) Aggregation behavior of long-chain ionic liquids in an ionic liquid. Phys Chem Chem Phys 10:4375–4377
37. Tong J, Ma X, Kong YX, Chen Y, Guan W, Yang JZ (2012) Ionic Parachor and its application II. Ionic liquid homologues of 1-Alkyl-3-methylimidazolium Propionate {[$C_n$mim][Pro] ($n = 2 - 6$)}. J Phys Chem B 116:5971–5976
38. Velasco SB, Turmine M, Caprio DD, Letellier P (2006) Micelle formation in ethyl-ammonium nitrate

(an ionic liquid). Colloids Surf A Physicochem Eng Asp 275:50–54
39. Guggenheim EA (1966) Equilibria of chemical reactions. Oxford University Press
40. Blesic M, Marques MH, Plechkova NV, Seddon KR, Rebelo LPN, Lopes A (2007) Self-aggregation of ionic liquids: micelle formation in aqueous solution. Green Chem 9:481–490
41. Fröba AP, Wasserscheid P, Gerhard D, Kremer H, Leipertz A (2007) Revealing the influence of the strength of coulomb interactions on the viscosity and interfacial tension of ionic liquid Cosolvent mixtures. J Phys Chem B 111:12817–12822
42. Liu WW, Cheng LY, Zhang YM, Wang HP, Yu MF (2008) The physical properties of aqueous solution of room-temperature ionic liquids based on imidazolium: database and evaluation. J Mol Liq 140:68–72
43. Fang DW, Hu XH, Liang KH, Yan Q, Wei J (2019) The excess molar volume and the molar surface Gibbs energy of the binary of the ether-functionalized ionic liquids [$C_2$2O1IM][TfO] with ethanol and isomeric propanols at T = (288.15–318.15) K. Thermochim Acta 682:178383
44. Gao YA, Zhao XY, Dong B, Zheng L, Li N, Zhang SH (2006) Inclusion complexes of β-Cyclodextrin with ionic liquid surfactants. J Phys Chem B 110:8576–8581
45. Adamson AW (1986) Physical chemistry of surfaces, 3rd edn. Wiley, New York
46. Wang Q, Wang H, Guo FS, Liu Y, Fang DW, Zang SL (2010) Estimation of physico-chemical properties of ionic liquid [C_7mim][BF_4]. Fluid Phase Equilib 299:300–303
47. Tong J, Liu QS, Xu WG, Fang DW, Yang JZ (2008) Estimation of physicochemical properties of ionic liquids 1-Alkyl-3-methylimidazolium chloroaluminate. J Phys Chem B 112:4381–4386
48. Sun SG, Wei Y, Fang DW, Zhang QG (2008) Estimation of properties of the ionic liquid BMIZn_3Cl_7. Fluid Phase Equilib 273:27–30
49. Wang JY, Zhao FY, Liu RJ, Hu YQ (2011) Thermophysical properties of 1-methyl-3-methylimidazolium dimethylphosphate and 1-ethyl-3-methylimidazolium diethylphosphate. J Chem Thermodyn 43:47–50
50. Deetlefs M, Seddon KR, Shara M (2006) Predicting physical properties of ionic liquids. Phys Chem Chem Phys 8:642–649
51. Adamson AW (1986) Physical chemistry of surfaces, 3rd edn. Wiley, New York, 1976. Translated by TR Gu, Science Press, Beijing
52. Yang JZ, Lu XM, Gui JS, Xu WG (2004) A new theory for ionic liquids – the interstice model. Green Chem 6:541–543
53. Guggenheim EA (1945) The principle of corresponding states. J Chem Phys 13(7):253–261
54. Zaitsau DH, Kabo GJ, Strechan AA, Paulechka YU, Tschersich A, Verevkin SP, Heintz A (2006) Experimental vapor pressures of 1-Alkyl-3-methylimidazolium Bis(trifluoromethylsulfonyl)imides and a correlation scheme for estimation of vaporization enthalpies of ionic liquids. J Phys Chem A 110:7303–7306
55. Tong J, Yang HX, Liu RJ, Chi L, Xia LX, Yang JZ (2014) Determination of the enthalpy of vaporization and prediction of surface tension for ionic liquid 1-Alkyl-3-methylimidazolium propionate [$C_n$mim][Pro](n=4,5,6). J Phys Chem B 118:12972–12978
56. Mountain BW, Seward TM (2003) Hydrosulfide/sulfide complexes of copper(I): experimental confirmation of the stoichiometry and stability of $Cu(HS)_2^-$ to elevated temperatures. Geochim Cosmochim Ac 67:3005–3014
57. Bandrés I, Giner B, Artigas H, Royo FM, Lafuente C (2008) Thermophysic comparative study of two isomeric Pyridinium-based ionic liquids. J Phys Chem B 112:3077–3084

Surfactant Behavior of Ionic Liquids Involving a Drug

Arghajit Pyne, Sangita Kundu and Nilmoni Sarkar
Department of Chemistry, Indian Institute of Technology, Kharagpur, WB, India

Introduction

The organic salts comprising of sterically mismatched ions and also with relatively low melting point (generally below 100 °C) but excellent thermal stability are known as ionic liquids (ILs). In recent times, they are extensively used in different research fields; but historically these ILs are not very new. Although the first published review on room temperature ionic liquid (RTIL) came in the year of 1999 by Thomas Welton, the earliest RTIL, ethylammonium nitrate (EAN, [$EtNH_3$][NO_3]), was reported by Paul Walden in 1914. However, in India, Rây and Sen did excellent works and made significant contributions in this particular field since 1911. Besides the RTILs, the ILs having long alkyl hydrophobic chains and inherent amphiphilic characteristics are known as surface-active ionic liquids (SAILs). The structural dissection of the ILs reveals that most of the ILs containing imidazolium or pyrrolidinium head groups and long hydrophobic alkyl chains lead to

their aggregation in different media. Such aggregations result in several interesting molecular assemblies like micelles, vesicles, reverse micelles, microemulsions, etc. These IL-induced microheterogeneous aggregates show significant amounts of contributions in drug delivery, gene delivery, nanocarrier, bioimaging, photodynamic therapy, etc. Nevertheless, among all these applications, the IL-related aggregate-induced drug delivery is the most important.

Background

Surfactants are generally organic molecules having polar, ionic, or nonionic head groups with extended apolar, organic residues [1]. These surfactants undergo intra- and intermolecular assemblies to form various molecular architectures like micelle, vesicles, microemulsions, etc. The history of such surfactant assembly is not very new. Kaler and coworkers in 1989 reported the formation of thermodynamically stable vesicles between the cationic surfactant, cetyltrimethylammonium tosylate (CTAT), and the anionic surfactant, sodium dodecylbenzenesulfonate (SDBS), at appropriate mixing ratio in aqueous solution [2]. They discussed about the role of the production of ion-pair amphiphile (IPA) which act as double-chained zwitterionic surfactant in the formation of vesicular aggregates. Although these surfactant-based aggregated systems are highly stable and very easy to prepare, in recent times, due to the breakthrough surface-active properties and excellent aggregation behaviors, these surfactants are gradually replaced by more fascinating and sophisticated surfactant systems, known as ILs [3].

Results and Discussion

This particular section has been subdivided into two parts: in the first part, we have discussed the synthesis and characterization of ILs and surfactants-induced different aggregated nanostructures. The second part of this section deals with the discussion about the surfactant properties of the ILs with the abilities of the studied aggregates as efficient drug nanocarriers. This section also includes different photophysical studies associated with the drugs inside these IL-derived different aggregated morphologies.

Synthesis and Characterization of Different Aggregated Nanostructures

Conventional Surfactant Derived Aggregated Structures

The aggregated structures formation due to the assembly of the surfactants is quite conventional one, and a significant numbers of contributions in terms of their synthesis and morphological characterization as well as applications in diverse research fields have been made. Although, till date, a large number of reports are published on this particular topic, one of the oldest works in this field was reported by Kaler et al. [2], where they showed that spontaneous vesicle having radius in the range of 30–80 nm formed when appropriate concentrations of oppositely charged surfactants, CTAT and SDBS, in water were mixed. The formation of alkyltrimethylammonium bromide containing (C_nTAB, $n = 12$, 14, and 16) micelles and cholesterol-induced respective vesicles were also reported [1]. The structural and morphological characterizations of the systems were performed using dynamic light scattering (DLS) and transmission electron microscopy (TEM) measurements. Moreover, cholesterol-induced micelle-to-vesicle transition of the system as mentioned was also probed through studying the excited-state intramolecular double proton transfer (ESIDPT) dynamics of a well-known probe molecule, 2,2′-Bipyridine-3,3′-diol ($BP(OH)_2$). Now, apart from these studies, Kuchlyan et al. [4] also discussed about the formation of stable unilamellar vesicles from zwitterionic *N*-hexadecyl-*N*,*N*-dimethylammonio-1-propanesulfonate (SB-16) and cationic poly-L-lysine (PLL) surfactants, which were characterized in detail employing turbidity measurement, DLS, cryo-TEM, zeta potential, conductivity, and steady-state emission studies. The results were assembled and shown in Fig. 1.

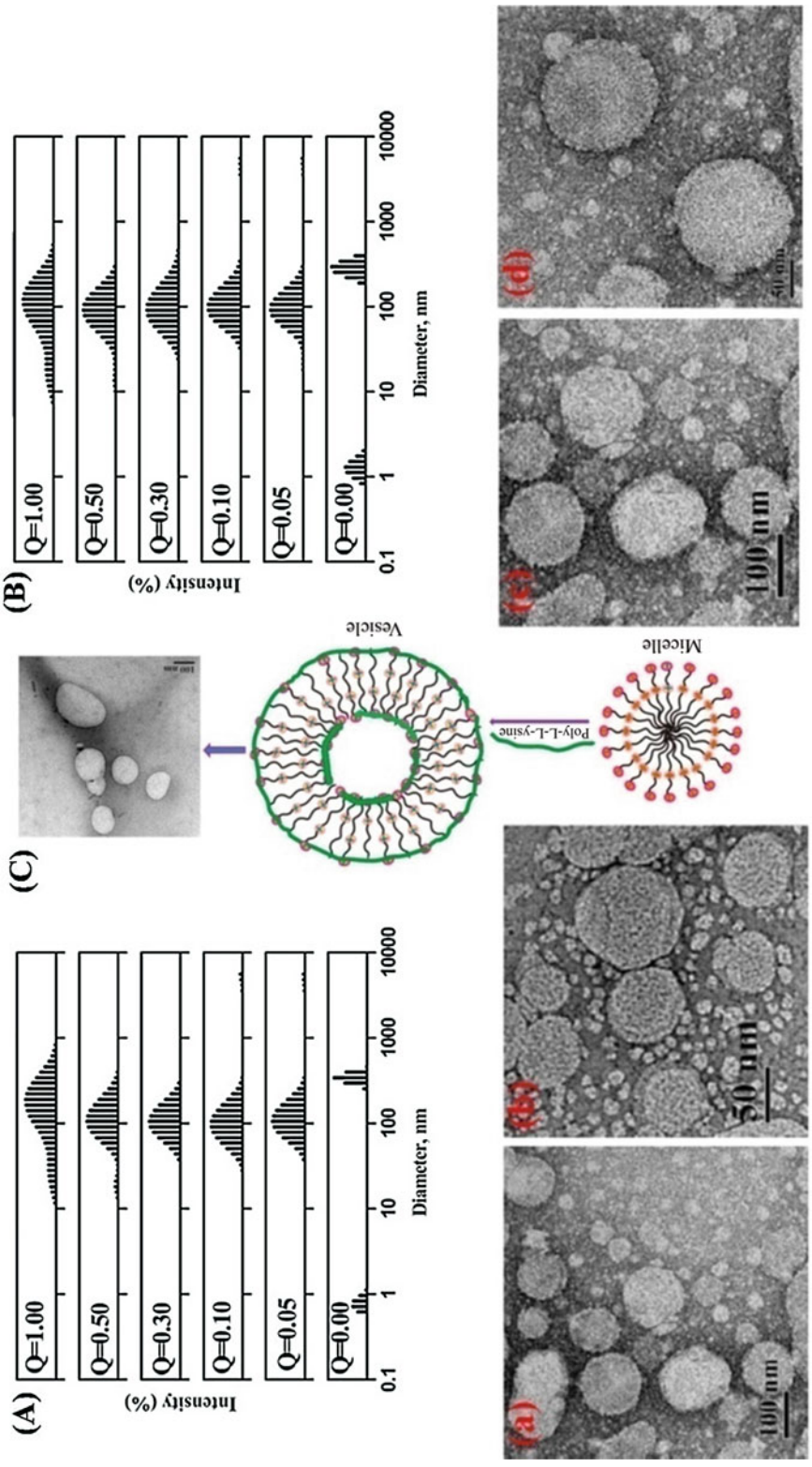

Surfactant Behavior of Ionic Liquids Involving a Drug, Fig. 1 DLS intensity size distribution histograms of (**A**) CTAB/cholesterol and (**B**) TTAB/cholesterol supramolecular aggregates; TEM images of the vesicles composed of CTAB/cholesterol, (**a**, **b**) Q = 1.0 and TTAB/cholesterol, (c, d) Q = 1.0 (Q = concentration of cholesterol/concentration of surfactant); (**C**) schematic diagram of the vesicle formation between zwitterionic surfactant, *N*-hexadecyl-*N*,*N*-dimethylammonio-1-propanesulfonate (SB-16), and cationic poly(amino acid), poly-L-lysine (PLL). (Images (**A**, **B**, **a**, **b**, **c**, and **d**) are reprinted with permission from J. Phys. Chem. B 2014, 118, 9329–9340 (copyright 2014, American Chemical Society), and image **C** is reprinted with permission from J. Phys. Chem. B 2015, 119, 8285–8292 (copyright 2015, American Chemical Society))

IL-Surfactant-Based Aggregated Nanostructures

There are significant applications of the conventional surfactants and respective surfactant-based aggregates; but in recent times, the corresponding uses of these surfactants are reduced to some extent because of their high toxicity and comparatively complex methods are involved in converting these materials to respective biodegradable ones. Now, although, some ILs show some amount of cytotoxicity, in general, the ILs are considered as "green solvents," and since the solvent properties of the ILs can be tuned very easily, these "designer solvents" are efficiently used as replacements of common solvents and also different conventional surfactants [3]. However, a detailed study on the micelle-vesicle-micelle transition, involving anionic surfactant, SDBS, and cationic imidazolium-based ILs, $C_n$mimCl ($n = 12, 16$), was performed [5]. A similar study including cationic surfactant, CTAB, and anionic IL, 1-butyl-3-methylimidazolium octylsulfate [C_4mim][C_8SO_4], was also carried out [6]. The detailed characterization results of these two studies were summarized in Fig. 2.

IL-IL-Based Aggregated Nanostructures

The structural dissection of various ILs reveals that opposite ion pairs with long hydrophobic alkyl chains lead to form corresponding micelles above a certain concentration (critical micelle concentration, CMC). These IL micelles result in respective vesicular aggregates in the presence or absence of any external additives. These IL-induced micelle-to-vesicle transitions in the presence or absence of foreign amphiphilic molecules are well known and very much important with respect to their applications in different research fields. In this respect, the aggregation between two oppositely charged ILs-cationic 1-dodecyl-3-methylimidazoium chloride ([C_{12}mim]Cl) and anionic 1-butyl-3-methylimidazolium *n*-octylsulfate ([C_4mim][C_8SO_4]) and, as a result, micelle-vesicle-micelle transitions were firmly established using turbidity, conductivity, DLS, TEM, and cryo-TEM measurements [7]. The DLS study indicated that the micellar solution of [C_4mim][C_8SO_4] IL gradually formed mixed micelle and vesicles with increasing concentrations of another IL additive, [C_{12}mim]Cl, which were further confirmed using TEM and cryo-TEM images (Fig. 3).

Now, microemulsions are thermodynamically stable microheterogeneous system containing an oil phase and aqueous phase stabilized by an interfacial film of surfactant or mixture of surfactants. Han and his co-workers first demonstrated the formation of IL-in-oil (IL/o) microemulsions containing IL as a polar domain. Subsequently, Eastoe et al. have studied this system using SANS experiments. Pramanik et al. [8] prepared nonaqueous microemulsion comprised of RTIL, *N*-methyl-*N*-propylpyrrolidinium bis(trifluoromethanesulfonyl)imide ([P13][Tf_2N]), nonionic surfactant, TX-100, and benzene as nonpolar phase and characterized it by electrical conductivity, DLS, and NMR measurements, and the dynamic properties were investigated using steady-state and time-resolved spectroscopic measurements (Fig. 4a).

In another report, Mandal et al. [9] investigated the fluorescence resonance energy transfer (FRET) study from coumarin 480 to rhodamine 6G in the microreactor of the microemulsion, where the polar IL, 1-ethyl-3-methylimidazolium *n*-butylsulfate ([C_2mim][C_4SO_4]), was stabilized by a mixture of polyoxyethylene sorbitan monooleate (Tween 80) and sorbitan laurate (Span 20) in the oil phase of IPM (shown in Fig. 4b). Nowadays, the conventional ILs are modified to form various novel ILs, and thus their surface-active properties are highly modulated [3]. The most promising and popular way for such modification involves replacing the Na^+ of common double-chain surfactant, aerosol-OT (NaAOT), with appropriate counterparts of ILs. Such replacement with imidazolium cations ($[C_n mim]^+$; $n = 8,12,16$) leads to the formation of new types of surface-active ILs which were observed to form giant vesicular aggregates in aqueous buffer solution as described by Banerjee et al. [10] The detailed characterizations of these aggregates were performed using nuclear magnetic resonance (NMR), TEM, fluorescence lifetime imaging microscopy (FLIM), and fluorescence correlation spectroscopy (FCS) studies. Pyne et al. [11] also used this concept to synthesize a novel cholesterol and glycine-derived AOT-based [Chol-Gly][AOT] SAIL. This modified

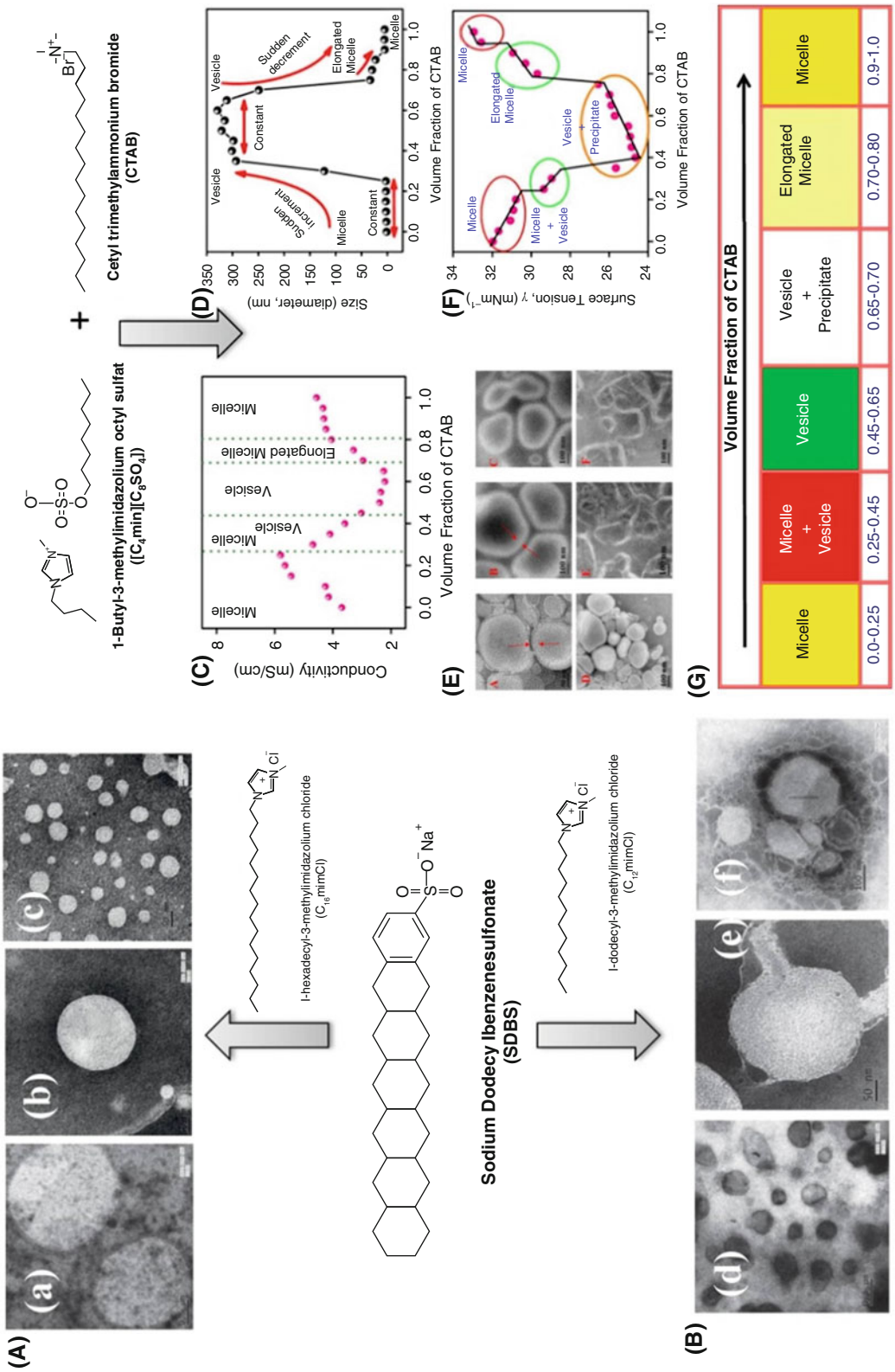

Surfactant Behavior of Ionic Liquids Involving a Drug, Fig. 2 (continued)

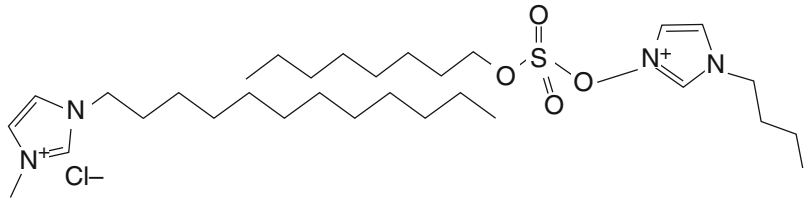

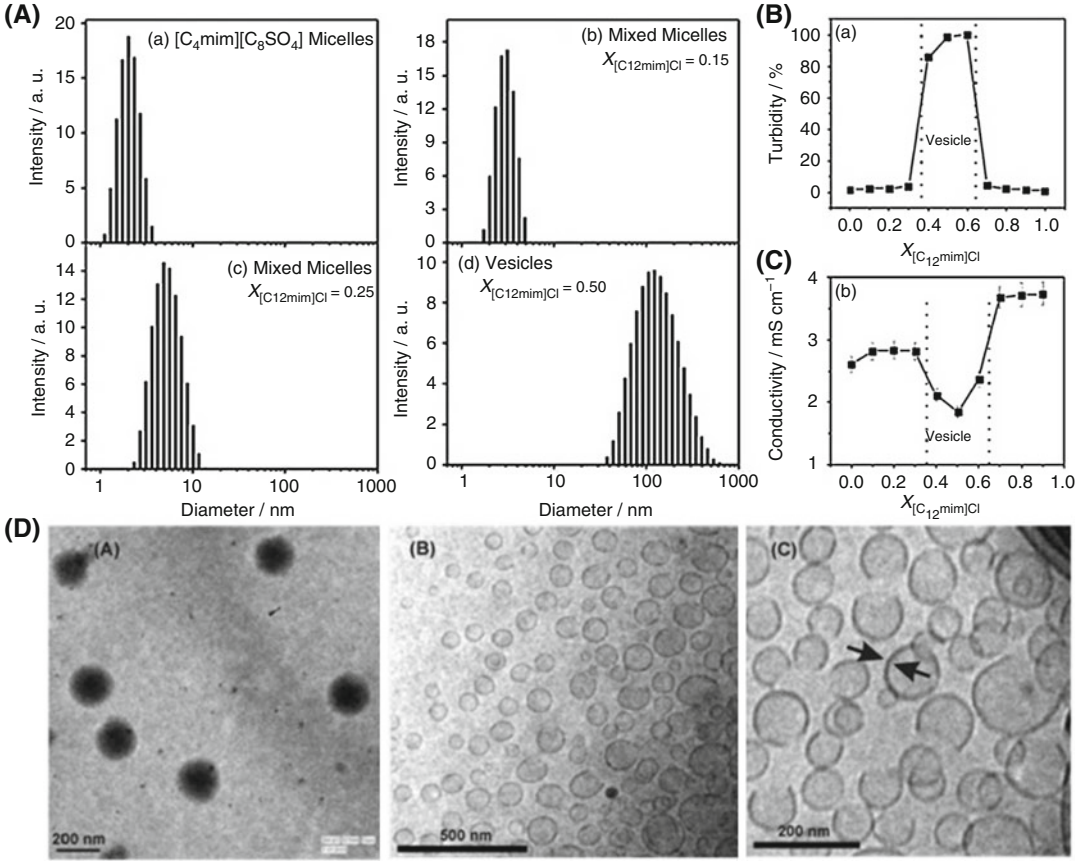

Surfactant Behavior of Ionic Liquids Involving a Drug, Fig. 3 (**A**–**D**) DLS intensity versus size profile, normalized turbidity, conductivity, and TEM micrographs, respectively, of $[C_4mim][C_8SO_4]/[C_{12}mim]Cl$ vesicles. (Images (**A**–**D**) are reprinted with permission from ChemPhysChem 2014, 15, 3544–3553 (copyright 2014, Wiley))

Surfactant Behavior of Ionic Liquids Involving a Drug, Fig. 2 TEM images of (**A**) SDBS/$[C_{16}mim]Cl$ vesicular aggregates at (**a**) $\chi_{C_{16}mimCl} = 0.50$ (**b**) $\chi_{C_{16}mimCl} = 0.20$ and (**c**) $\chi_{C_{16}mimCl} = 0.65$; (**B**) SDBS/$[C_{12}mim]Cl$ vesicular aggregates at (**d**) $\chi_{C_{12}mimCl} = 0.50$ (**e**) $\chi_{C_{12}mimCl} = 0.20$ and (f) $\chi_{C_{16}mimCl} = 0.65$. (**C**–**F**) Conductivity, size (determined by DLS), TEM, and surface tension measurements of $[C_4mim][C_8SO_4]$/CTAB solution at different volume fractions of CTAB; (**G**) pictorial representation to summarize micelle-vesicle-micelle transition of $[C_4mim][C_8SO_4]$/CTAB system. (Images (**A**, **B**) are reprinted with permission from J. Colloid Interface Sci. 2017, 490, 762–773 (copyright 2017, Elsevier), and images (**C**–**G**) are reprinted with permission from Langmuir 2013, 29, 10066–10076 (copyright 2013, American Chemical Society))

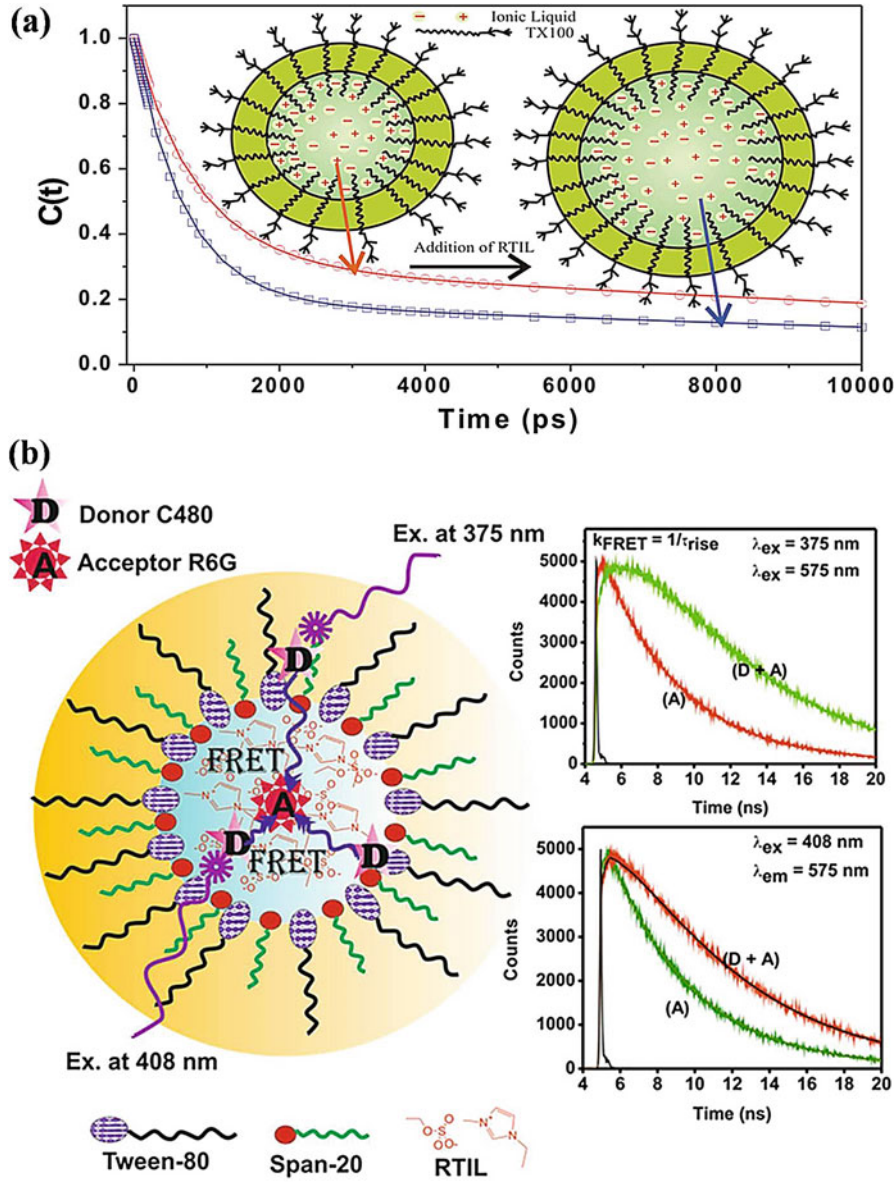

Surfactant Behavior of Ionic Liquids Involving a Drug, Fig. 4 (**a**) Change in solvation correlation time of probe C480 with the addition of RTIL ([P13][Tf_2N]) in TX100/benzene system; (**b**) picosecond time-resolved fluorescence decays of the acceptor R6G with the addition of donor C480 in RTIL microemulsion system comprised of [C_2mim][C_4SO_4] IL, surfactant mixtures of Tween 80 and Span 20, and oil phase IPM. (Image **a** is reprinted with permission from J. Phys. Chem. B 2011, 115, 2322–2330 (copyright 2011, American Chemical Society), and Image **b** is reprinted with permission from J. Phys. Chem. B 2013, 117, 3221–3231 (copyright 2013, American Chemical Society))

surfactant [Chol-Gly][AOT] is very much important since it was reported to form IL-in-oil microemulsion in the presence of 1-ethyl-3-methylimidazolium octylsulfate ([Emim][Os]) IL and IPM oil phase as well as stable vesicles in aqueous solution. The microemulsion was characterized by constructing ternary phase diagram, DLS, ^{1}H NMR, steady-state emission using

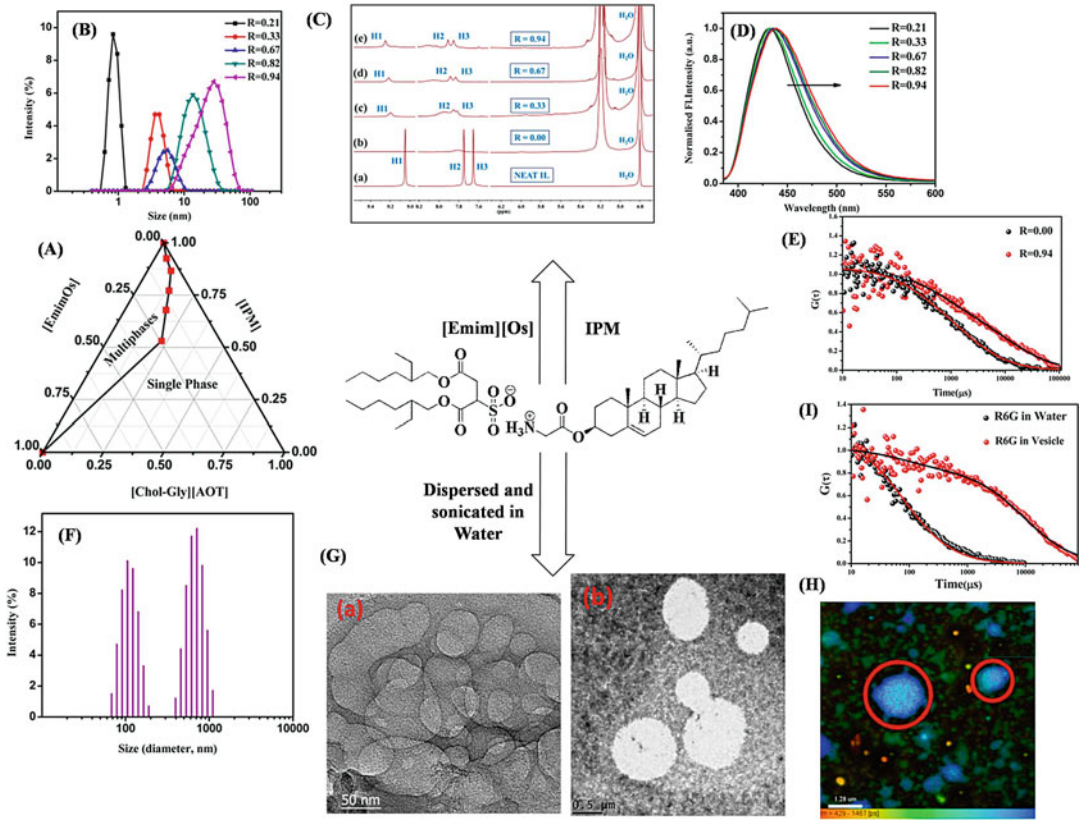

Surfactant Behavior of Ionic Liquids Involving a Drug, Fig. 5 (**A**) Ternary phase diagram, (**B**) DLS size distribution analysis, (**C**) ^{1}H NMR study, (**D**) steady-state emission study, and (**E**) FCS study to characterize EmimOs/[Chol-Gly][AOT]/IPM microemulsion; (**F**) DLS histogram, (**G**) TEM images, (**H**) FLIM image, and (**I**) FCS study for systematic characterization of the vesicles formed by [Chol-Gly][AOT] in water. (Images (**A**–**I**) are reprinted with permission from Langmuir 2017, 33, 5891–5899 (copyright 2017, American Chemical Society))

coumarin 480 as the fluorophore, and also by recording the diffusion behavior of rhodamine 6G (R6G) in microemulsion droplets through FCS techniques (Fig. 5A–E). The ternary phase diagram indicated the presence of three microregions, IL-in-oil, oil-in-IL, and bicontinuous regions, whereas other mentioned measurement techniques confirmed that with increasing EmimOs IL content, the size of the microemulsion droplets increased. On the other hand, the formation of vesicle dispersion in water was established employing DLS, TEM, cryo-TEM, field emission scanning electron microscopy (FESEM), atomic force microscopy (AFM), FCS, and FLIM measurements, as shown in Fig. 5F–I. All these characterization techniques clearly tells that both small and large vesicular aggregates were formed in the aqueous dispersion of the synthesized [Chol-Gly][AOT].

IL-Biomolecules Aggregated Nanostructures

The above three sections deal with the aggregation results of IL with different surface-active molecules. In this section, we would like to discuss about the interactions and consequently aggregations between ILs and some biologically important molecules. These biomolecules range from proteins, nucleotides, and amino acids to bile salts, vitamins, etc. The impact of ILs on protein actually depends on the properties of IL and proteins as well as several external factors like pH, temperature, ionic strength of the

S

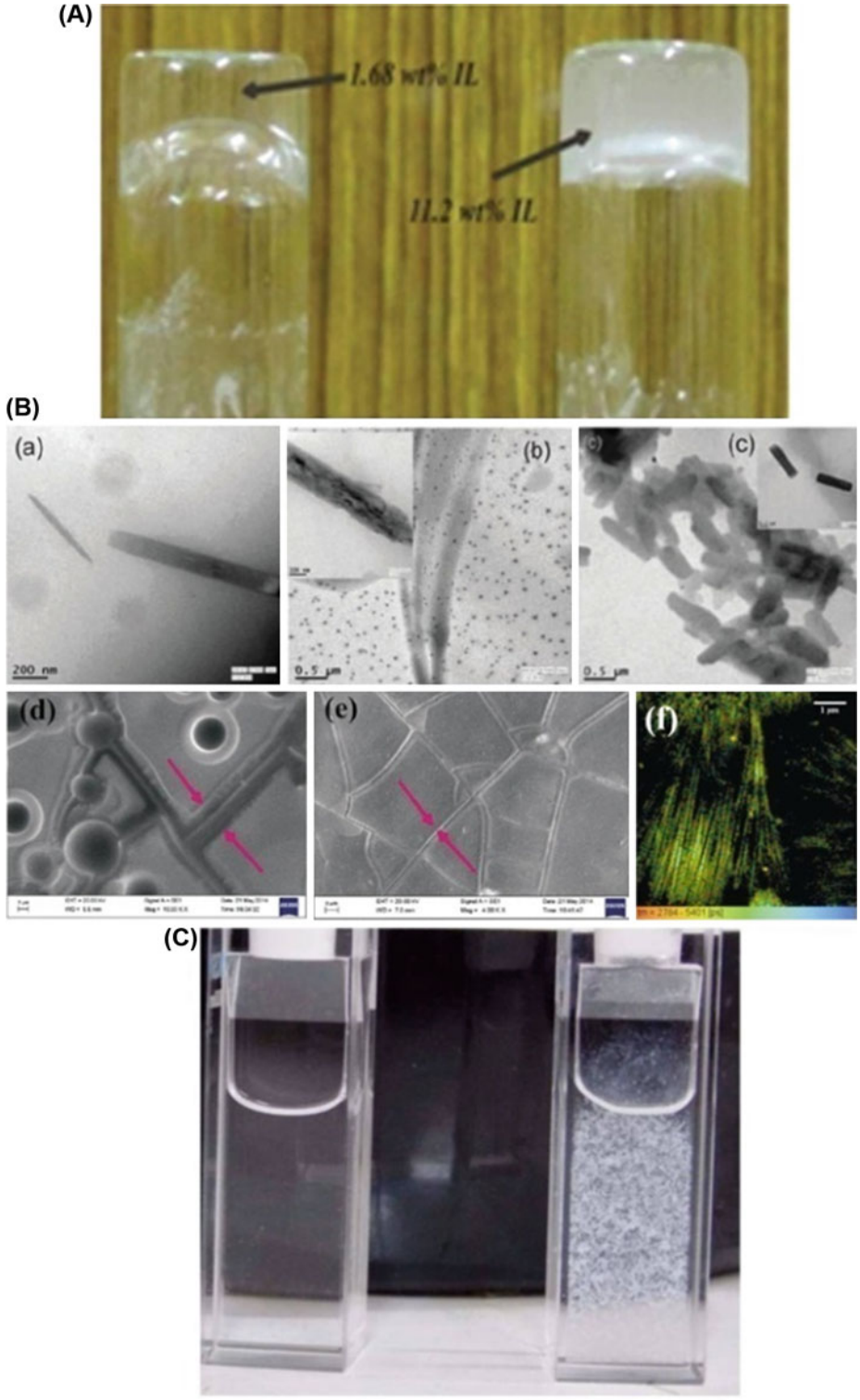

Surfactant Behavior of Ionic Liquids Involving a Drug, Fig. 6 (continued)

solution, etc., and depending on these parameters, some ILs may induce aggregation or denaturation of protein, while some other ILs may provide stability to the biomolecular system. The ILs also can provide solubility and long-term stability to several other biomolecules and thus can be effectively used as preservation medium. Moreover, recently a large number of biocompatible ILs, derived from biomolecules like amino acids, are known which have potential applications in biological, medical, and pharmaceutical research fields. However, the most promising IL-biomolecules aggregation involves that between ILs and bile salts which result in various types of aggregated morphologies.

Bile salts are the important biological amphiphiles, involved in digestion of fats, fat-soluble compounds, and lipids. Kundu et al. have discussed that at low IL concentrations, elongated rodlike bile salt (sodium deoxycholate, NaDC) aggregates were obtained, which transformed into small aggregates at higher IL concentrations [12]. This was supported using TEM, SEM, and FLIM techniques, as shown in Fig. 6.

Different IL Systems Involving Drug Molecules

IL-Drug Assembly and Drug-Containing ILs

The large and diverse studies in the field of ILs result in a broad focus on the synthesis and applications of drug-containing IL systems and different aggregated microstructures involving drugs and ILs. The reports on the aggregation behaviors of ibuprofenate (Ibu)-derived [$C_n$mim][Ibu] (n = 4, 6, 8) [13] in aqueous medium shed light on the formation of aggregated architectures from the active pharmaceutical ingredients (APIs). The experimental (DLS, cryo-TEM and ^{1}H NMR) as well as molecular dynamics simulation studies showed that with increasing alkyl chain lengths of imidazolium cations, [$C_n$mim][Ibu] micellar sizes increase, and micelle to large globular aggregates were formed which upon dilution transformed into spherical vesicular aggregates.

In the second part, the discussion will be based on the assembly between ILs and drug molecules and subsequent characterizations of the respective system.

Pyne et al. [14] showed recently that one of the most important and popular anticancer drugs, doxorubicin hydrochloride (Dox), formed spherical vesicular aggregates with eight carbon containing IL, [C_8mim]Cl, and further this vesicular aggregates were transformed into rodlike fibrillar networks in the presence of another important biomolecule, sodium cholate (NaCh) bile salt. In Fig. 7, the measurement techniques (DLS, FLIM, TEM, FESEM, and AFM) used to characterize both these vesicular and fibrillar aggregates are shown. The report suggested that spherical Dox/IL aggregates were formed mainly due to the presence of π-π and cation-π interactions along with hydrophobic and hydrogen bonding interactions between the Dox and imidazolium IL. On the other hand, the electrostatic and hydrophobic interactions between the IL and bile salt as well as IL and Dox resulted in the disruption of spherical aggregates to rodlike fibrillar aggregates. These Dox containing vesicular and fibrillar aggregates are expected to have potential applications in different biomedical and pharmaceutical research fields.

Drug Molecules Inside the ILs Forming Assemblies

The conventional strategy for developing drug delivery system consists of loading drug molecules inside the aggregated networks formed by different amphiphilic molecules. In previous

Surfactant Behavior of Ionic Liquids Involving a Drug, Fig. 6 (**A**) Digital micrographs of the viscous solution of 20 mM NaDC in the presence of 1.68 wt% and 11.2 wt% [bmim]-BF_4; (**B**) TEM images of NaDC aggregates in the presence of 1.12 wt% (**a**), 1.68 wt% (**b**), and 11.2 wt% (**c**) [bmim]-BF_4, FESEM images of the aggregates of 20 mM NaDC in the presence of (**d**) 1.68 wt % and (**e**) 5.6 wt% [bmim]-BF_4, and (**f**) FLIM image of 20 mM NaDC aggregates in the presence of 3 wt% [bmim]-BF_4; (**C**) digital images of NaDC solution in 5.68 wt% [bmim]-BF_4, above and below CMC. (Images (**A**–**C**) are reprinted from Phys. Chem. Chem. Phys. 2015, 17, 25216–25227 with permission from the PCCP Owner Societies)

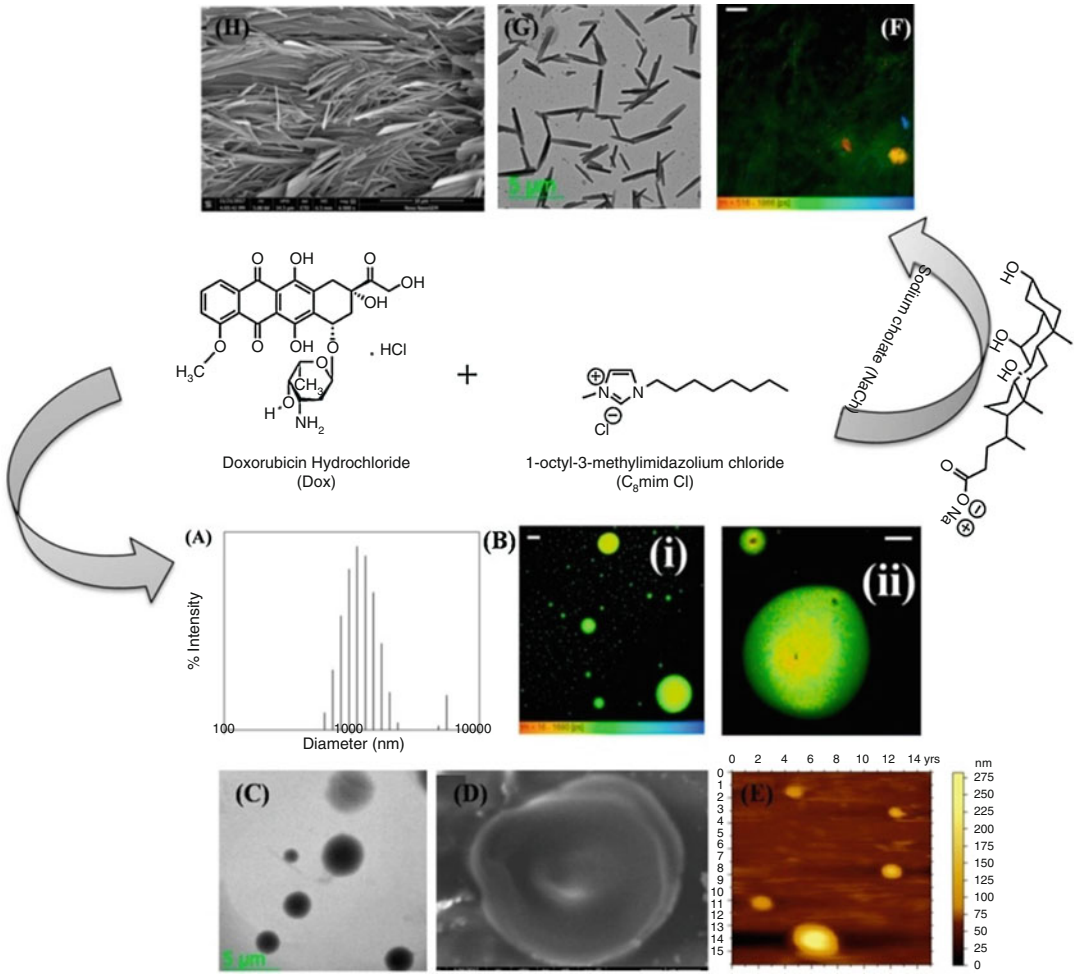

Surfactant Behavior of Ionic Liquids Involving a Drug, Fig. 7 (**A**) DLS, (**B**) FLIM, (**C**) TEM, (**D**) FESEM, and (**E**) AFM images of Dox/[C_8mim]Cl spherical vesicular aggregates; (**F**) FLIM, (**G**) TEM, and (**H**) FESEM images of the rodlike fibrillar Dox/[C_8mim]Cl/NaCh aggregates. (Images (**A**–**H**) are reprinted with permission from Langmuir 2018, 34, 3296–3306 (copyright 2018, American Chemical Society))

sections, we have discussed elaborately that ILs can serve as potential candidates for the formation of the aggregated architectures. A large number of literature studies clearly support our standpoint. The ILs are documented to provide stability, increase solubility of several drug molecules, and, as a consequence, serve as drug delivery systems for a huge number of drug molecules. Curcumin is a commonly used organic molecule, obtained from turmeric and is highly pharmaceutically active molecule. The therapeutic efficacy and medicinal applications of curcumin are well known, and thus, its nanoformulations also have excellent pharmaceutical applications. The entrapment and subsequently photophysical behavior of curcumin inside [Bmim][Os] IL micelle were studied by Ghatak et al. [15] The study provides us informations regarding the high stability of curcumin inside the IL micelle and also large partition coefficient ($K_p = 8.59 \times 10^3$) of the drug from water to micellar phase, which established the micellar system as an effective drug delivery system. Again, Roy et al. [16] reported that aqueous solution of sorbitan stearate (Span 60) formed vesicles in the presence of [C_{16}mim]Cl IL, which again resulted an

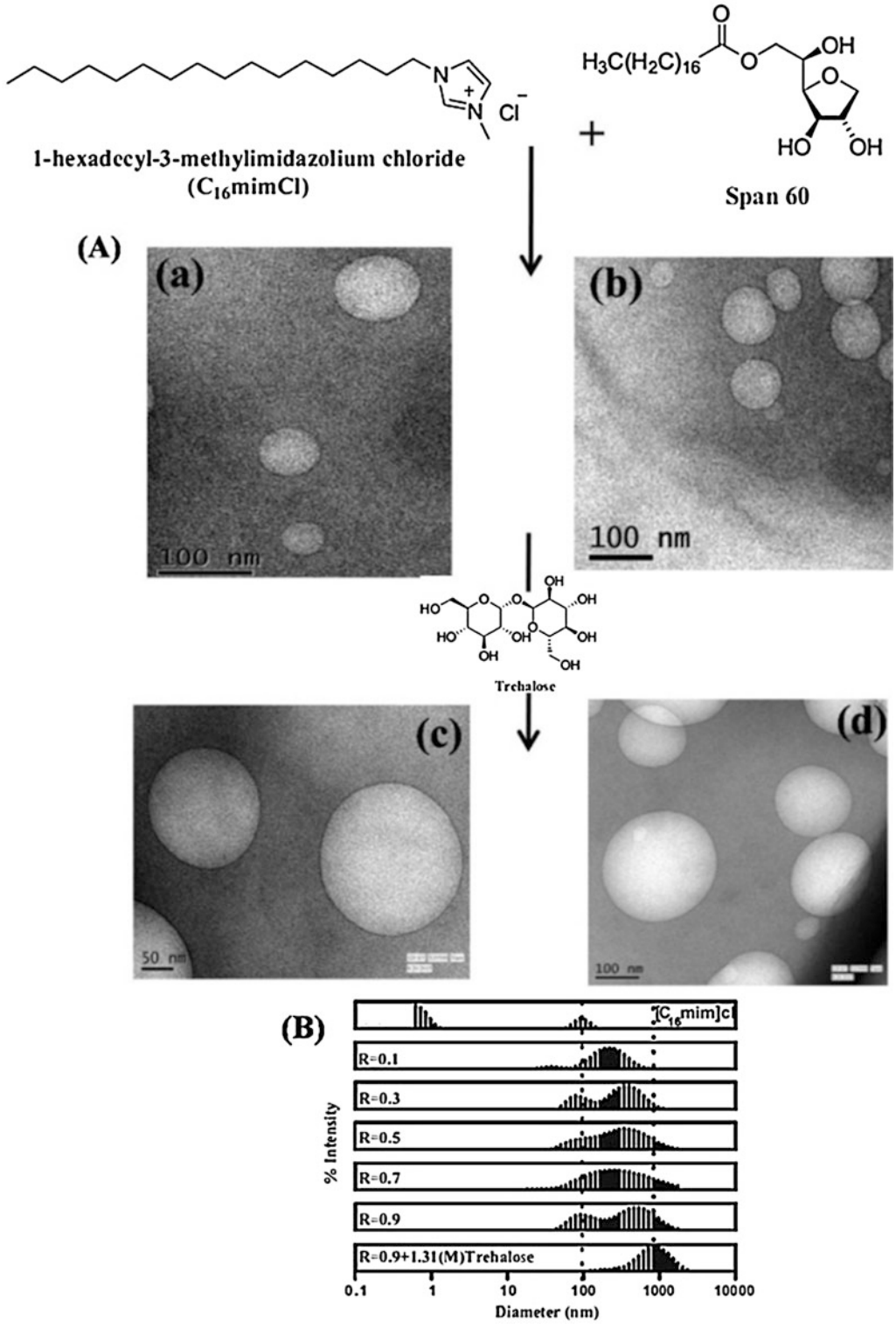

Surfactant Behavior of Ionic Liquids Involving a Drug, Fig. 8 (continued)

increment in size in the presence of trehalose. Now, due to favorable interactions between cationic [C_{16}mim]Cl IL and curcumin, the drug molecules were shown to encapsulate effectively inside the IL micelle and corresponding vesicles. Moreover, microenvironments of the IL-Span 60 aggregates and the same in the presence of trehalose were reported to affect the proton transfer (ESIPT) dynamics of curcumin significantly compared to that in IL micelle. The results are summarized and shown in Fig. 8.

Furthermore, Mahajan et al. [17] investigated the possible location of two important drug molecules, dopamine hydrochloride (DH) and acetylcholine chloride (AC), inside the micelle formed by the SAIL, 1-tetradecyl-3-methylimidazolium bromide (C_{14}mimBr) (Fig. 9).

Due to their small size, narrow size distribution, biocompatibility, and stability, micelles are more potent as a drug carrier. Through a comparative study using several experimental techniques, they have concluded that the SAIL-based micellar environment is better for encapsulation of the drug molecules than the conventional cationic surfactant tetradecyltrimethylammonium bromide ([TTA][Br]) micelles. Among these two drugs, DH was bound more strongly than AC with the C_{14}mimBr and [TTA][Br] because of the cation-π interaction between the aromatic moieties of drugs and positive charges of the imidazolium and ammonium cations of C_{14}mimBr and [TTA][Br], respectively. Furthermore, due to more hydrophilicity of DH, the hydrogen bonding ability of the polar groups of DH with water helps to locate the drug in the water micellar interface compared to the another one. As a consequence, the critical micelle concentration was reduced more in the presence of DH which was also the reason for the favorable interaction with DH. Again, Goto and co-workers reported that IL can be successfully used for the formulation of

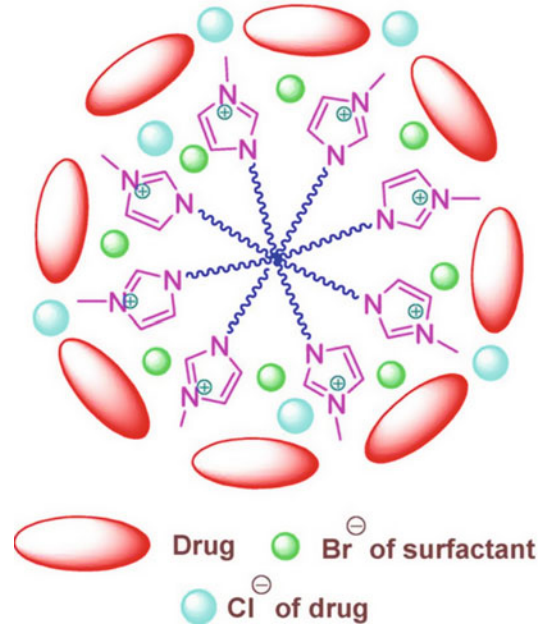

Surfactant Behavior of Ionic Liquids Involving a Drug, Fig. 9 Possible location of adsorption of drugs (DH and AC) inside the [C_{14}mim][Br] micelles. (This image is reprinted with permission from Langmuir 2012, 28, 17238–17246 (copyright 2012, American Chemical Society))

nonaqueous microemulsion which was effectively used as a transdermal and topical drug delivery system of several sparingly soluble drugs such as acyclovir (ACV), methotrexate (MTX), and dantrolene sodium (shown in Scheme 1) [18].

Now, in the previous section, we have discussed the IL-based microemulsion systems and their properties in details. Therefore, in this section, we are going to discuss about the drug delivery abilities of these systems, where the drug molecules were loaded inside the core of the microemulsions droplets and the surfactant-containing oil phase was used to stabilize the system as well as to overcome the stratum corneum barrier, a well-known barrier of

Surfactant Behavior of Ionic Liquids Involving a Drug, Fig. 8 (**A**) TEM images of the vesicles formed by [Span60] and [C_{16}mim]Cl (**a**, **b**), whereas the effect of trehalose on the vesicles (**a**, **b**) is shown in the figures (**c**, **d**); (**B**) DLS intensity versus size distribution histograms of [C_{16}mim]Cl micelle, [C_{16}mim]Cl-Span 60 vesicles, and vesicle in the presence of 1.31(M) trehalose. (Images (**A**, **B**) are reprinted with permission from Chem. Phys. Lett. 2016, 665, 14–21 (copyright 2016, Elsevier))

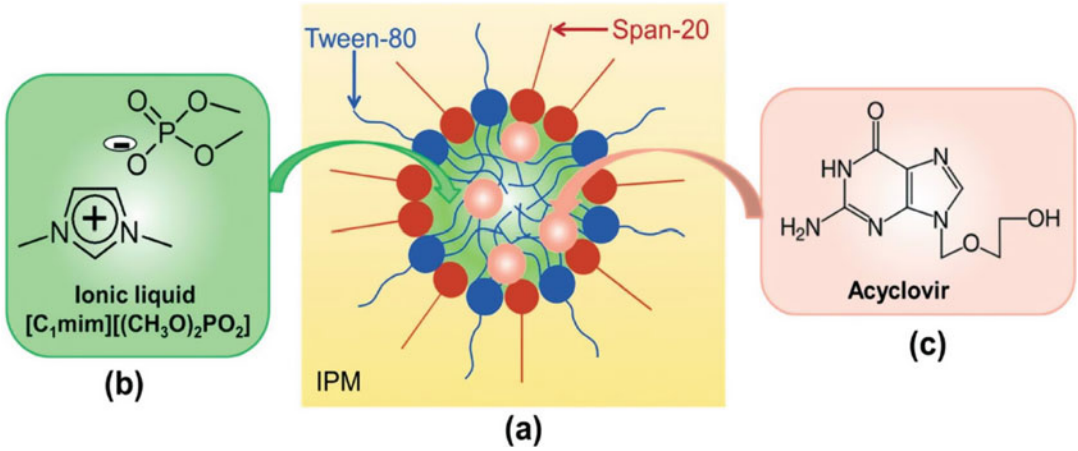

Surfactant Behavior of Ionic Liquids Involving a Drug, Scheme 1 Schematic diagrams of an IL-in-oil microemulsions (IL/o MEs) (**a**), IL [C_1mim][DMP] (**b**), and ACV drug (**c**). (This image is reprinted from J. Colloid Interface Sci. 2010, 352, 136–142 (copyright 2010, Elsevier))

topical drug delivery system. Among a set of hydrophilic ILs tested, dimethylimidazolium dimethylphosphate [C_1mim][DMP] formed stable droplets in IPM continuous phase stabilized by a blend of surfactants, Span 20 and Tween 80. It is true that pure IL are not completely biocompatible, but this microemulsion contained low concentration of IL and thus showed over 80% cell viability of a cancerous cell line compared to the Dulbecco's phosphate-buffered saline (D-PBS), IL, IPM, and water-in-oil (without IL) microemulsion. The similar approach was followed by Goindi and co-workers for the preparation of another IL/o microemulsion by coupling 1-butyl-3-methylimidazolium bromide (BMIMBr) with IPM and Span 20/Tween 80 surfactant assembly. This system showed potential applications as the drug carrier of 5-fluorouracil and exhibited some promising results. This IL/o microemulsion enhanced the therapeutic efficacy of 5-fluorouracil by increasing the solubility and permeability of the drug in the presence of the microsemulsion [19]. Again, ex vivo permeation results through mouse skin showed 4-fold and 1.6-fold enhancement in the percentage of drug penetration ability of the system as compared to the aqueous solution and without microemulsion. In addition, in vivo experiments against dimethylbenz(a)anthracene (DMBA)/12-*O*-tetradecanoylphorbol-13-acetate (TPA)-induced mice skin carcinogenesis showed that IL/o microemulsion system was efficient to cure the skin cancer in 4 weeks without any side effects. The histopathological studies indicated no anatomic and pathological change in the skin structure of mice. The same type of IL stabilized formulation containing 1-butyl-3-methylimidazolium hexafluorophosphate ($BMIMPF_6$), Tween 80, and ethanol was also used to solubilize and deliver the water insoluble drug etodolac (ETO). The ETO loaded microemulsion is known to provide excellent anti-inflammatory and antiarthritic activities in rodent models. Now, piroxicam is an anti-inflammatory, nonsteroidal drug belongs to the family of the compounds classified as oxicams which have antipyretic and analgesic properties and broadly used in the treatment of musculoskeletal and joint disorders, arthritis, and postoperative pain. The most promising route of the administration of the compound is through the topical delivery system compared to the oral route as the latter has some adverse effects. So, Ng et al. have developed IL/o nanoemulsions composed of different types of ILs such as hydrophilic IL, 1-hexyl-3-methylimidazolium chloride [Hmim][Cl], hydrophobic IL, 1-butyl-3-methylimidazolium hexafluorophosphate [Bmim][PF_6], and

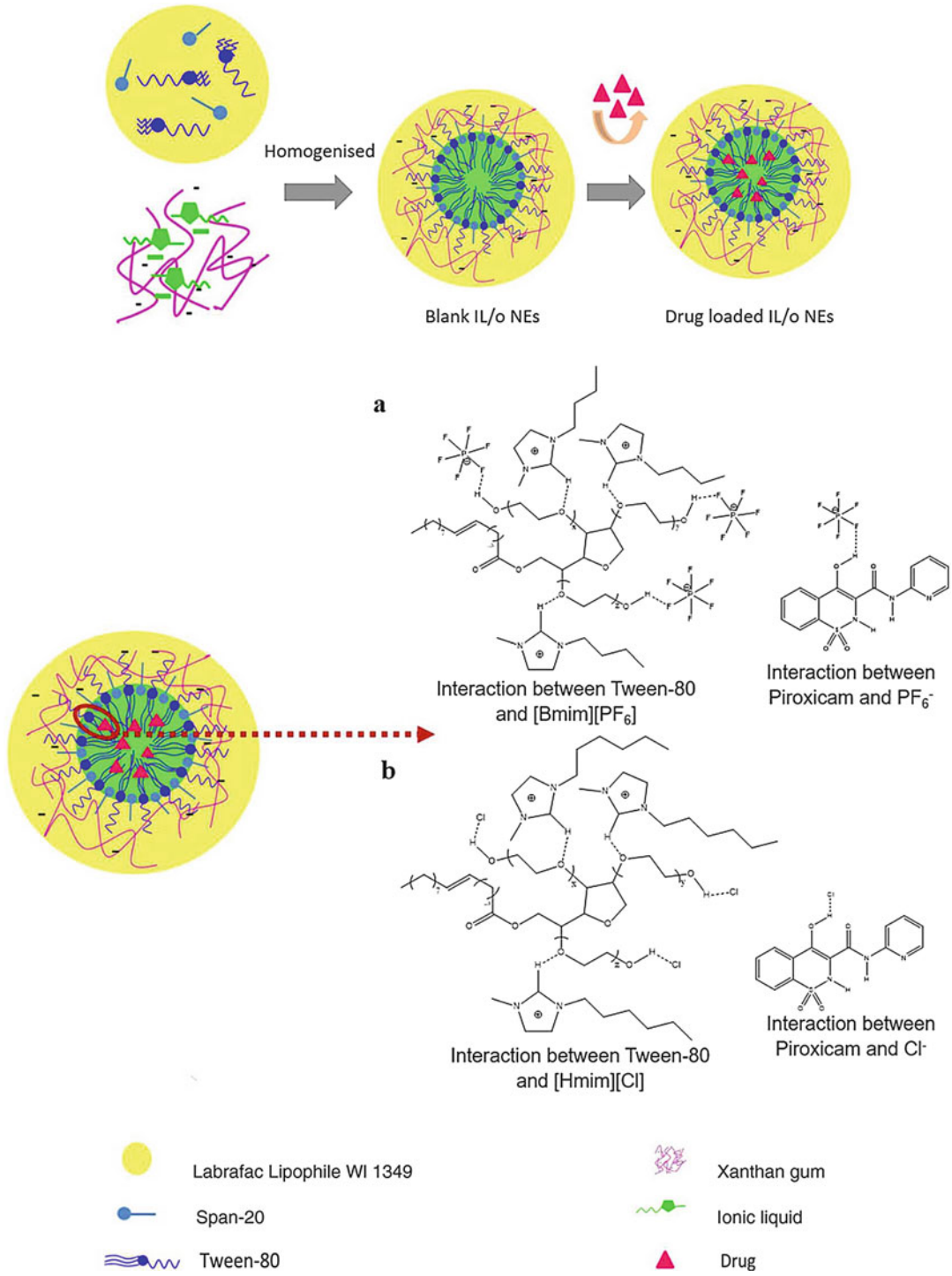

Surfactant Behavior of Ionic Liquids Involving a Drug, Scheme 2 Proposed mechanism for formation of IL/o microemulsion. (**a**) Hydrogen bond interaction between Tween 80 and [Bmim][PF_6], (**b**) hydrogen bond interaction between Tween 80 and [Hmim][Cl]. (This image is reprinted with permission from J. Mol. Liq. 2017, 234, 30–39 (copyright 2017, Elsevier))

surfactant mixtures (Tween 80 and Span 80). The hydrogen bonding interaction between the polar groups of piroxicam and IL anions is the main driving force for the encapsulation of piroxicam in the ILs [20]. Such encapsulations inside the core of the formed micelles are further stabilized by the hydrogen bonding with the surfactant, Tween 80.

The mechanism of the formation is elaborated in Scheme 2. The drug-loaded nanoemulsions were showing good physicochemical stability giving excellent result in the in vitro drug release study that confirms the good permeability and partitioning of the drug inside the microemulsion.

Conclusion

In summary, the discussion presented here combines synthesis and characterization of a large number of IL-derived aggregates and also drug delivery behaviors of these aggregates. The aggregates presented here are mainly IL-based micelle, vesicle, and microemulsion systems. Furthermore, this study discussed about the different IL-drug assemblies and also drug-containing IL assembled systems, where the drug serves as the constituting component of the IL and subsequently their applications as nanocarriers of the drug molecules. A significant number of literature reports are presented, where synthesis, characterization, and applications of different IL-based aggregated assemblies are elaborately discussed. All of the discussions finally conclude that the versatile uses of ILs as conventional surfactants along with as biocompatible drug delivery systems will surely open up a new horizon in colloid science as well as in biological and pharmaceutical research areas.

References

1. Ghosh S, Kuchlyan J, Roychowdhury S, Banik D, Kundu N, Roy A, Sarkar N (2014) Unique influence of cholesterol on modifying the aggregation behavior of surfactant assemblies: investigation of photophysical and dynamical properties of 2,2′-bipyridine-3,3′-diol, $BP(OH)_2$ in surfactant micelles, and surfactant/cholesterol forming vesicles. J Phys Chem B 118:9329–9340
2. Kaler EW, Murthy AK, Rodriguez BE, Zasadzinski JAN (1989) Spontaneous vesicle formation in aqueous mixtures of single-tailed surfactants. Science 245:1371–1374
3. Dutta R, Kundu S, Sarkar N (2018) Ionic liquid-induced aggregate formation and their applications. Biophys Rev 10:861–871
4. Kuchlyan J, Banik D, Roy A, Kundu N, Sarkar N (2015) Vesicles formation by zwitterionic micelle and poly-L-lysine: solvation and rotational relaxation study. J Phys Chem B 119:8285–8292
5. Dutta R, Ghosh S, Banerjee P, Kundu S, Sarkar N (2017) Micelle-vesicle-micelle transition in aqueous solution of anionic surfactant and cationic imidazolium surfactants: alteration of the location of different fluorophores. J Colloid Interface Sci 490:762–773
6. Ghosh S, Ghatak C, Banerjee C, Mandal S, Kuchlyan J, Sarkar N (2013) Spontaneous transition of micelle–vesicle–micelle in a mixture of cationic surfactant and anionic surfactant-like ionic liquid: a pure nonlipid small unilamellar vesicular template used for solvent and rotational relaxation study. Langmuir 29:10066–10076
7. Mandal S, Kuchlyan J, Banik D, Ghosh S, khorwal V, Sarkar N (2014) Ultrafast FRET to study spontaneous micelle-to-vesicle transitions in an aqueous mixed surface-active ionic-liquid system. ChemPhysChem 15:3544–3553
8. Pramanik R, Sarkar S, Ghatak C, Rao VG, Sarkar N (2011) Ionic liquid containing microemulsions: probe by conductance, dynamic light scattering, diffusion-ordered spectroscopy NMR measurements, and study of solvent relaxation dynamics. J Phys Chem B 115:2322–2330
9. Mandal S, Ghosh S, Banerjee C, Kuchlyan J, Banik D, Sarkar N (2013) A novel ionic liquid-in-oil microemulsion composed of biologically acceptable components: an excitation wavelength dependent fluorescence resonance energy transfer study. J Phys Chem B 117:3221–3231
10. Banerjee C, Roy A, Kundu N, Banik D, Sarkar N (2016) A new strategy to prepare giant vesicles from surface active ionic liquids (SAILs): a study of protein dynamics in a crowded environment using a fluorescence correlation spectroscopic technique. Phys Chem Chem Phys 18:14520–14530
11. Pyne A, Kuchlyan J, Maiti C, Dhara D, Sarkar N (2017) Cholesterol based surface active ionic liquid that can form microemulsions and spontaneous vesicles. Langmuir 33:5891–5899
12. Kundu N, Banik D, Roy A, Kuchlyan J, Sarkar N (2015) Modulation of the aggregation properties of sodium deoxycholate in presence of hydrophilic imidazolium based ionic liquid: water dynamics study to probe the structural alteration of the aggregates. Phys Chem Chem Phys 17:25216–25227
13. Péteilh CT, Coasne B, In M, Brevet D, Devoisselle JM, Vioux A, Viau L (2014)

Surfactant behavior of ionic liquids involving a drug: from molecular interactions to self-assembly. Langmuir 30:1229–1238
14. Pyne A, Kundu S, Banerjee P, Sarkar N (2018) Unveiling the aggregation behavior of doxorubicin hydrochloride in aqueous solution of 1-octyl-3-methylimidazolium chloride and the effect of bile salt on these aggregates: a microscopic study. Langmuir 34:3296–3306
15. Ghatak C, Rao VG, Mandal S, Ghosh S, Sarkar N (2012) An understanding of the modulation of photophysical properties of curcumin inside a micelle formed by an ionic liquid: a new possibility of tunable drug delivery system. J Phys Chem B 116:3369–3379
16. Roy A, Dutta R, Sarkar N (2016) Influence of trehalose on the interaction of curcumin with surface active ionic liquid micelle and its vesicular aggregate composed of a non-ionic surfactant sorbitan stearate. Chem Phys Lett 665:14–21
17. Mahajan S, Sharma R, Mahajan RK (2012) An investigation of drug binding ability of a surface active ionic liquid: micellization, electrochemical, and spectroscopic studies. Langmuir 28:17238–17246
18. Moniruzzaman M, Kamiya N, Goto M (2010) Ionic liquid based microemulsion with pharmaceutically accepted components: formulation and potential applications. J Colloid Interface Sci 352:136–142
19. Goindi S, Arora P, Kumar N, Puri A (2014) Development of novel ionic liquid-based microemulsion formulation for dermal delivery of 5-fluorouracil. AAPS PharmSciTech 15:810–821
20. Nor SBM, Woi PM, Ng SH (2017) Characterisation of ionic liquids nanoemulsion loaded with piroxicam for drug delivery system. J Mol Liq 234:30–39

Synthesis of Polymers in Ionic Liquids

Haq Nawaz and Feng Xu
Beijing Key Laboratory of Lignocellulosic Chemistry, Beijing Forestry University, Beijing, China

Introduction

Ionic liquids (ILs) are a new and emerging class of solvents for dissolution, regeneration, and chemical modification of natural and synthetic polymers. Based on their outstanding features such as chemically stable, non-flammable, less vapor pressure, easily recyclable, biodegradability, functional variability, and highly soluble, the ILs are widely synthesized and utilized in chemical industries for the fabrication of functional materials [1–4]. In addition, the synthesis of diverse ionic liquids based on various cations and anions structures are achieving more and more substantial roles in extensive applications such as separation, electrochemistry, energy conversion, catalysis, purification, photoluminescence, analysis, and biomass processing [5, 6]. Besides natural polymers, synthetic polymers are being widely synthesized in ionic liquids for multipurpose applications. The reason behind it is very clear that many polymeric reactions taking place in ionic liquids not only replace the toxic and volatile organic solvents but also affect the properties of polymers synthesized in ionic liquids. In addition, the ionic liquids possess hydrophilic groups such as cations and/or anions and hydrophobic groups such as long alkyl chains which interact with the monomer molecules thereby breaking the hydrogen bonding and imparting special features to the prepared polymers. On the other hand, such abilities are lacking in common organic solvents such as nitromethane, DMF, and halogen containing solvents in polymer synthesis. Furthermore, different mechanisms are involved in the synthesis of polymers in ionic liquids which are briefly discussed below.

Free Radical Polymerization

The molecules or monomers having vinylic group undergo free radical polymerization. Although free radical polymerization has been successfully accomplished in volatile organic solvents by controlling the gel effect and viscosity, however, the resulted environmental pollution forced the researcher to think about the use of green solvents for radical polymerization as an alternatives of organic solvents. For this purpose, ionic liquids have been utilized and proved to be a better choice with enhanced polymeric properties. The free radical polymerization of methyl methacrylate (MMA) was carried out in ionic liquid 1-butyl-3-methylimidazolium phosphorus hexafluoride ([Bmim][PF_6]) and in volatile organic solvents

and the results were compared. The results revealed that the rate of polymerization was increased and the polymer product was achieved with high molecular weight in ionic liquid when compared to organic solvent. These results might be attributed to the decreased rate of chain termination in ionic liquid. Furthermore, free radical polymerization of styrene and methyl methacrylate was carried out in [Bmim][PF_6] and in organic solvent like benzene and the results were compared. The results demonstrated that the rate of polymerization and molecular weight of the prepared polymers was much higher in ionic liquid as compared to benzene. The reason might be the high viscosity, better phase separation of macroradicals, and diffusion controlled termination phenomenon in ionic liquids [7]. The proposed mechanism of free radical polymerization of methyl methacrylate is shown in Fig. 1a. The ionic liquid [Bmim][PF_6] is widely employed in free radical polymerization due to its easy synthesis and commercial availability. However, it has some drawbacks such as it gets hydrolyzed and produces harmful hydrofluoric acid in the reaction.

Ring Opening Polymerization

The ring opening polymerization using ionic liquids was firstly reported in 2006 [8]. In this study, the ε-caprolactone was polymerized in 1-butyl-3-methylimidazolium tetrafluoroborate ([Bmim][BF_4]) using ZnO as a catalyst under microwave conditions (Fig. 1b). The results demonstrated that the rate of polymerization was effectively improved and no more catalyst was required in polymerization process at high temperature above

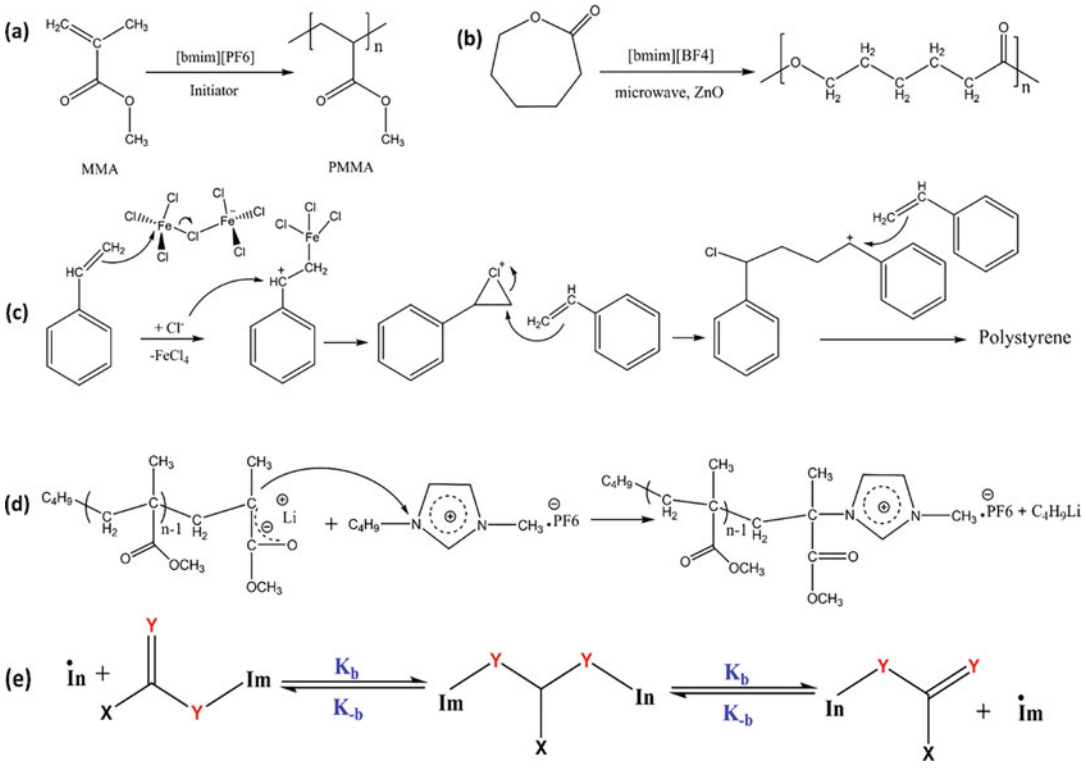

Synthesis of Polymers in Ionic Liquids, Fig. 1 Schemes and proposed mechanisms. (**a**) Free radical polymerization of methyl methacrylate in [Bmim][PF_6]; (**b**) ring opening polymerization of ε-caprolactone in [Bmim][BF_4] using ZnO as a catalyst; (**c**) cationic polymerization of styrene in [Bmim][Fe_2Cl_7] ionic liquid; (**d**) anionic polymerization of methyl methacrylate in [Bmim][PF_6]; (**e**) the equilibrium in the RAFT polymerization

200 °C. In addition, the ring opening polymerization is also affected by the counter ions of the ionic liquids using triflates of rare earth metals as a catalyst. The study revealed that the ionic liquids with counter ions such as [PF6] and $[SbF_6]^-$ proved to be effective solvents and yielded high molecular weight polymers while the ionic liquids with counter ions such as $[BF_4]^-$ was not succeeded for polymer synthesis [9]. These results demonstrated that the counter ions might interact with rare earth metals and form complexes which are auspicious for the process of polymerization. Furthermore, the ionic liquid-based polymerization process leads to the lower energy of activation as compared to organic solvents. It is suggested that the ions of ionic liquids can affect the association constant of polymer chain end and thus reduce the time of polymerization. In addition, the ionic liquids can be recycled and reused several times by adding water in the reaction product, filtering the polymers and removing the water by distillation.

Cationic Polymerization

For the first time, Higashimura and Kennedy groups discovered cationic and/or controlled polymerization process four decades ago and it is still considered to be the most promising method in the polymer synthesis. In this cationic polymerization method, the reactive carbocation intermediate is produced by the attack of active hydrogen onto monomers which is further generated by the reaction between water and lewis acids such as $AlCl_3$, $SnCl_4$, $TiCl_4$, and BF_3. The generated cationic intermediates undergo successive reactions with monomer molecules resulting in the preparation of long polymer chains. The proficiency of cationic polymerization is competently influenced by several parameters such as solvent polarity, nature of lewis acids, and the type of salts added for stabilizing the carbocations. The ionic nature of the ionic liquids makes them capable of solvating the organic/inorganic materials, hence making it a perfect candidate for the cationic polymerization [10]. The cationic polymerization of styrene has been reported in an iron containing ionic liquids such as 1-n-butyl-3-methylimidazolium ($[Bmim]^+$) along with $[Fe_2Cl_7]^-$ which acted as miniemulsion with H_2O. The results indicated that the polymer was produced with small particle size of 150–172 nm diameter in just 6 h and in the temperature range of 70 °C to 90 °C [11]. It was further inferred that the molecular weight of the polymer was increased when compared to that obtained by conventional process. The mechanism is presented in Fig. 1c. Furthermore, the rate of reaction was almost slow indicating its controllable nature thereby achieving desired high molecular weight polymers. The imidazolium-based ionic liquids, such as (Rmim-LA) where, R = ethyl, butyl and LA = aluminum trichloride, aluminum tribromide, boron tribromide, iron trichloride, gallium trichloride, and isobutyl aluminum dichloride, were prepared and were employed for cationic polymerization of isobutylene molecules. The results demonstrated that the ionic liquid such as ethylmethylimidazolium chloride exhibited excellent performance for monomer conversion into polymers when interacted with metal salts such as $AlCl_3$, $FeCl_3$, and $GaCl_3$ [12].

Anionic Polymerization

The monomers having active center to stabilize the negative charge undergo anionic polymerization. The common monomers that underdo anionic polymerization are styrene and dienes because of their ability to stabilize the negative charge by the process of delocalization. In this method, the most important factor is the properties of initiator such as electron affinity, nature of solvent, and structural characteristics of produced carbanions. The initiator should not attack on the side chain but only react with monomers. The anionic polymerization of methyl methacrylate has been reported in different ionic liquids such as 1-ethyl-3-methylimidazolium bis (trifluoromethane sulfonyl) amide [Emim][NTf_2], 1-butyl-3-methylimidazolium hexafluoro phosphate [Bmim][PF6], trimethylsulfonium bis(trifluoromethane sulfonyl)amide [Me_3S][NTf_2], and *N, N*-diethyl-*N*-methyl-*N*-(2-methoxyethyl) ammonium bis(trifluoromethane sulfonyl)amide [deme][NTf_2]. The diphenylhexyl lithium and

n-butyl lithium were employed as initiators [13]. The results indicated that the polymerization was only succeeded in [Bmim][PF_6] with very low yield. These results demonstrated that there might be a reaction that took place between the ionic liquids and the initiators. It was further suggested that to proceed the anionic polymerization in ionic liquids successfully, some points must be considered such as the polymerization must be carried out in low melting ionic liquids under low temperature; the cations and anions should not contain any reactive site and the basicity of initiator must be lower than that of alkyl lithium to overcome deactivation step. In another study, the anionic polymerization of methyl methacrylate was carried out in imidazolium based ionic liquids with counter ions $[BF_4]^-$ and $[PF_6]^-$ and alkyl lithium was utilized as an initiator. However, the results were not successful and MMA with terminated ionic group was appeared which was further confirmed by MALDI TOF MS technique [14]. The results demonstrated that at position-1 of imidazolium cation, the alkyl groups were attached as the head groups instead of alkyl lithium initiator. Furthermore, the new anionic moieties might have attacked onto nitrogen atom of ionic liquid and removed one of the larger groups from nitrogen and subjected to the chain transfer phenomenon (Fig. 1d).

Condensation Polymerization

In this method, the smaller molecules undergo successive condensation to form a large polymeric material with the loss of small molecules. This method is also named as "polycondensation." There are many synthetic polymers such as polyamides, polyesters, polysulfones, polyimides, and polyhydrazides which are synthesized in common organic solvents by employing this technique. Because of environment unfriendly nature of organic solvents, the thrust to explore the green solvents has been the subject of interest in last few years. Therefore, green solvents like ionic liquids have been investigated in the condensation process of polymers to replace organic solvents. Moreover, it has been recognized that the polycondensation phenomenon in ionic liquids has several advantages, such as it does not need to convert the functional groups into reactive species which indicate that there would be a direct process which can reduce the possibilities of hazardous side reactions. In addition, the effects of reaction conditions such as temperature, time, properties of the monomers used such as structure, viscosities, and the type of ionic liquids like cations/anions behavior on the synthesis and yield of polymers have been well studied by several researchers [15].

The large-scale production of poly(ethylene terephthalate) has been realized using phenyl alkyl pyrrolidinium-based ionic liquids. This method was eco-friendly and involved less time frame for completion. The ionic liquids were synthesized by the reaction of phenyl alkyl bromide with *N*-methyl pyrrolidine at ambient temperature and ion exchange method was performed by $[PF_6]^-$ and $[Tf_2N]^-$, thereby producing poly(ethylene terephthalate) with the molecular weight of around 1.9×10^4 $gmol^{-1}$. In addition, the high molecular weight poly(ethylene terephthalate) were achieved by the process of polycondensation of bis-β-hydroxyethyl terephthalate in the prepared ionic liquids [16]. In another study, the polycondensation of amino acids such as b-alanine was realized in imidazolium-based ionic liquids and triphenylphosphine was utilized as a condensing agent. The results demonstrated that the poly(β-alanine) was obtained with high molecular weight and degree of polymerization of 49.5 by employing 1,3-dimethyl imidazolium dimethyl phosphate as a reaction medium. It was further inferred that the polypeptides can be synthesized from natural amino acids like L-isoleucine and L-valine by employing the most common ionic liquid [Emim]Cl as a reaction medium [17].

Atom Transfer Radical Polymerization (ATRP)

In this phenomenon, an equilibrium reaction is established between the inactive species (RZ) and an active radical (R*). The presence of redox reaction between the transition metal complex and (RZ) retain the equilibrium.

Furthermore, the generated radicals involve in the polymerization of vinylic monomers resulting in a polyvinylic polymers. On the other hand, the metal halides react with the propagating radical to decrease the oxidation state of metals in the complex. This back and forth mechanism leads to the formation of polymers. In addition, the concentration of radicals must keep low in order to ensure the controlled atom transfer radical polymerization reaction [18]. For the first time, the controlled radical polymerization of methyl methacrylate (MMA) was recognized in ionic liquid [Bmim][PF_6] using ATRP technique. In this method, the CuBr/N-propyl-2-pyridylmethanimine was employed as a catalyst and ethyl-2-bromoisobutyrate was utilized as an initiator. The results demonstrated that the reaction proceeded faster in ionic liquid medium compared to organic solvents. Furthermore, this process was advantageous because the cupper catalyst remained in the ionic liquids phase and was used again and again instead of its purification as a cupper salt from ionic liquids [19]. The non-polar toluene was utilized to extract the polymer from the reaction medium. Methyl methacrylate was further polymerized using ATRP method. The phosphorous-based ionic liquid such as 1-phenyl-3-methylimidazole diphenyl phosphate was employed as a reaction medium and $CuBr_2$ was used as a catalyst. The results demonstrated that the polymerization was progressed via a controlled/living fashion due to the formation of ionic liquid/catalyst complex. In addition, the prepared complex revealed an outstanding solubility, hence leading to ATRP product [20].

Reversible Addition-Fragmentation Chain Transfer (RAFT) Polymerization

It is a type of controlled living radical polymerization in which a series of reversible addition-fragmentation steps takes place on the basis of degenerative chain transfer. In this method, the inactive chains are converted to active propagating chains to start the reaction. Such kind of polymerization takes place in the presence of thiocarbonyl thiol compounds and the proposed mechanism of the polymerization is presented in Fig. 1e where thiocarbonyl groups is designated as "C=Y". Perrier and his co-workers reported the first reversible addition–fragmentation chain transfer polymerization (RAFT) in ionic liquids such as 1-alkyl-3-methylimidazolium hexafluoroborate having different alkyl side chains (n = 4, 6, and 8). Three monomers were used such as acrylates, methacrylates, and styrene. The results demonstrated that the acrylates and methacrylates underwent smooth and controlled polymerization. However, the styrene did not undergo complete polymerization due to its precipitation in the ionic liquids [21]. The influence of ionic liquid [Bmim][PF_6] on the RAFT polymerization of butyl methacrylate was investigated. The results revealed that the rate of polymerization of butyl methacrylate was increased in the presence of 2-cyano-2-propyl dodecyl trithiocarbonate-RAFT agent in ionic liquid. These findings were further attributed to the formation of radical-IL complex during the reaction [22]. In addition, block copolymerization of butyl methacrylate and methyl methacrylate was also investigated and PBMA-block-PMMA was successfully prepared.

Concluding Remarks

In summary, ionic liquids with their outstanding ionic properties are being widely investigated in synthetic chemistry and in material sciences. Because of their unique properties such as low vapor pressure, excellent solubility, chemical stability, and recyclability, they are effectively employed in polymer sciences. Sometimes, they are directly involved in a chemical reactions and sometimes acting as a catalyst. Several types of polymers are being synthesized such as polystyrene, polyamides, poly(methyl methacrylate), poly(butyl methacrylate), poly (glycolic acid), and polyvinyl chloride by using different polymerization mechanisms such as free radical, cationic, anionic, ring opening, condensation, and living polymerization. The resulting polymers demonstrated the high molecular weight, enhanced thermal properties, and chemical stability and resulted in controlled and eco-friendly polymerization processes.

References

1. Zhang JM, Wu J, Yu J, Zhang X, He J, Zhang J (2017) Application of ionic liquids for dissolving cellulose and fabricating cellulose-based materials: state of the art and future trends. Mater Chem Front 1:1273–1290
2. Fabre E, Murshed SMS (2021) A review of the thermophysical properties and potential of ionic liquids for thermal applications. J Mater Chem A 9: 15861–15879
3. Curreri AM, Mitragotri S, Tanner EEL (2021) Recent advances in ionic liquids in biomedicine. Adv Sci 8:2004819
4. Pesic J, Watson M, Papovic S, Vranes M (2021) Ionic liquids: review of their current and future industrial applications and their potential environmental impact. Recent Pat Nanotechnol 15:225–244
5. Mohammed H, Al-Othman A, Nancarrow P, Elsayed Y, Tawalbeh M (2021) Enhanced proton conduction in zirconium phosphate/ionic liquids materials for high-temperature fuel cells. Int J Hydrog Energy 46:4857–4869
6. Liu K, Wang Z, Shi L, Jungsuttiwong S, Yuan S (2021) Ionic liquids for high performance lithium metal batteries. J Energy Chem 59:320–333
7. Hong K, Zhang H, Mays JW, Visser AE, Brazel CS, Holbrey JD, Reichert WM, Rogers RD (2002) Conventional free radical polymerization in room temperature ionic liquids: a green approach to commodity polymers with practical advantages. Chem Commun:1368–1369
8. Liao L, Liu L, Zhang C, Gong S (2006) Microwave-assisted ring-opening polymerization of ε-Caprolactone in the presence of ionic liquid. Macromol Rapid Commun 27:2060–2064
9. Nomura N, Taira A, Nakase A, Tomioka T, Okada M (2007) Ring-opening polymerization of lactones by rare-earth metal triflates and by their reusable system in ionic liquids. Tetrahedron 63:8478–8484
10. Durga G, Kalra P, Verma VK, Wangdi K, Mishra A (2021) Ionic liquids: from a solvent for polymeric reactions to the monomers for poly(ionic liquids). J Mol Liq 335:116540
11. Alves RC, Agner T, Rodrigues TS, Machado F, Neto BAD, da Costa C, de Araújo PHH, Claudia Sayer C (2018) Cationic miniemulsion polymerization of styrene mediated by imidazolium based ionic liquid. Eur Polym J 104:51–56
12. Berezianko IA, Vasilenko IV, Kostjuk SV (2018) Acidic imidazole-based ionic liquids in the presence of diisopropyl ether as catalysts for the synthesis of highly reactive polyisobutylene: effect of ionic liquid nature, catalyst aging, and sonication. Polymer 145:382–390
13. Kokubo H, Watanabe M (2008) Anionic polymerization of methyl methacrylate in an ionic liquid. Polym Adv Technol 19:1441–1444
14. Biedron T, Kubisa P (2007) Chain transfer to ionic liquid in an anionic polymerization of methyl methacrylate. J Polym Sci Part A: Polym Chem 45: 4168–4172
15. Kubisa P (2009) Ionic liquids as solvents for polymerization processes; Progress and challenges. Prog Polym Sci 34:1333–1347
16. Dou J, Liu Z (2012) A simple and efficient synthetic method for poly(ethylene terephthalate): phenylalkyl pyrrolidinium ionic liquid as polycondensation medium. Green Chem 14:2305–2313
17. Zhang S, Goncalves LD, Lefebvre H, Tessier M, Rousseau B, Fradet A (2012) Direct poly(β-alanine) synthesis via polycondensation in ionic liquids. ACS Macro Lett 1:1079–1082
18. Sarbu T, Matyjaszewski K (2001) ATRP of methyl methacrylate in the presence of ionic liquids with ferrous and cuprous anions. Macromol Chem Phys 202:3379–3391
19. Carmichael AJ, Haddleton DM, Bon SAF, Seddon KR (2000) Copper mediated living radical polymerisation in an ionic liquid. Chem Commun:1237–1238
20. Liu XH, Zhu Q, Zhang YG, Zhang QY, Ding C, Li J (2017) Facile, simple, and inexpensive ionic liquid, 1-phenyl-3-methylimidazole diphenyl phosphate, as an efficient phosphorus-based ligand for copper-catalyzed reverse atom transfer radical polymerization of methyl methacrylate. RSC Adv 7:45022–45028
21. Perrier S, Davis TP, Carmichael AJ, Haddleton DM (2002) First report of reversible addition–fragmentation chain transfer (RAFT) polymerisation in room temperature ionic liquids. Chem Commun:2226–2227
22. Kumar ARSS, Roy M, Singha NK (2018) Effect of ionic liquids on the RAFT polymerization of butyl methacrylate. Eur Polym J 107:294–302